UCLA
COMPUTATIONAL AND APPLIED MATHEMATICS

A Treatment of Discontinuities in Shock Capturing Finite Difference Method

Mao De-kang

February 1989

CAM Report 89-06

Department of Mathematics
University of California, Los Angeles
Los Angeles, CA. 90024-1555

1. Introduction

As is well known, the initial value problem for hyperbolic conservation laws is as follows:

$$u_t + f(u)_x = 0 \tag{1.1a}$$

$$u(x,t) = u_0(x) \tag{1.1b}$$

where $u = (u_1, u_2, \cdots, u_m)^T$ is a state vector and $f(u)$, the flux, is a vector valued function of m components. The system is hyperbolic in the sense that the $m \times m$ Jacobian matrix

$$A(u) = \partial f(u)/\partial u$$

has m real eigenvalues

$$a_1(u) \le a_2(u) \le \cdots \le a_m(u)$$

and a complete set of m linearly independent right-eigenvectors. A weak solution to (1.1) is a bounded measurable function $u(x,t)$ which satisfies

$$\int_0^\infty \int_{-\infty}^{\infty} (u\phi_t + f(u)\,\phi_x)\, dxdt + \int_{-\infty}^{\infty} u_0(x)\,\phi(x,0)\, dx = 0 \tag{1.2}$$

for all $\phi \in C_0^2((-\infty,\infty)\times[0,\infty))$.

The main cause of the numerical difficulty in shock capturing methods is the occurrence of discontinuities. The fluid state variables may jump across shock curves, and it may have discontinuous derivatives across characteristics. Most currently used shock capturing schemes allow the computation to cross discontinuities. Therefore we have difficulty in the vicinity of the discontinuities: on one hand we adopt a scheme, which its consistency is usually based on the assumption that the exact solution to the problem is smooth; on the other hand we do not have the necessary smoothness there. That is why oscillations and smearing of discontinuities

often occur in the computations.

Since 1970's many efficient finite difference approximations to (1.1) have been developed. Particularly, the ENO schemes lately developed by Harten, Osher, Engquist, and Chakravarthy (see [1], [2], [3], [4]) have been very successful in dealing with shocks. These schemes use a local adaptive stencil to obtain information automatically from regions of smoothness when the solution develops discontinuities. Obviously, the idea of picking up information from smooth parts contains the attempt to prevent the computation from crossing discontinuities. As a result, approximations using these methods can obtain uniformly high order accuracy right up to discontinuities, while keeping a sharp, essentially nonoscillatory shock transition.

Two improvements of ENO schemes should be mentioned are as follows.

In [7] and [8] Shu and Osher constructed the pointwise ENO schemes by applying the adaptive stencil idea to the numerical flux and using a TVD Runge-Kutta type time discretization (see [9]). This greatly eases the implementation and simplifies the programming.

In [10] Yang designed an artificial compression method for ENO schemes by modification of the slop in the reconstruction procedure. This technique efficiently improves the performance of the ENO schemes at contact discontinuities.

Recently, Harten introduced a concept of "subcell resolution" to the ENO schemes. The main ingredient of it is the observation that the information in cell average of a discontinuous function contains the location of the discontinuity within the cell. Using this observation one can modify the ENO reconstruction to recover accurately any discontinuous function from its cell average. The modification of the ENO reconstruction, that is to extend the reconstruction function in each left and right adjacent cell to the recovered location of the discontinuity, efficiently prevent the computation from crossing the discontinuity. The application of this technique to the linearly degenerate characteristic field greatly sharpens the contact discontinuities.

Five years ago, the author began to work on a treatment of discontinuities for shock capturing methods, which is based on arbitrary schemes (see [11], [12], [13]). It is somehow similar to Harten's "subcell resolution", although with different origin. The essence of the treatment is that in some critical intervals which is suspected of harboring discontinuities, we modify the original scheme to prevent the computation from crossing discontinuities. The modification is done by adding artificial terms to the original scheme. The accurate location of discontinuity is obtained by adding the small artificial terms. The spurious oscillation and the smearing of discontinuities are essentially eliminated since the computation is not done across the discontinuities. We believe that the basic idea presented here also applies to the multi-dimension cases.

The paper is organized in the following manner: In Section 2, we describe the method in detail. In Section 3, we discuss the practical implementation of this treatment. Some shock tracking idea is introduced to make the method more efficient. Section 4 studies the effect of this treatment on variation of the numerical solution. Section 5 generalizes this treatment to the case of the Euler equations of gas dynamics. Section 6 contains several numerical examples to show the performance of the treatment.

2. Treatment of Discontinuities in the Scalar Case

We begin with the scalar, convex problem, i.e both u and f in (1.1) are scalars, and $f'' \geq 0$. Let us consider a general conservative difference scheme:

$$u_j^{n+1} = u_j^n - \lambda(\hat{f}^n_{j+\frac{1}{2}} - \hat{f}^n_{1-\frac{1}{2}}) , \tag{2.1}$$

where $\hat{f}^n_{j+\frac{1}{2}} = \hat{f}(u^n_{j-k+1}, \cdots, u^n_{j+k})$ is the numerical flux dependent on $2k$ variables. The flux is consistent with (1.1a) in the sense that

$$\hat{f}(u,u, \cdots, u) = f(u) , \tag{2.2}$$

λ is the mesh ratio, i.e. $\lambda = \tau/h$, where τ and h are the time and space increments respectively.

The key point of this paper is trying to prevent the computation from crossing the possible discontinuities. To describe the method in detail, we start with a simple and particular case. Suppose that on the level n we have a cell, say $[x_{j_1}, x_{j_1+1}]$, which is suspected of harboring a shock (or contact discontinuity). The numerical solution on each side of which is supposed to be "smooth" (as shown in Fig. 2.1). The first step is to extend the numerical solution, by some kind of extrapolation, from one side of the cell to the other side, and get a set of extrapolation values: $u^{n,+}_{j_1-k}, u^{n,+}_{j_1-k+1}, \cdots, u^{n,+}_{j_1}, u^{n,-}_{j_1+1}, u^{n,-}_{j_1+2}, \cdots, u^{n,-}_{j_1+k+1}$ (see Fig. 2.1). Then, on each side of the shock, the numerical solution on the level $n+1$ will be evaluated only with the numerical solution on the level n and its extrapolation values from the same side. For example, if point (x_j, t_{n+1}) is on the left of the shock, then u_j^{n+1} will be computed as

$$u_j^{n+1} = u_j^n - \lambda(\hat{f}^{n,-}_{j+\frac{1}{2}} - \hat{f}^{n,-}_{j-\frac{1}{2}}) \tag{2.3}$$

rather than (2.1), where

$$\hat{f}^{n,-}_{j+\frac{1}{2}} = \hat{f}(u^n_{j-k+1}, \cdots, u^n_{j_1}, u^{n,-}_{j_1+1}, \cdots, u^{n,-}_{j+k}) \tag{2.4}$$

Also if point (x_j,t_{n+1}) is on the right of the shock, then u_j^{n+1} will be computed as

$$u_j^{n+1} = u_j^n - \lambda(\hat{f}^{n,+}_{j+\frac{1}{2}} - \hat{f}^{n,+}_{j-\frac{1}{2}}) \tag{2.5}$$

rather than (2.1), where

$$\hat{f}^{n,+}_{j+\frac{1}{2}} = \hat{f}\,(u^{n,+}_{j-k+1}, \cdots, u^{n,+}_{j_1}, u^n_{j_1+1} \cdots, u^n_{j+k}) \tag{2.6}$$

In doing so, the computation is completely prevented from crossing the jump of the numerical solution, hence the oscillation and smearing are essentially eliminated.

An important problem is to obtain the correct speed of the shock. That is whether the jump of the numerical solution should stay in the original cell or move one cell to the left or right when it goes from the level n to the level $n+1$. If the jump moves one cell to the left, then the point (x_{j_1},t_{n+1}) should be on the right of the shock, and $u_{j_1}^{n+1}$ should be computed as

$$u_{j_1}^{n+1} = u_{j_1}^{n,+} - \lambda(\hat{f}^{n,+}_{j_1+\frac{1}{2}} - \hat{f}^{n,+}_{j_1-\frac{1}{2}}) \tag{2.7}$$

If the jump moves one cell to the right, then the point (x_{j_1+1},t_{n+1}) should be on the left of the shock, and $u_{j_1+1}^{n+1}$ should be computed as

$$u_{j_1+1}^{n+1} = u_{j_1+1}^{n,-} - \lambda(\hat{f}^{n,-}_{j_1+\frac{3}{2}} - \hat{f}^{n,-}_{j_1+\frac{1}{2}}) \tag{2.8}$$

(as shown in Fig. 2.2). In [1], Harten dealt with this problem by involving the location and the speed of the discontinuity. In this paper we are dealing with it in a different way.

Obviously, the modified scheme is not conservative across the cell $[x_{j_1},x_{j_1+1}]$. However we can write it in a conservation-like form by introducing some artificial terms along x and t directions, i.e. we rewrite the scheme in the form

$$u_j^{n+1} = u_j^n - \lambda(\tilde{f}^n_{j+\frac{1}{2}} - \tilde{f}^n_{j-\frac{1}{2}}) + p^n_{j+\frac{1}{2}} - p^n_{j-\frac{1}{2}} + q_j^{n+1} - q_j^n \tag{2.9}$$

where

$$\tilde{f}^{n}_{j+\frac{1}{2}} = \begin{cases} \hat{f}^{n,-}_{j+\frac{1}{2}} & j \le j_1 \\ \hat{f}^{n,+}_{j+\frac{1}{2}} & j \ge j_1+1 \end{cases} \tag{2.10}$$

The introduced artificial terms are as follows. If the jump of the numerical solution on the level $n+1$ remains in the the cell $[x_{j_1},x_{j_1+1}]$, then:

$$\begin{aligned} & p^{n}_{j+\frac{1}{2}} = 0 && \forall j \\ & q^{n+1}_{j} = 0 && \forall j \ne j_1 \\ & q^{n+1}_{j_1} = q^{n}_{j_1} + \lambda(\hat{f}^{n,+}_{j_1+\frac{1}{2}} - \hat{f}^{n,-}_{j_1+\frac{1}{2}}) . \end{aligned} \tag{2.11}$$

If the jump moves one cell to the left, then:

$$\begin{aligned} & p^{n}_{j+\frac{1}{2}} = 0 && \forall j \ne j_1 \\ & p_{j_1-\frac{1}{2}} = -q^{n}_{j_1} + (u^{n}_{j_1} - u^{n,+}_{j_1}) + \lambda(\hat{f}^{n,-}_{j_1-\frac{1}{2}} - \hat{f}^{n,+}_{j_1-\frac{1}{2}}) \\ & q^{n+1}_{j} = 0 && \forall j \ne j_1-1 \\ & q^{n+1}_{j_1-1} = -p^{n}_{j_1-\frac{1}{2}} . \end{aligned} \tag{2.12}$$

If the jump moves one cell to the right, then:

$$\begin{aligned} & p^{n}_{j+\frac{1}{2}} = 0 && \forall j \ne j_1 \\ & p^{n}_{j_1+\frac{1}{2}} = q^{n}_{j_1} + \lambda(\hat{f}^{n,+}_{j_1+\frac{1}{2}} - \hat{f}^{n,-}_{j_1+\frac{1}{2}}) \\ & q^{n+1}_{j} = 0 && \forall j \ne j_1+1 \\ & q^{n+1}_{j_1+1} = q^{n}_{j_1} + (u^{n,-}_{j_1+1} - u^{n}_{j_1+1}) + \lambda(\hat{f}^{n}_{j_1+\frac{3}{2}} - \hat{f}^{n,-}_{j_1+\frac{3}{2}}) . \end{aligned} \tag{2.13}$$

Instead of u_j^n, quantity $u_j^n - q_j^n$ is conservative in the modified scheme (2.9).

A very important point in our treatment is that these artificial terms given in (2.11), (2.12), and (2.13) are regarded as the "truncation error" at the discontinuity. In fact, if multiply (2.9) by $\phi_j^n \tau$, sum it with respect to j and n, and sum it by parts, we get

$$\sum_{n=0}^{\infty}\sum_{j=-\infty}^{\infty}\frac{\phi_j^n-\phi_j^{n-1}}{\tau}u_j^n\tau h+\sum_{n=0}^{\infty}\sum_{j=-\infty}^{\infty}\frac{\phi_{j+1}^n-\phi_j^n}{h}\tilde{f}^n_{j+\frac{1}{2}}\tau h+\sum_{j=-\infty}^{\infty}\phi_j^0u_j^0h$$

$$=\sum_{n=1}^{\infty}\frac{\phi_{j_n}^n-\phi_{j_{n-1}}^{n-1}}{\tau}q_{j_n}^n\tau h+\phi_{j_0}^0q_{j_0}^0h+\sum_{n=0}^{\infty}\frac{\phi_{j_n+1}^n-\phi_{j_n}^n}{\tau}p^n_{j_n+\frac{1}{2}}\tau h \qquad (2.14)$$

where $\phi_j^n=\phi(x_j,t_n)$, ϕ is a twice differentiable test function, $[x_{j_n},x_{j_n+1}]$ contains a jump on the level n. Comparison of (1.2) with (2.14) implies that the smaller the artificial terms are, the closer the numerical solution is to the exact solution. Therefore we need to keep these artificial terms small in the computation. Since $p_{j_n+\frac{1}{2}}$ is related to $q_{j_{n+1}}^{n+1}$, practically it suffices only to take care of the latter one, and this will automatically give us a criterion to control the jump's moving. We calculate for each case the corresponding $q_{j_{n+1}}^{n+1}$, compare them, and choose the case which corresponds to the smallest $|q_{j_{n+1}}^{n+1}|$. In doing so, we can get an accurate shock location on each time level.

The above method involves artificial terms along both x and t directions. Thus we refer to it as the $x-t$ version of the treatment. Another version of this treatment is the x version, in which only artificial terms along x direction are involved, and the jump of numerical solution occupies at least two cells. Here we will only give a brief description of it, for further details interested reader is refer to [11], [12].

Suppose that we have an interval $[x_{j_1-1},x_{j_1+1}]$ on the level n, which is suspected of containing a shock. First we extend the numerical solution from one side of the interval to the other side, and get a set of extrapolation values: $u_{j_1-k-1}^{n,+}, \cdots, u_{j_1}^{n,+}, u_{j_1}^{n,-}, \cdots, u_{j_1+k+1}^{n,-}$. Then the computation on each side of the possible shock will be implemented only with the

numerical solution and its extrapolation values from the same side (just as done by (2.3) - (2.8)). Instead of requiring $|q_{j_{n+1}}^{n+1}|$ to be small, we require the numerical solution to have the least variation within the interval in the x version, i.e. we require

$$|u_{j_1}^n - 0.5(u_{j_1+1}^n + u_{j_1-1}^n)|$$

to be small, where $u_{j_1}^n$ is the value of the numerical solution at the middle point of the interval (see [11]). This will also give us a criterion to control the moving of the jump, i.e. whether the jump should stay in the original interval or move one cell to the left or right when it goes from the level n to the level $n+1$.

Remark 2.1 Harten's subcell resolution only involves the artificial terms along x direction, so his method is an x version. If the basic scheme is the ENO scheme, we believe that the x version of this treatment is similar to the Harten's method.

Remark 2.2 Suppose that the basic scheme (2.1) is *rth* order. This order of accuracy will be kept in the region of smoothness for the modified scheme in both the x and the $x-t$ version if the extrapolation employed above is more than *rth* order accurate. This means that the treatment will cause little error even if it is applied to the region of smoothness. However, numerical experiments show that in many cases lower order (even zero order) extrapolation works well, especially in dealing with shocks.

3. Implementation of the Treatment

1) Formation of the Generated Intervals. The first problem is to determine the cells which need the treatment. In this paper we refer to these cells as generated intervals (in [11] and [12] we refer to them as generated sections). Generally, we choose a quantity which is related to the numerical solution as the measure of non-smoothness. Then the criterion of selection is based on the observation of this measure. Obviously, the simplest choice of this measure is $|u_{j+1}^n - u_j^n|$. Correspondingly, in the candidate cell or interval, $|u_{j+1}^n - u_j^n|$ should be relatively large. In the case of $f'' > 0$, $u_{j+1}^n - u_j^n < 0$ is also required so that the treatment is only applied to shocks, not rarefaction waves. This is the criterion used in [12]. The main drawback of it is that we could neglect some weak shocks and contact discontinuities, and apply the treatment to cells or intervals which have somewhat large slops, but still should be regarded as "smooth" according to the global structure of the numerical solution. A further consideration along this direction is to involve some high order difference quotient of numerical solution in the measure of non-smoothness.

The criterion suggested by Harten in [1] is based on the ENO reconstruction, and involves difference quotients of high order. An important point of his criterion is that the measure of non-smoothness in the candidate cell should attain a local maximum. If $|u_{j+1}^n - u_j^n|$ is the measure of non-smoothness, his criterion is analogous to require that $|u_{j+1}^n - u_j^n|$ be greater than both $|u_j^n - u_{j-1}^n|$ and $|u_{j+2}^n - u_{j+1}^n|$. This criterion greatly avoids neglecting weak shocks and contact discontinuities.

Obviously, no criterion can strictly distinguish shocks and contact discontinuities from the smooth parts of the numerical solution, especially in the case of spontaneous shocks. This means that we can not completely avoid the "accidental effect" of this treatment to the smooth region. However, remark 2.1 tells us that such accidental effect is tolerated in computation.

In this paper, we combine the criterion in [12] and [1]. It takes $|u_{j+1}^n - u_j^n|$ as the measure of non-smoothness, and requires that this measure in candidate cells be relatively large, say greater than a constant α_1, and also attain a local maximum. In the case of $f'' > 0$, $u_{j+1}^n - u_j^n < 0$ is required as well.

Usually, the generated interval in the $x-t$ version only occupies one cell. But in the x version it occupies at least two cells. Therefore, the candidate cells obtained by the above criterion in the x version should be extended to the intervals of more than one cells to become generated intervals. We merge the adjacent candidation cells into one interval, and extend the isolated candidate cell to its left or right adjacent cell by choice. In [12] we extend the isolated candidate cell as follows: check the difference quotient in each left and right adjacent cell, then extend the candidate cell to the one with greater difference quotient. In doing so we expect to eliminate some spurious oscillation.

Finally, the cells or intervals containing the jumps coming from the level n should be precedently accepted as the generated intervals on the level $n+1$. For example in $x-t$ version, suppose we have a generated interval $[x_{j_1},x_{j_1+1}]$ on the level n, then one of the intervals $[x_{j_1},x_{j_1+1}]$, $[x_{j_1+1},x_{j_1+2}]$, and $[x_{j_1-1},x_{j_1}]$ should be accepted as generated interval on the level $n+1$ according to the different case of moving, unless the corresponding jump is too weak, say $|u_{j_1+1}^{n+1}-u_{j_1}^{n+1}|$, $|u_{j_1+2}^{n+1}-u_{j_1+1}^{n+1}|$, or $|u_{j_1}^{n+1}-u_{j_1-1}^{n+1}|$ is smaller than a constant $\alpha_2(<\alpha_1)$. A similar handling for x version is given in [11]. In doing so, we have introduced some shock front tracking idea into the algorithm to make it more efficient. However, unlike the traditional front tracking methods (refer to [16], [17], [18]), no lower dimensional adaptive grid is introduced to fit the front of discontinuity, and the whole algorithm is much simpler.

The efforts to set up even more efficient and reasonable criterion are welcome.

2) Performance of the Treatment. Here we only focus our attention to the $x-t$ version. For the detail of the x version see [11].

Suppose that there is a generated interval $[x_{j_1},x_{j_1+1}]$ on the level n. At first we calculated $s=(f(u_{j_1+1}^n)-f(u_{j_1}^n))/(u_{j_1+1}^n-u_{j_1}^n)$, and check if it is greater than 0. The positive s indicates that the shock (or contact discontinuity) should move to the right. Therefore only two cases of moving should be considered: either the jump on the level $n+1$ still stays in cell $[x_{j_1},x_{j_1+1}]$ or moves one cell to the right. The case of $s \le 0$ can be treated similarly.

The treatment can be performed by adding some artificial terms to the basic scheme (2.1), i.e. the modified scheme can be written into the form

$$u_j^{n+1} = u_j^n - \lambda(\hat{f}^n_{j+\frac{1}{2}} - \hat{f}^n_{j-\frac{1}{2}}) + p^n_{j+\frac{1}{2}} - p^n_{j-\frac{1}{2}} + q_j^{n+1} - q_j^n \tag{3.1}$$

Suppose $s > 0$. If the jump remains in cell $[x_{j_1}, x_{j_1+1}]$, we take the artificial terms as follows:

for $j_1-k+1 \le j \le j_1-1$

$$p^n_{j+\frac{1}{2}} = \lambda(\hat{f}^n_{j+\frac{1}{2}} - \hat{f}^{n,-}_{j+\frac{1}{2}}), \tag{3.2}$$

for $j_1 \le j \le j_1+k+1$

$$p^n_{j+\frac{1}{2}} = \lambda(\hat{f}^n_{j+\frac{1}{2}} - \hat{f}^{n,+}_{j+\frac{1}{2}}), \tag{3.3}$$

and

$$\begin{aligned} q_j^{n+1} &= 0 \qquad\qquad \forall\ j \neq j_1 \\ q_{j_1}^{n+1} &= q_{j_1}^n + \lambda(\hat{f}^{n,+}_{j_1+\frac{1}{2}} - \hat{f}^{n,-}_{j_1+\frac{1}{2}}) \end{aligned} \tag{3.4}$$

If the jump moves one cell to the right we take the artificial terms as follows:

for $j_1-k+1 \le j_1 \le j_1-1$

$$p^n_{j+\frac{1}{2}} = \lambda(\hat{f}^n_{j+\frac{1}{2}} - \hat{f}^{n,-}_{j+\frac{1}{2}}), \tag{3.5}$$

for $j = j_1$

$$p^n_{j_1+\frac{1}{2}} = q^n_{j_1} + \lambda(\hat{f}^n_{j_1+\frac{1}{2}} - \hat{f}^{n,-}_{j_1+\frac{1}{2}}), \tag{3.6}$$

for $j_1+1 \le j \le j_1+k-1$

$$p^n_{j+\frac{1}{2}} = \lambda(\hat{f}^n_{j+\frac{1}{2}} - \hat{f}^{n,+}_{j+\frac{1}{2}}), \tag{3.7}$$

and

$$q_j^{n+1} = 0 \qquad \forall\, j \neq j_1+1$$
$$q_{j_1+1}^{n+1} = q_{j_1}^n + u_{j_1+1}^{n,-} - u_{j_1+1}^n + \lambda(\hat{f}^{n,+}_{j_1+\frac{3}{2}} - \hat{f}^{n,-}_{j_1+\frac{3}{2}}) . \tag{3.8}$$

Obviously, when the extrapolation employed in the treatment is of rth order, the terms $\lambda(\hat{f}^{n,+}_{j_1+\frac{1}{2}} - \hat{f}^{n,-}_{j_1+\frac{1}{2}})$, and $u^{n,-}_{j_1+1} - u^n_{j_1+1} + \lambda(\hat{f}^{n,+}_{j_1+\frac{3}{2}} - \hat{f}^{n,-}_{j_1+\frac{3}{2}})$ that occur in the expressions of $q^{n+1}_{j_1}$ and $q^{n+1}_{j_1+1}$ and the terms $p^n_{j+\frac{1}{2}}$ are all of $(r+1)th$ order. This justifies the statement in Remark 2.2.

3) High Resolution Technique. The moving of discontinuity fully depends on the artificial term along t direction. This implies that this artificial term contains the location of the discontinuity within the generated interval. Therefore one can use it to find out the more accurate location of discontinuity within the cell. We refer to this technique as the "high resolution" technique. As in [11], we use the following formula to compute the coordinate of the location s^n in $x-t$ version.

$$s^n = x_{j_1} + h(\frac{1}{2}(u^n_{j_1} - u^n_{j_1+1}) - q^n_{j+1})/(u^n_{j_1} - u^n_{j_1+1}) . \tag{3.9}$$

An analogous formula for the x version can be found in [11]. An example using (3.9) was presented in [11] and [12] showing the result of the technique. Suppose that the initial value problem (1.1) is a Riemann problem which its solution is a moving shock between two constant states. If we use a general 3-point scheme with the treatment of this paper. then the numerical solution is exactly the true solution. Also the shock location obtained by the high resolution technique on each time level is exact. In fact, the early idea of this treatment was motivated from this example.

4) Interaction of Generated Intervals. Until now we have only considered the case that involves a single discontinuity, on each side of which the numerical solution is supposed to be smooth. However, a general initial value problem may involve several shocks and contact

discontinuities, which could collide with each other. Therefore, inevitably we have to deal with the interactions of numerical discontinuities.

Without the loss of generality we only consider the interaction of two generated intervals in the $x-t$ version. Suppose that $[x_{j_1}, x_{j_1+1}]$ and $[x_{j_2}, x_{j_2+1}]$ are two generated intervals on the level n (as shown in Fig. 3.1). If the extrapolation in the treatment is of rth order, the extrapolation values on each side are evaluated with the $r+1$ values of the numerical solution on the other side. However, when the two generated intervals are close such that the number of the space points between them is less than $r+1$, the rth order extrapolation is impossible. Therefore we should reduce the order of the extrapolation. Hence, at that time the $u^{n,+}_{j_1-k,m}, \cdots, u^{n,+}_{j_1,m}$, and $u^{n,-}_{j_2+1,m}, \cdots, u^{n,-}_{j_2+k+1,m}$ are evaluated by the extrapolation of the order lower than r, where $u^{n,+}_{j,m}$ and $u^{n,-}_{j,m}$ denote the extrapolation values obtained from the part of the numerical solution between these two generated intervals (see Fig. 3.1).

When the number of the space points between the two generated intervals are less than $2k$, the stencils of some these points will cross both the two generated intervals. Therefore, in order to pick up the information only from one side, the computations at these points will use the following terms for numerical flux,

$$\hat{f}\,(u^{n,+}_{j-k+1,m}, \cdots, u^{n,+}_{j_1,m}, u^{n}_{j_1+1}, \cdots u^{n}_{j_2}, u^{n,-}_{j_2+1,m}, \cdots u^{n,-}_{j+k,m})\,. \tag{3.10}$$

The collision of generated intervals happens only when we are tracking the discontinuities. A typical case is as follows: Suppose that the two generated intervals are adjacent, i.e. $j_2 = j_1+1$, and the jump in the left (right) one should move to the right (left), while the jump in the right (left) one should remain in the original cell (as shown in Fig. 3.2 a, b). Obviously, there would be two overlapped generated intervals on the level $n+1$. Let $q^{n+1}_{j_1,l}$ and $q^{n+1}_{j_1,r}$ ($q^{n+1}_{j_1-1,l}$ and $q^{n+1}_{j_1-1,r}$) denote the artificial terms corresponding to the left and right generated intervals respectively. In that case, we take $q^{n+1}_{j_1}$ $(q^{n+1}_{j_1-1}) = q^{n+1}_{j_1,l} + q^{n+1}_{j_1,r}$ $(q^{n+1}_{j_1-1,l} + q^{n+1}_{j_1-1,r})$, and accept the two overlapped generated intervals on the level $n+1$ as a single generated interval.

If the jumps in both generated intervals should move towards each others (see Fig. 3.2 c). In that case we should accept $[x_{j_1-1},x_{j_1+1}]$ on the level n as a single generated interval of two cells. The treatment of the generated interval of two cells is the naive extension of the treatment of the generated interval of one cell. First we still extrapolate the numerical solution from each side to the other side. Then the numerical solution on the next level will be computed by (2.3) - (2.8). Unlike the case of generated interval of one cell, here we have four possible cases of jump moving. The generated interval on the level $n+1$ could be one of the $[x_{j_1-2},x_{j_1-1}]$, $[x_{j_1-1},x_{j_1}]$, $[x_{j_1},x_{j_1+1}]$, and $[x_{j_1+1},x_{j_1+2}]$. We calculate the corresponding artificial terms for each case by solving the following system:

$$
\begin{aligned}
u_j^{n+1} &= u_j^n - \lambda(\tilde{f}^n_{j+\frac{1}{2}} - \tilde{f}^n_{j-\frac{1}{2}}) + p^n_{j+\frac{1}{2}} - p^n_{j-\frac{1}{2}} - q_j^n && j < k \\
u_k^{n+1} &= u_k^n - \lambda(\tilde{f}^n_{k+\frac{1}{2}} - \tilde{f}^n_{k-\frac{1}{2}}) + p^n_{k+\frac{1}{2}} - p^n_{k-\frac{1}{2}} + q_k^{n+1} - q_k^n && j = k \qquad (3.11) \\
u_j^{n+1} &= u_j^n - \lambda(\tilde{f}^n_{j+\frac{1}{2}} - \tilde{f}^n_{j-\frac{1}{2}}) + p^n_{j+\frac{1}{2}} - p^n_{j-\frac{1}{2}} - q_j^n && j > k\ ,
\end{aligned}
$$

where $\tilde{f}^n_{j+\frac{1}{2}}$ is defined by (2.10), $p^n_{j_1-\frac{3}{2}} = p_{j_1+\frac{3}{2}} = 0$, and k is taken to be j_1-2, j_1-1, j_1, and j_1+1 respectively. We compare those $|q_k^{n+1}|$'s, and then choose the case which has the smallest $|q_k^{n+1}|$.

We can also handle the above situation in the following easy way. Treat the left generated interval as its jump does not move, and still let the jump in the right one move to the left, or conversely. Then merge the two overlapped generated intervals on the level $n+1$.

The handling of collision of the generated intervals for x version (only for the zero order extrapolation) is given in [11]. Since each generated interval in that case at least occupies two cells, the handling of collision is more complicated than that for $x-t$ version.

4. TVD property of the treatment, uniformly boundedness of the artificial terms.

In this section we study the effects of this treatment on the variation of the numerical solution. Here we only consider the $x-t$ version in the case $f'' > 0$. An analogue discussion for the x version can be founded in [11].

An important class of difference schemes are the TVD schemes. These schemes do not increase the total variation of the numerical solution. We will show in this section that our treatment keeps the TVD property of the scheme if the interactions of discontinuities are ignored.

Suppose (2.1) is a TVD scheme which can be written in the form (see [5], [19]).

$$u_j^{n+1} = u_j^n + C^{n,+}_{j+\frac{1}{2}} \Delta^n_{j+\frac{1}{2}} u - C^{n,-}_{j-\frac{1}{2}} \Delta^n_{j-\frac{1}{2}} u \tag{4.1}$$

here

$$\begin{aligned} &C^{n,+}_{j+\frac{1}{2}} \geq 0 \quad , \quad C^{n,-}_{j+\frac{1}{2}} \geq 0; \\ &C^{n,+}_{j+\frac{1}{2}} + C^{n,-}_{j+\frac{1}{2}} \leq 1 \end{aligned} \tag{4.2}$$

$$\begin{aligned} C^{n,+}_{j+\frac{1}{2}} &= \lambda \frac{f(u_j^n) - \hat{f}^n_{j+\frac{1}{2}}}{\Delta^n_{j+\frac{1}{2}} u} \\ C^{n,-}_{j+\frac{1}{2}} &= \lambda \frac{f(u_{j+1}^n) - \hat{f}^n_{j+\frac{1}{2}}}{\Delta^n_{j+\frac{1}{2}} u} \end{aligned} \tag{4.3}$$

and

$$\lambda \left| (f(v_j) - \hat{f}_{j+\frac{1}{2}}) + (f(v_{j+1}) - \hat{f}_{j+\frac{1}{2}}) \right| \leq |v_{j+1} - v_j| \tag{4.4}$$

It is easy to see that (4.4) implies

$$\hat{f}(v_{j-k+1}, \ldots, v_{j-1}, w, w, v_{j+2}, \ldots, v_{j+k}) = f(w) \tag{4.5}$$

Such essentially 3-point scheme includes, beside the standard 3-point scheme, several recently constructed second- order accurate converging schemes (refer to [19]). By the *rth* order treatment we mean the treatment which uses the *rth* order extrapolation.

THEOREM 4.1 *The zero order treatment keeps the TVD property in the vicinity of the generated intervals.*

We use the "vicinity" to indicate the region the treatment could affect. When the basic scheme is $(2k+1)$-point scheme and $[x_{j_1}, x_{j_1+1}]$ is the generated interval, this region is the interval $[x_{j_1-k}, x_{j_1+k+1}]$. Hence, we need to show

$$\sum_{j=j_1-k}^{j_1+k} |\Delta^{n+1}_{j+\frac{1}{2}} u| \le C^{n,+}_{j_1+k+\frac{1}{2}} |\Delta^{n}_{j_1+k+\frac{1}{2}} u| + (1 - C^{n,-}_{j_1+k-\frac{1}{2}}) |\Delta^{n}_{j_1+k-\frac{1}{2}} u|$$

$$+ \sum_{j=j_1-k+1}^{j_1+k-1} |\Delta^{n}_{j+\frac{1}{2}} u| + (1 - C^{n,+}_{j_1-k+\frac{1}{2}}) |\Delta^{n}_{j_1-k+\frac{1}{2}} u| + C^{n,-}_{j_1-k-\frac{1}{2}} |\Delta^{n}_{j_1-k-\frac{1}{2}} u| \tag{4.6}$$

Proof: Assume that $[x_{j_1}, x_{j_1+1}]$ is a generated interval on level n. Without loss of generality we assume $s = (f(u^n_{j_1+1}) - f(u_{j_1}))/(u_{j_1+1} - u_{j_1}) \ge 0$, i.e. the shock moves to the right. When $j \le j_1-1$, or $j \ge j_1+2$, the u^{n+1}_j is evaluated by (2.3) or (2.5). Since the scheme (2.1) can be written in the form of (4.1), we have

$$u^{n+1}_j = u^n_j + C^{n,+}_{j+\frac{1}{2},l} \Delta^n_{j+\frac{1}{2}} u - C^{n,-}_{j-\frac{1}{2},l} \Delta^n_{j-\frac{1}{2}} u \qquad j \le j_1-1 , \tag{4.7}$$

and

$$u^{n+1}_j = u^n_j + C^{n,+}_{j+\frac{1}{2},r} \Delta^n_{j+\frac{1}{2}} u - C^{n,-}_{j-\frac{1}{2},r} \Delta^n_{j-\frac{1}{2}} u \qquad j \ge j_1+2 . \tag{4.8}$$

Here

$$C^{n,+}_{j+\frac{1}{2},l} = \lambda \frac{f(u^n_j) - \hat{f}^{n,-}_{j+\frac{1}{2}}}{\Delta^n_{j+\frac{1}{2}} u}$$
$$C^{n,-}_{j+\frac{1}{2},l} = \lambda \frac{f(u^n_{j+1}) - \hat{f}^{n,-}_{j+\frac{1}{2}}}{\Delta^n_{j+\frac{1}{2}} u} \qquad (4.9)$$

and

$$C^{n,+}_{j+\frac{1}{2},r} = \lambda \frac{f(u^n_j) - \hat{f}^{n,+}_{j+\frac{1}{2}}}{\Delta^n_{j+\frac{1}{2}} u}$$
$$C^{n,-}_{j+\frac{1}{2},r} = \lambda \frac{f(u^n_{j+1}) - \hat{f}^{n,+}_{j+\frac{1}{2}}}{\Delta^n_{j+\frac{1}{2}} u}, \qquad (4.10)$$

and both the couples (4.9) and (4.10) satisfy (4.2). Obviously, the modified scheme still has a TVD form at these points, but with different coefficients.

When the jump on the level $n+1$ remains in $[x_{j_1}, x_{j_1+1}]$, the $u^{n+1}_{j_1}$ and $u^{n+1}_{j_1+1}$ still given by (2.3) and (2.4) respectively. Bearing in mind (4.5) and that the extrapolation is of zero order, we have:

$$u^{n+1}_{j_1} = u^n_{j_1} - C^{n,-}_{j_1-\frac{1}{2},l} \Delta_{j_1-\frac{1}{2}} u$$
$$u^{n+1}_{j_1+1} = u^n_{j_1+1} + C^{n,+}_{j_1+\frac{3}{2},r} \Delta^n_{j_1+\frac{3}{2}} u \,. \qquad (4.11)$$

Hence,

$$\Delta^{n+1}_{j_1-\frac{1}{2}} u = (1 - C^{n,+}_{j_1-\frac{1}{2},l} - C^{n,-}_{j_1-\frac{1}{2},l}) \Delta^n_{j_1-\frac{1}{2}} u + C^{n,-}_{j_1-\frac{3}{2},l} \Delta^n_{j_1-\frac{3}{2}} u$$
$$\Delta^{n+1}_{j_1+\frac{1}{2}} u = \Delta^n_{j_1+\frac{1}{2}} u + C^{n,-}_{j_1+\frac{3}{2},r} \Delta^n_{j_1+\frac{3}{2}} u + C^{n,-}_{j_1-\frac{1}{2},l} \Delta^n_{j_1-\frac{1}{2}} u \qquad (4.12)$$
$$\Delta^{n+1}_{j_1+\frac{3}{2}} u = C^{n,+}_{j_1+\frac{5}{2},r} \Delta^n_{j_1+\frac{5}{2}} u + (1 - C^{n,+}_{j_1+\frac{3}{2},r} - C^{n,-}_{j_1+\frac{3}{2},r}) \Delta^n_{j_1+\frac{3}{2}} u \,.$$

When the jump moves one cell to the right, correspondingly we have

$$\begin{aligned} u_{j_1}^{n+1} &= u_{j_1}^n - C^{n,-}_{j_1-\frac{1}{2},l}\Delta^n_{j_1-\frac{1}{2}}u \\ u_{j_1+1}^{n+1} &= u_{j_1}^n \end{aligned} \tag{4.13}$$

and

$$\begin{aligned} \Delta^n_{j_1-\frac{1}{2}}u &= (1 - C^{n,+}_{j_1-\frac{1}{2},l} - C^{n,-}_{j_1-\frac{1}{2},l})\Delta^n_{j_1-\frac{1}{2}}u + C^{n,-}_{j_1-\frac{3}{2},l}\Delta^n_{j_1-\frac{3}{2}}u \\ \Delta^{n+1}_{j_1+\frac{1}{2}}u &= C^{n,-}_{j_1-\frac{1}{2},l}\Delta^n_{j_1-\frac{1}{2}}u \\ \Delta^{n+1}_{j_1+\frac{3}{2}} &= C^{n,+}_{j_1+\frac{5}{2},r}\Delta^n_{j_1+\frac{5}{2}}u + (1 - C^{n,+}_{j_1+\frac{3}{2},r})\Delta^n_{j_1+\frac{3}{2}}u + \Delta^n_{j_1+\frac{1}{2}}u \ . \end{aligned} \tag{4.14}$$

However, both (4.13) and (4.14) with (4.7) and (4.8) lead to (4.6), and the proof is complete.

When the order of extrapolation is higher than zero, (4.11) and (4.13) should be replaced by

$$\begin{aligned} u_{j_1}^{n+1} &= u_{j_1}^n + C^{n,+}_{j_1+\frac{1}{2},l}\Delta^n_{j_1+\frac{1}{2},l}u - C^{n,-}_{j_1-\frac{1}{2},l}\Delta^n_{j_1-\frac{1}{2}}u \\ u_{j_1+1}^{n+1} &= u_{j_1+1}^n + C^{n,+}_{j_1+\frac{3}{2},r}\Delta^n_{j_1+\frac{3}{2}}u - C^{n,-}_{j_1+\frac{1}{2}}\Delta^n_{j_1+\frac{1}{2},r}u \end{aligned} \tag{4.15}$$

and

$$\begin{aligned} u_{j_1}^{n+1} &= u_{j_1}^n + C^{n,+}_{j_1+\frac{1}{2},l}\Delta^n_{j_1+\frac{1}{2},l}u - C^{n,-}_{j_1-\frac{1}{2},l}\Delta^n_{j_1-\frac{1}{2}}u \\ u_{j_1+1}^{n+1} &= u_{j_1}^n + (u_{j_1+1}^{n,-} - u_{j_1}^n) + C^{n,+}_{j_1+\frac{3}{2},l}\Delta^n_{j_1+\frac{3}{2},l}u - C^{n,-}_{j_1+\frac{1}{2},l}\Delta^n_{j_1+\frac{1}{2},l}u \end{aligned} \tag{4.16}$$

Where

$$\begin{aligned} \Delta^n_{j_1+\frac{3}{2},l}u &= u_{j_1+2}^{n,-} - u_{j_1+1}^{n,-} \\ \Delta^n_{j_1+\frac{1}{2},l}u &= u_{j_1+1}^{n,-} - u_{j_1}^n \\ \Delta^n_{j_1+\frac{1}{2},r}u &= u_{j_1+1}^n - u_{j_1}^{n,+} \end{aligned} \tag{4.17}$$

It is possible that the appearance of the terms in (4.17) could kill the TVD property in the vicinity of the generated interval. However, these terms are only of $O(h)$ by the assumption that the numerical solution is "smooth" on each side of the discontinuity. Hence the error caused by them is also of $O(h)$ on each time level. Therefore, the total variation of the numerical solution will be bounded if there is only a single (or a finite number of discontinuities without interactions) in the problem.

The cases with interactions of generated intervals remain to be studied, and it is possible that the treatment in that cases will also not cause much damage to the TVD property.

If the difference scheme is conservative, the uniform bounded variation of the numerical solution guarantees the existence of a subsequence of the numerical solutions which converges to a weak solution. If the entropy condition is satisfied, the uniqueness of the weak solution and then the convergence of the scheme will follow. In the present case, due to the introduction of q_j^n, which makes the scheme not conservative at some points, the boundedness of total variation is not enough for obtaining a convergent sequence of the numerical solutions. However, according to (2.14), it suffices to require the uniform boundedness of q_j^n in addition to the uniform boundedness of the total variation.

According to (2.11) and (2.13), when the extrapolation is of zero order, $q_{j_1}^{n+1}$ in the first case and $q_{j_1+1}^{n+1}$ in the second case are given by

$$q_{j_1}^{n+1} = q_{j_1}^n + \lambda(f(u_{j_1+1}^n) - f(u_{j_1}^n)) \tag{4.18}$$

and

$$q_{j_1+1}^{n+1} = q_{j_1}^n + (u_{j_1}^n - u_{j_1+1}^n) + \lambda(\hat{f}^{n,+}_{j_1+\frac{3}{2}} - f(u_{j_1}^n)) \tag{4.19}$$

respectively. Because $s = (f(u_{j_1+1}^n) - f(u_{j_1}^n))/(u_{j_1+1}^n - u_{j_1}^n))$, and $u_{j_1}^n - u_{j_1+1}^n$ are supposed to be positive, so $f(u_{j_1+1}^n) - f(u_{j_1})$ is negative. If $(u_{j_1}^n - u_{j_1+1}^n) + \lambda(\hat{f}^{n,+}_{j_1+\frac{3}{2}} - f(u_{j_1}^n))$ is

positive, then since our treatment picks up the smaller one of the $|q_{j_1}^{n+1}|$ and $|q_{j_1+1}^{n+1}|$, it automatically keep this artificial term uniformly bounded with respect to n. Since $u_{j_1}^n - u_{j_1+1}^n > 0$, the positiveness of the term $u_{j_1}^n - u_{j_1+1}^n + \lambda(\hat{f}_{j_1+\frac{3}{2}}^{n,+} - f(u_{j_1}^n))$ always can be achieved by placing a limitation on λ. In fact

$$\begin{aligned} & u_{j_1}^n - u_{j_1+1}^n + \lambda(\hat{f}_{j_1+\frac{3}{2}}^{n,+} - f(u_{j_1}^n)) \\ & = u_{j_1}^n - u_{j_1+1}^n + \lambda(f(u_{j_1+1}^n) - f(u_{j_1}^n)) - C_{j_1+\frac{3}{2}}^{n,+} \Delta_{j_1+\frac{3}{2}}^n u \end{aligned} \tag{4.20}$$

The last term in (4.20) is of $O(h)$, so the limitation is close to the CFL-condition. If we replace the original selection by choosing the case which corresponds to the smaller one between $|q_{j_1}^{n+1}|$ and $|q_{j_1}^n + u_{j_1}^n - u_{j_1+1}^n + \lambda(f(u_{j_1+1}^n) - f(u_{j_1}^n))|$ (rather than $|q_{j_1}^{n+1}|$), we will have the following inequality as the criterion of selection

$$q_{j_1+1}^n \le \frac{1}{2}(u_{j_1+1}^n - u_{j_1}^n) + \lambda(f(u_{j_1+1}^n) - f(u_{j_1}^n)). \tag{4.21}$$

If it is true, the jump moves one cell to the right, otherwise the jump remains in the original cell. This is the criterion suggested in [11]. The numerical experiments shows that it also works quite well.

If the extrapolation is of the order high than zero, according to (2.11) and (2.13)

$$q_{j_1}^{n+1} = q_{j_1}^n - C_{j_1+\frac{1}{2},r}^{n,-} \Delta_{j_1+\frac{1}{2},r}^n u + \lambda(f(u_{j_1+1}^n) - f(u_{j_1}^n)) + C_{j_1+\frac{1}{2},l}^{n,+} \Delta_{j_1+\frac{1}{2},l}^{n,+} u \tag{4.22}$$

$$\begin{aligned} q_{j_1+1}^{n+1} &= q_{j_1}^n + u_{j_1}^n - u_{j_1+1}^n + \lambda(\hat{f}_{j_1+\frac{3}{2}}^{n,+} - f(u_{j_1}^n)) \\ &+ (u_{j_1+1}^{n,-} - u_{j_1}^n) - C_{j_1+\frac{3}{2}}^{n,-} \Delta_{j_1+\frac{3}{2},l}^n u + \lambda(f(u_{j_1+1}^{n,-}) - f(u_{j_1}^n)) \end{aligned} \tag{4.23}$$

Obviously, all the extra terms in (4.22)and (4.23) are of $O(h)$. Therefore, the above discussion still hold if $u_{j_1}^n - u_{j_1+1}^n$ is big enough.

5. Application of the Treatment to the Euler Equations of Gas Dynamics

In this section, we describe how to apply this treatment to the Euler equations of gas dynamics for a polytropic gas:

$$u_t + f(u)_x = 0 \tag{5.1a}$$

$$u = (\rho, m, E)^T \tag{5.1b}$$

$$f(u) = qu + (0, p, qp)^T \tag{5.1c}$$

$$p = (\gamma-1)(E - \frac{1}{2}pq^2) \tag{5.1d}$$

Here ρ, q, p, and E are the density, velocity, pressure and total energy, respectively; $m = \rho q$ is the momentum and γ is the ratio of specific heats.

The eigenvalues of the Jacobian matrix $A(u) = \partial f / \partial u$ are:

$$a_1(u) = q - u, \quad a_2(u) = q, \quad a_3(u) = q + u \tag{5.2}$$

where $c = (\gamma p / \rho)^{\frac{1}{2}}$ is the sound speed.

In [1], Harten applied his "subcell resolution" only to the linear degenerate characteristic field, i.e. he did a (linear) field-by-field decomposition and then applied the technique to the second locally defined characteristic variable only. In this paper we are going to apply our treatment to all the different kinds of discontinuities in a nonlinear way. However, in the present work we only use this treatment as a tracking technique to track the discontinuities for the system case. Correspondingly, all the numerical examples for the Euler system reported in the next section are of the piecewise smooth solution with a finite number of discontinuities. No spontaneous shock is involved.

Only $x-t$ version is under concern.

We begin with a simple case that contains only one discontinuity, the numerical solution on each side of which is smooth. As is well known there are three different kinds of

discontinuities in the Euler system: the left shock, the right shock, and the contact discontinuity. Therefore, the generated intervals should also be classified into three different kinds: the left shock generated interval (LSGI), the right shock generated interval (RSGI), and the contact discontinuity generated interval (CDGI). Each of them can be identified by solving the $RP(u_{j_1}^n, u_{j_1+1}^n)$ (the Riemann problem which has $u_{j_1}^n$ and $u_{j_1+1}^n$ as its left and right states). Here $[x_{j_1}, x_{j_1+1}]$ is the corresponding generated interval. The solution to the $RP(u_{j_1}^n, u_{j_1+1}^n)$ in an LSGI or an RSGI should have a relatively strong left or right shock, while the solution to the $RP(u_{j_1}^n, u_{j_1+1}^n)$ in a CDGI should have a relatively strong contact discontinuity.

Suppose $[x_{j_1}, x_{j_1+1}]$ is the generated interval on the level n. At first, we extrapolate the numerical solution from one side of the generated interval to the other side. The extrapolation values are $u_{j_1-k}^{n,+}$, $u_{j_1-k+1}^{n,+}$, ..., $u_{j_1}^{n,+}$, $u_{j_1+1}^{n,-}$, $u_{j_1+2}^{n,-}$, ..., $u_{j_1+k+1}^{n,-}$. In the system case, if we use (2.3) - (2.8) to compute the numerical solution, the treatment will affect the other fields. Therefore, we revise our algorithm. Suppose $[x_{j_1}, x_{j_1+1}]$ is an LSGI. We solve the Riemann problem $RP(u_{j_1-i}^n, u_{j_1-i}^{n,+})$ $(i = 0, ..., k)$, and get a set of left middle states $u_{j_1-i,*}^{n,l}$ $(i = 0, \ldots, k)$ (as shown in Fig. 5.1). Then in the computation we replace the $u_{j_1-i}^{n,+}$ in (2.3) - (2.8) by these left middle states. If $[x_{j_1}, x_{j_1+1}]$ is a RSGI, we solve the Riemann problem $RP(u_{j_1+i}^{n,-}, u_{j_1+i}^n)$ $(i = 1, ..., k+1)$, and replace the $u_{j_1+i}^{n,-}$ in (2.3) - (2.8) by the corresponding right middle states $u_{j_1+i,*}^{n,r}$.

It is not difficult to see that if the original system is a linear constant coefficient system such a handling is equivalent to applying the treatment in a field-by-field way. That is doing the field-by-field decomposition at first, and then applying the treatment to each characteristic variable. But in the nonlinear case (such as Euler system) they are different, especially when strong discontinuities are involved. We believe that the present one is more precise, for it seems as involving a "nonlinear" field-by-field decomposition.

Accordingly, the treatment to the CDGI should be as follows: Solve the Riemann problem $RP(u_{j_1-i}^n, u_{j_1-i}^{n,+})$ and get the left middle states $u_{j_1-i,*}^{n,l}$ $(i = 0, \cdots, k)$, solve the Riemann problems $RP(u_{j_1+i}^{n,-}, u_{j_1+i}^n)$ and get the right middle states $u_{j_1+i,*}^{n,r}$ $(i = 1, ..., k+1)$,

and then in the computation we replace $u_{j_1-i}^{n,+}$ by $u_{j_1-i,*}^{n,l}$, and $u_{j_1+i}^{n,-}$ by $u_{j_1+i,*}^{n,r}$ in (2.3) - (2.8). However, the practical treatment used in this work is simpler than the above. For the contact discontinuity, the density is discontinuous, but the velocity and the pressure are still continuous. Therefore, in the computation we only extrapolate ρ, and take the original values of the numerical solution for the velocity q and the pressure p. The examples presented in Section 6 shows that such a treatment works well.

The moving of the generated interval is still controlled by keeping $|q_{j_1}^n|$ small, here $q_{j_1}^n$ is the artificial terms along t direction. Because the $q_{j_1}^n$ is a vector with three components now, $|q_{j_1}^n|$ should be some norm of $q_{j_1}^n$. For example, a natural candidate would be

$$|q_{j_1}^n| = \sum_{l=1}^{3} |q_{j_1}^{n,(l)}| \tag{5.3}$$

where $q_{j_1}^{n,(l)}$ is a component of $q_{j_1}^n$. However, the three components of the system (5.1) may have quite different scales, hence the presently used $|q_{j_1}^n|$ in this paper is

$$|q_{j_1}^n| = \sum_{l=1}^{3} |q_{j_1}^{n,(l)}/(u_{j_1}^{n,(l)} - u_{j_1+1}^{n,(l)})| \tag{5.4}$$

Here $u_j^{n,(l)}$ is the component of u_j^n.

Sometimes the solution to the Riemann problem $RP(u_{j_1}^n, u_{j_1+1}^n)$ may have more than one strong discontinuity. This situation occurs very often when two generated intervals of different kinds collide with each other. We refer to this kind of generated intervals as the nodes. A typical case is that the $RP(u_{j_1}^n, u_{j_1+1}^n)$ contains precisely a left and a right shock with a middle state u_*. The main idea in treating these cases is the consideration that we have more than one different, overlapped generated intervals in $[x_{j_1}, x_{j_1+1}]$, and the treatment should be precisely applied to each of them. Let's use the above typical case to describe the algorithm.

Suppose the generated interval is $[x_{j_1}, x_{j_1+1}]$. In the vicinity of this generated interval we introduce two auxiliary initial value problems. The initial value of the first problem has the left

part of the u^n as its left part, and the middle state u_* as its right part, with an LSGI $[x_{j_1}^n, x_{j_1+1}^n]$. The initial value of the second problem has the right part of the u^n as its right part, and the middle state u_* as its left part, with an RSGI $[x_{j_1}, x_{j_1+1}]$. However, the computation of these two problems are only run in the background, and the results are only used as information to direct the moving of the two generated intervals. In the numerical solution, the computation is still performed just as only a single generated interval exists. The two different generated intervals are located in the same cell for the first several time-steps until they separate, and then the middle state appears between them.

It is also not difficult to show that if the original system is a linear constant coefficient system, such a handling is equivalent to applying the treatment in a field-by-field way.

The more complicated cases of nodes, such as that the $RP(u_{j_1}^n, u_{j_1+1}^n)$'s involve three different discontinuities, can be treated in a similar way.

6. Numerical Experiments

In this section we present some results to show the performance of our treatment.

EXAMPLE 1. This is a repetition of the Example 2. in [11]. We solve the following initial value problem

$$\begin{aligned} &u_t + (\frac{u^2}{2})_x = 0 \qquad -1 \le x \le 1 \\ &u(x,0) = \frac{1}{4} + \frac{1}{2}\sin\pi x \end{aligned} \tag{6.1}$$

The exact solution is smooth up to $t = \frac{2}{\pi}$, then it develops a moving shock which interacts with the rarefaction waves. We get the exact solution by using a Newton iteration. For details, see [4].

The Lax-Friedrichs (LF) scheme, Lax-Wendroff (LW) scheme, and Majda-Osher (MO) scheme (see [14]) are chosen to be the basic schemes. The LF scheme only has first order accuracy, the LW scheme produces spurious oscillations near the shocks, and the MO scheme smear the shock too much (usually about 4 to 5 transition point).

We take $\lambda = 0.5$ and the parameter $\alpha = 0.1$. The latter is used in the formation of the generated intervals. Only the results of the LW scheme is presented here. For results of the LF and MO schemes see [11].

In Fig. 6.1-a and 6.1-b we show the numerical solution of $\Delta x = \frac{1}{10}$ computed with the zero order x version and $x-t$ version treatment respectively, where t is taken to be 0.5, 0.65, and 1.1. In Fig. 6.2-a and 6.2-b we show the corresponding results for $\Delta x = \frac{1}{40}$.

The results of the LW scheme have a very good resolution to the exact solution in both smooth and nonsmooth parts. In all these examples, the numerical shock (or shocks) develops before $t = \frac{2}{\pi}$, and in some cases the treatment of interactions of generated intervals has been used. However, the effects of this treatment to the smooth part seem to creat little error to the experiment.

In the Table 6.1-a and 6.1-b we make the comparisons of the locations between the numerical and exact shocks. The former is obtained by the high resolution technique described in Section 2. Table 6.1-a displays the results of the x version with $\Delta x = \frac{1}{10}$ from the 14th to 22th time-step, and Table 6.1-b displays the results of the $x-t$ version with $\Delta x = \frac{1}{40}$ from the 52th to 88th time-step. Clearly, we have very accurate shock locations in both examples. Usually, the $x-t$ version has no shock transition point, but the x version has one shock transition point. Hence, the $x-t$ version generally has the higher resolution for shock than the x version does. In addition, we found in the experiment that the $x-t$ version is easier to program than the x version, especially in dealing with the interactions of generated intervals.

We also did the numerical experiments for higher order treatments. The results of them are similar to that of the zero order, and occasionally the result of zero order treatment is even a little better than that of the high order ones. According to Remark 2.2, the zero order treatment causes an $O(1)\, L^\infty$ truncation error, hence it kills the consistency at the corresponding points. However, shock has a self-sharpening mechanism due to the converging characteristics. It strongly prevent this $O(1)$ error to be transported to the smooth region. That is why the zero order treatment causes little error to the smooth part.

EXAMPLE 2. This is the example 3. in [11] revisited. We use the following linear IVP to test our $x-t$ version treatment

$$u_t + u_x = 0 \tag{6.2a}$$

$$u_0(x+0.5) = \begin{cases} -x\sin(\frac{3}{2}\pi x^2) & -1 < x < -\frac{1}{3} \\ |\sin(2\pi x)| & |x| < \frac{1}{3} \\ 2x - 1 - \sin(3\pi x)/6 & \frac{1}{3} < x < 1 \end{cases} \tag{6.2b}$$

$$u_0(x+2) = u_0(x) \tag{6.2c}$$

Lax-Wendroff scheme is chosen to be the basic scheme, and we let $\Delta x = \frac{1}{30}$, $\lambda = 0.8$. The solution to this IVP involves three contact discontinuities and one weak discontinuity (i.e. its derivative is discontinuous). In Fig. 6.3-a we present the numerical results without treatment at $t = 2$ and $t = 8$. The poor resolution is almost unacceptable.

At first the treatment is applied to the contact discontinuities only. In Fig. 6.3-b to Fig. 6.3-d we display the results with the zero order, the first order, and the second order treatment respectively. Obviously, the higher the order of the treatment is, the better the resolution. Due to the lack of converging characteristics, the numerical results are somewhat sensitive to the order of the treatment.

However, the figures show that the weak discontinuities also causes trouble to the computations. Supposing that the idea of preventing the computation from crossing the discontinuity applies to the weak discontinuity, we naively use the treatment to the weak one. The corresponding result is displayed in Fig. 6.3-e. It is much better than any previous one. In Fig. 6.4 we display the result of the second order treatment with $\Delta x = \frac{1}{60}$. It can be seen that the numerical solutions at both $t = 2$ and $t = 8$ very close to the exact solution (the corresponding result without the treatment, which we have omitted in order to save space, is as poor as that displayed in Fig. 6.3-a in quality).

In order to test the long-term preformance of the treatment, we computed the numerical solution at $t = 16, 32, 64$ (4800 time-steps) respectively. The results are also presented in Fig. 6.4. These results show that the long-term performance of the treatment is still good. Particularly at $t = 64$, except the second one, the discontinuities have very good resolution, even though the smooth part of the numerical solution has been seriously damped by the Lax-Wendroff scheme.

In all the examples with the second order treatment, the second discontinuity still has some problem. There is some "sinking" on its right side, and seemingly, it is just this "sinking" that causes the deviation of the discontinuity location. The possible cause of this "sinking" might be the "wrong up-wind computation" at the right endpoint of the generated interval. An

appropriate evaluation of u_j^n at each point should mainly use the information from the left side due to the positive speed of wave propagation. But at that endpoint, the use of the extrapolation values makes the computation essentially get the information from the right side. However, it seems that the " wrong up-wind computation" does not always affect the computation. The numerical experiment shows that sometime it does and sometime it does not. The problem is not clear yet and is expected to be studied.

In the following examples for the Euler system, we use the treatment as a tracking technique to track the discontinuities, and choose the Lax-Wendroff scheme as the basic scheme. The treatment is of the second order and $\gamma = 1.4$ is used.

EXAMPLE 3. We apply our treatment to the Riemann problems for the Euler equations of gas dynamics (5.1) with following two sets of initial condition known as the Sod problem and the Lax Problem respectively:

$$\begin{aligned} (\rho_l, q_l, p_l) &= (1., 0., 1.) \\ (\rho_r, q_r, p_r) &= (0.125, 0., 0.1) \end{aligned} \tag{6.3}$$

and

$$\begin{aligned} (\rho_l, q_l, p_l) &= (0.445, 0.698, 3.528) \\ (\rho_r, q_r, p_r) &= (0.5, 0., 0.571) \end{aligned} \tag{6.4}$$

Both problems have a left rarefaction wave, a right shock, and a contact discontinuity. The treatment of node works in the first several time-steps. Inspired by the Example 2., in which the treatment is also applied to the weak discontinuity, we are going to apply this treatment to the edges of the rarefaction wave. However, the naive application is unacceptable. If we did so, we could get a rarefaction shock. The solution is as follows: Suppose that we are now dealing with the back edge of the left rarefaction. Because the basic scheme is a 3-point scheme, the extrapolation values used on each side of the generated interval are only $u_{j_1}^{n,+}$ and $u_{j_1+1}^{n,-}$. In order to expand the rarefaction wave we replace the $u_{j_1+1}^{n,-}$ by the original data $u_{j_1+1}^n$. The back edge of the right rarefaction wave can be treated in a similar way. But the locations of the

edge of the right rarefaction wave can be treated in a similar way. But the locations of the back edges captured by this technique are not very accurate. Moreover, the analogue treatment to the front edge of the rarefaction wave fails to capture the weak discontinuities (it almost disappears after several time-steps). However, this technique still can be used to expand the rarefaction wave near its center without oscillations. The more proper treatment to the rarefaction wave is under investigation.

For the Sod problem we use $\Delta x = 0.01$ and $CFL = 0.4$. The numerical result is displayed in Fig. 6.5-a. There are some oscillation in the smooth region. We assume that the oscillation is caused by the basic scheme itself and add a second order viscosity term introduced in [4] to the smooth part, which eliminate the oscillation. The corresponding numerical result is displayed in Fig. 6.5-b.

For the Lax problem, we use $\Delta x = 0.01$ and $CFL = 0.8$. The numerical result is displayed in Fig. 6.6. No oscillation occurs in this experiment.

EXAMPLE 4. (The blast waves problem). Here we consider the Euler system with following initial condition

$$u_0 = \begin{cases} u_l & 0. \le x < 0.1 \\ u_m & 0.1 \le x < 0.9 \\ u_r & 0.9 \le x \le 1. \end{cases} \tag{6.5}$$

where

$$\begin{aligned} \rho_l = \rho_m = \rho_r = 1., \quad q_l = q_m = q_r = 0. \\ p_l = 10^3, \quad p_m = 10^{-2}, \quad p_r = 10^2 \end{aligned} \tag{6.6}$$

and the two boundaries are assumed to be solid walls. See [15] for the details of the solution and the comparison of the performance of various schemes.

We take $\Delta x = 0.005$, $CFL = 0.7$. The numerical solution at $t =$ 0.010, 0.016, 0.026, 0.028, 0.030, 0.032, 0.034 and 0.038 are presented in Fig. 6.7-a to 6.7-h. The solid lines in these figures are the numerical solutions of 4th-order ENO scheme with 800 space points, and

is considered here as a "converged solution".

At the time around $t = 0.032$ there is a rarefaction wave with two front edges (its right edge moves to the right), which is generated from the collision of a shock and a contact discontinuity. If we use the Lax-Wendroff scheme as the basic scheme, we will get a rarefaction shock due to the failure of the treatment to the weak discontinuities. In order to expand the rarefaction wave, we add a first order viscosity term to the basic scheme (hence it is still a 3-point scheme) and reduce the order of the treatment to the first order for 20 time-steps at that time. It creats some error to the smooth part, especially to the velocity. "Sinking" phenomenon is still seen in the left sides of some contact discontinuities, which is caused by the so called "wrong up-wind computation".

Acknowledgement

The author thanks Stanley Osher, Ami Harten, Chi-Wang Shu, Huanan Yang, and Emad Fatemi for helpful discussion and/ or for suggesting numerical examples, as well as correcting English errors in the manuscript.

Reference

[1] A. Harten; ENO Schemes with Subcell Resolution. ICASE Report 87-65 (August 1987).

[2] A. Harten; Preliminary Results on the Extension of ENO Schemes to Two-Dimensional Problems. in Proceedings of the International Conference on Hyperbolic Problems, Siant-Etienne, January 1986.

[3] A. Harten and S. Osher; Uniformly High-order Accurate Nonoscillatory Scheme I. SIAM J. Numer. Anal. Vol. 24 (1987) pp. 279-309.

[4] A. Harten, B. Engquist, S. Osher and Chakravarthy; Uniformly High Order Accurate Essentially Nonoscillatory Schemes III. J. Comput. Phys. Vol. 71 (1987), pp. 231-303.

[5] A. Harten; High resolution Scheme for Hyperbolic Conservation Laws. J. Comput. Phys. Vol. 49 (1983) pp. 357-393.

[7] C-W. Shu and S. Osher; Efficient Implementation of Essentially Nonoscillatory Shock Capturing Schemes. ICASE Report 87-33, J. Comput. Phys. to appear.

[8] C-W. Shu and S. Osher; Efficient Implementtation of Essentially Nonoscillatory Shock Capturing Schemes II. preprint.

[9] C. Shu; TVD Time Discretizations. UCLA Mathematics Department Report, Los Angeles, CA 90024 (May, 1986).

[10] Huanan Yang; An Artificial Compression Method for ENO Schemes. The Solp Modification Method. Preprint

[11] Mao De-Kang; A treatment of Discontinuities in Shock Capturing Finite Difference Methods. I. Single Conservation Laws. UCLA Report 88-32

[12] Mao De-kang; A Treatment of Discontinuity in Shock Capturing Finite Difference Methods I. UCLA CAM Report 88-08 March 1988

[13] Mao De-kang; A Finite Difference Scheme for Shock Calculation. J. Comput. Math. No. 3 (1985) pp. 256-282 (in Chinese).

[14] A. Majda and S Osher; Numerical Viscosity and the Entropy Condition. Comm. Pure Appl. Math. Vol. 32 (1979) pp. 797-838.

[15] P. Woodward and P. Collela; The Numerical Simulation of Two-dimensional fluid with stron shocks. J. Comp.Phys. Vol.54 (1984) pp.115-173

[16] I-L Chen, J. Glimm, O. McBryan, B. Plohr, and S. Yaniv; Front Tracking for Gas Dynamics. J. Comp. Physics. Vol. 62 (1986) pp. 83-110.

[17] R. Richtmyer and K. Morton; Difference Methods for Initial Value Problems. Interscience, New York, 1976.

[18] Wu Xiong Hua and Zhu You Lan; A Scheme of the Singularity- Separating Method for the Nonconvex Problem. Comput. & Fluid. Vol. 13, No. 4 (1985) pp. 473-484.

[19] E. Tadmor; Numerical Viscosity and Entropy Condition for Conservative Difference Schemes. Math. Comp. Vol. 43 (1984) pp. 369-381

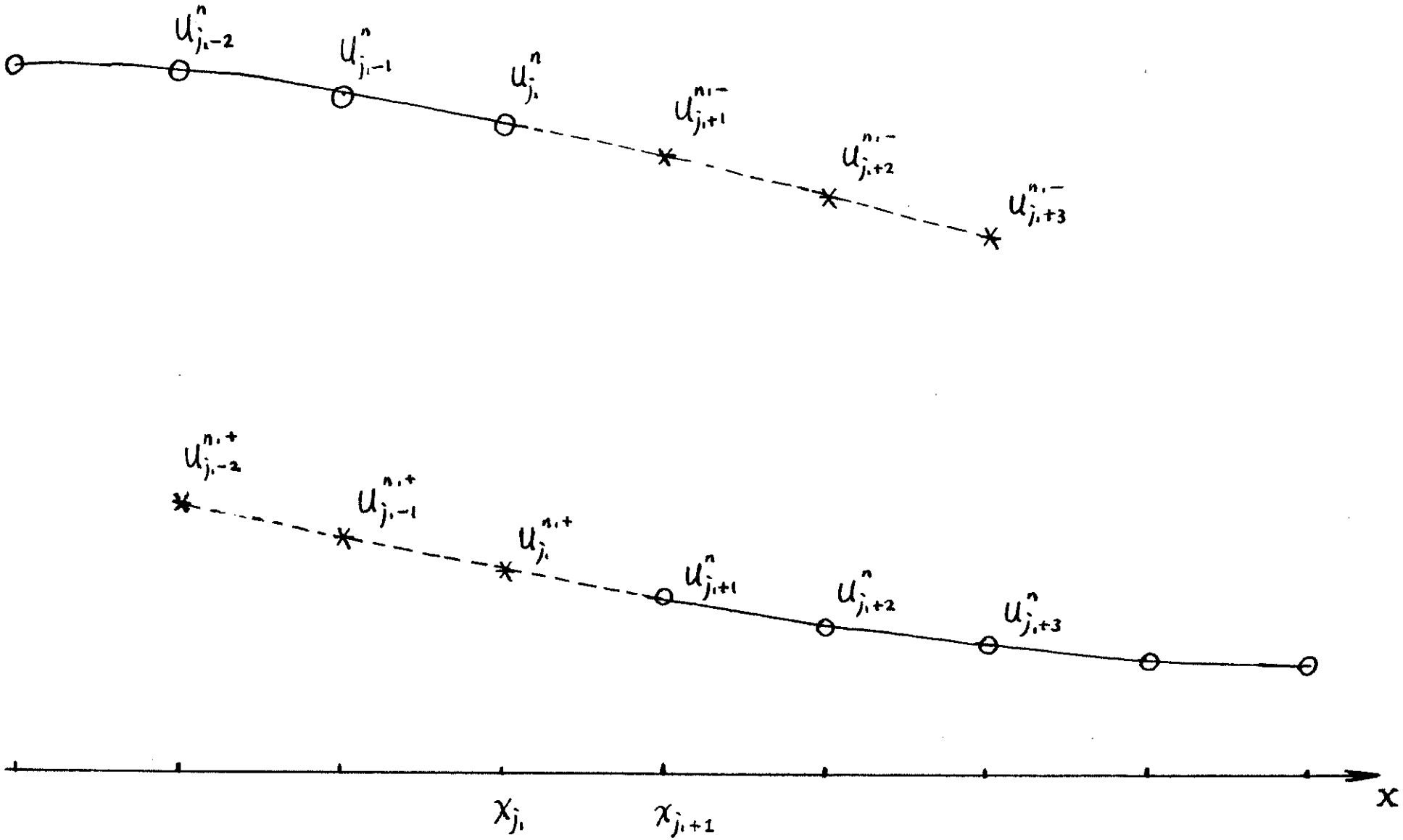
$u^n_{j_1-2}$
$u^n_{j_1-1}$
$u^n_{j_1}$
$u^{n,-}_{j_1+1}$
$u^{n,-}_{j_1+2}$
$u^{n,-}_{j_1+3}$
$u^{n,+}_{j_1-2}$
$u^{n,+}_{j_1-1}$
$u^{n,+}_{j_1}$
$u^n_{j_1+1}$
$u^n_{j_1+2}$
$u^n_{j_1+3}$
x
x_{j_1}
x_{j_1+1}

Fig. 2.1

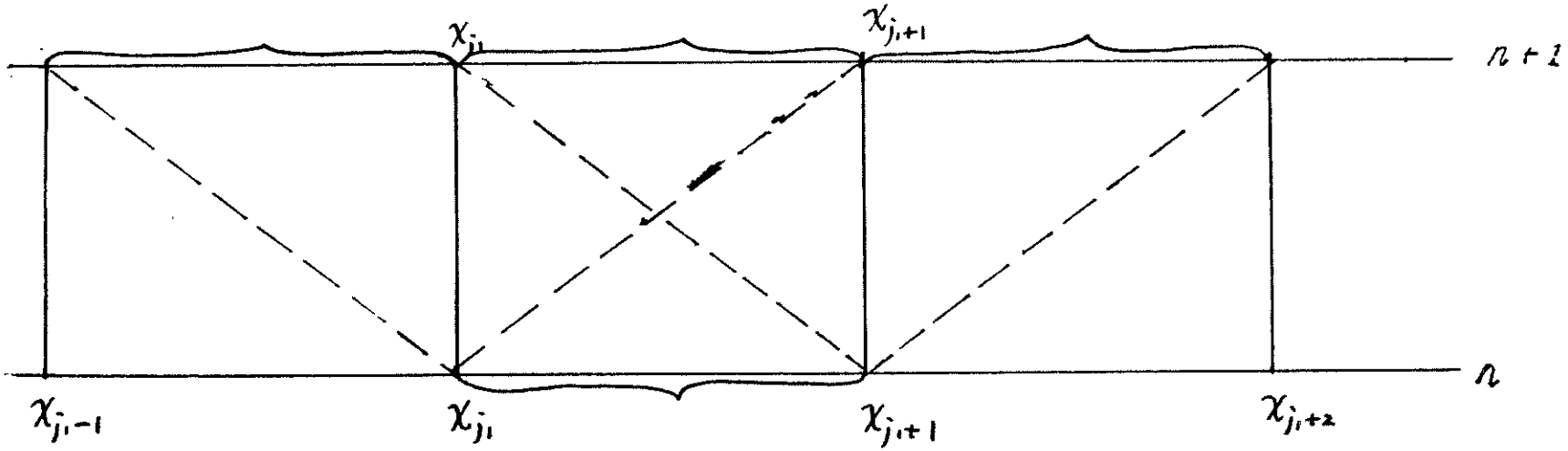

Fig. 2.2

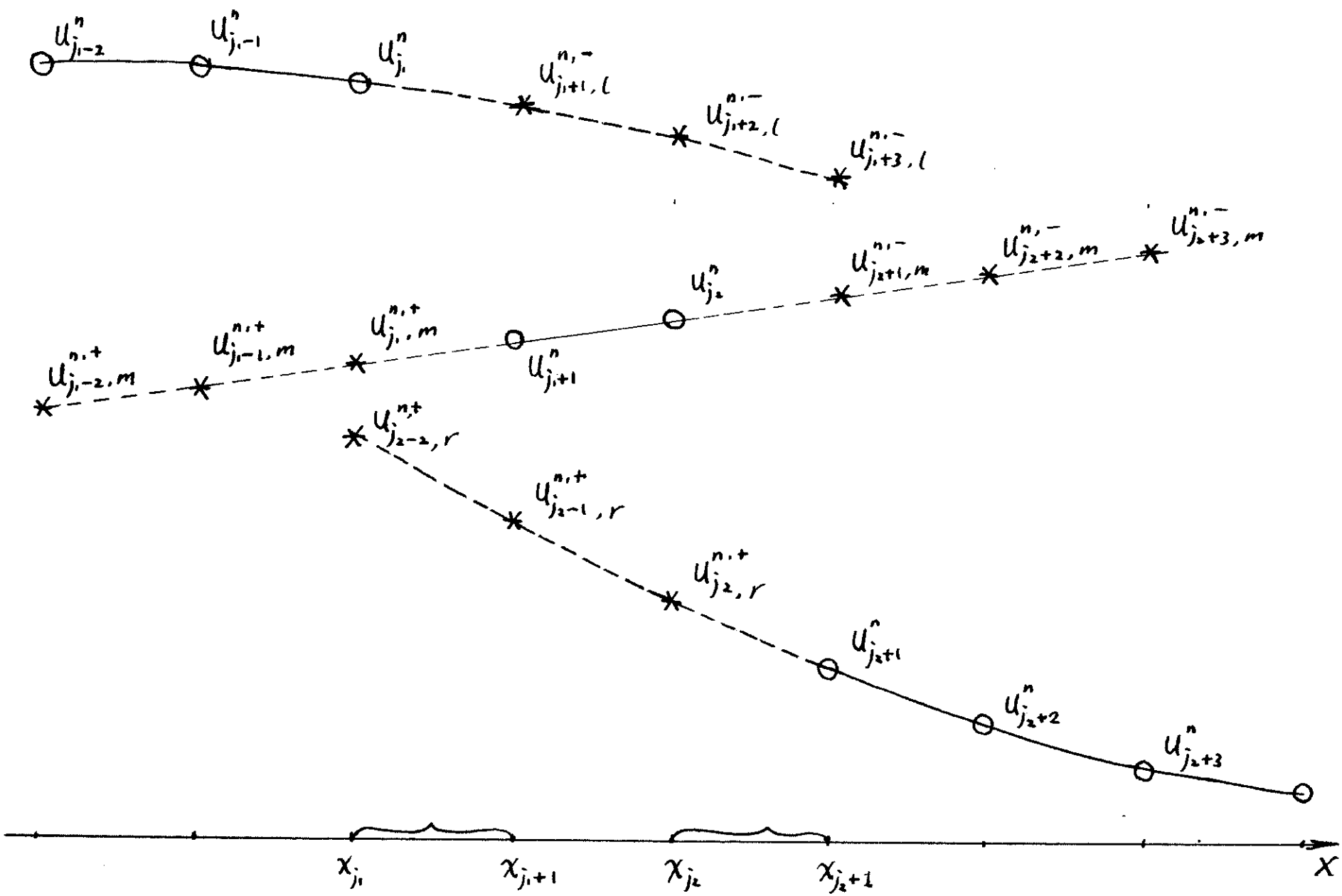
$u^n_{j_1-2}$
$u^n_{j_1-1}$
$u^n_{j_1}$
$u^{n,-}_{j_1+1,l}$
$u^{n,-}_{j_1+2,l}$
$u^{n,-}_{j_1+3,l}$
$u^{n,-}_{j_2+3,m}$
$u^{n,-}_{j_2+2,m}$
$u^{n,-}_{j_2+1,m}$
$u^n_{j_2}$
$u^{n,+}_{j_1,m}$
$u^{n,+}_{j_1-1,m}$
$u^{n,+}_{j_1-2,m}$
$u^n_{j_1+1}$
$u^{n,+}_{j_2-2,r}$
$u^{n,+}_{j_2-1,r}$
$u^{n,+}_{j_2,r}$
$u^n_{j_2+1}$
$u^n_{j_2+2}$
$u^n_{j_2+3}$
x_{j_1}
x_{j_1+1}
x_{j_2}
x_{j_2+1}
x

Fig. 3.1

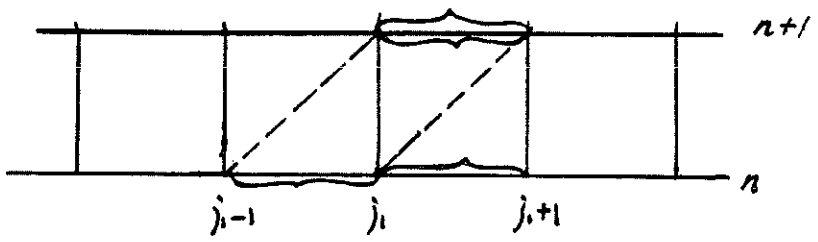

a.

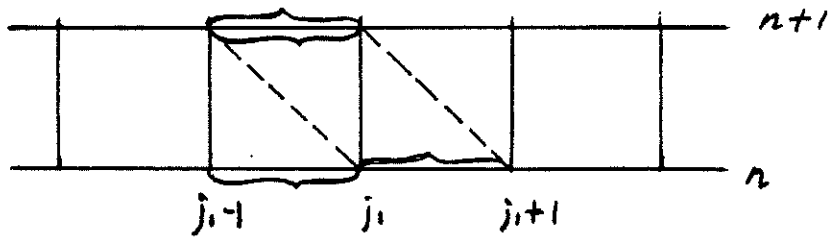

b.

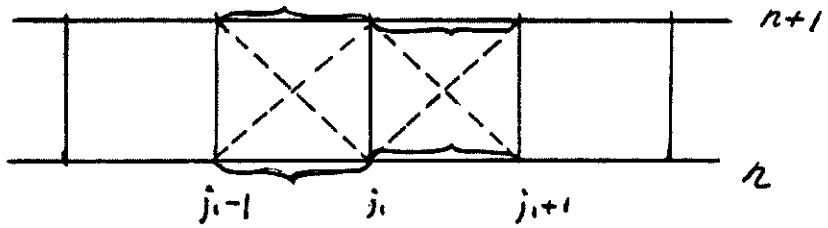

c.

Fig. 3.2

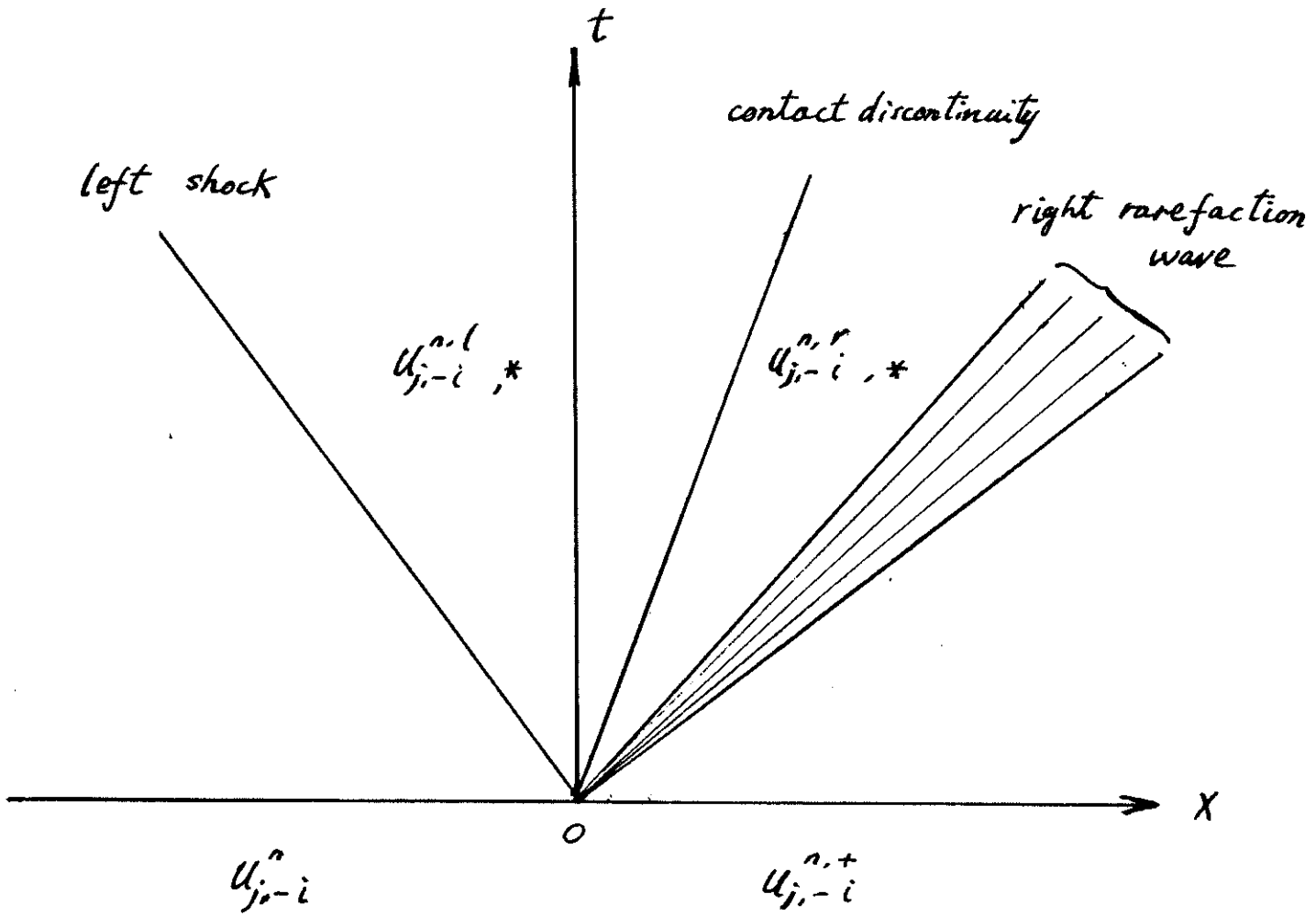
t
contact discontinuity
left shock
right rarefaction wave
$u^{n,l}_{j,-i}$,*
$u^{n,r}_{j,-i}$,*
X
0
$u^{n}_{j,-i}$
$u^{n,+}_{j,-i}$

Fig. 5.1

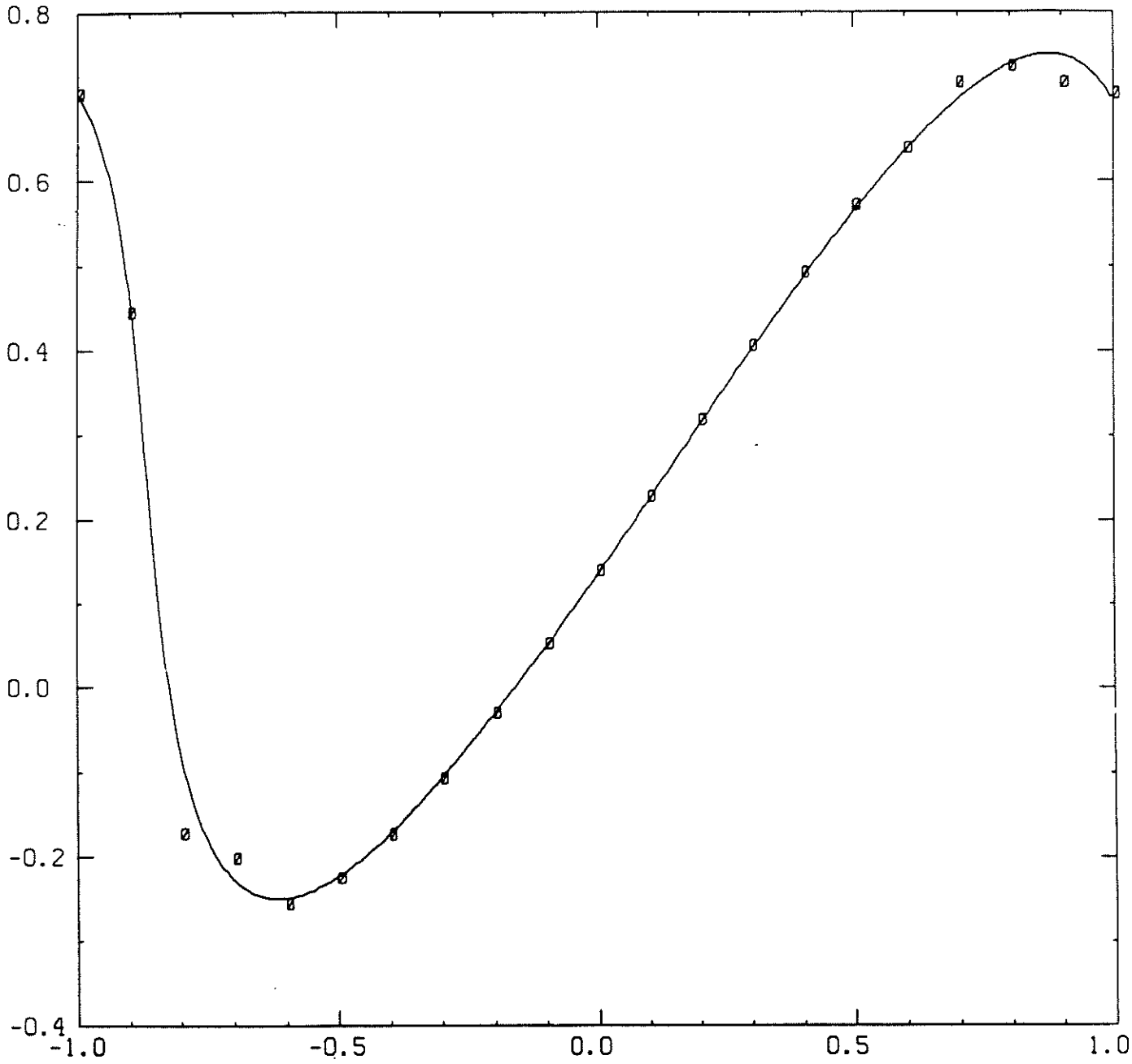

Figure 6.1-a

$T = 0.5$

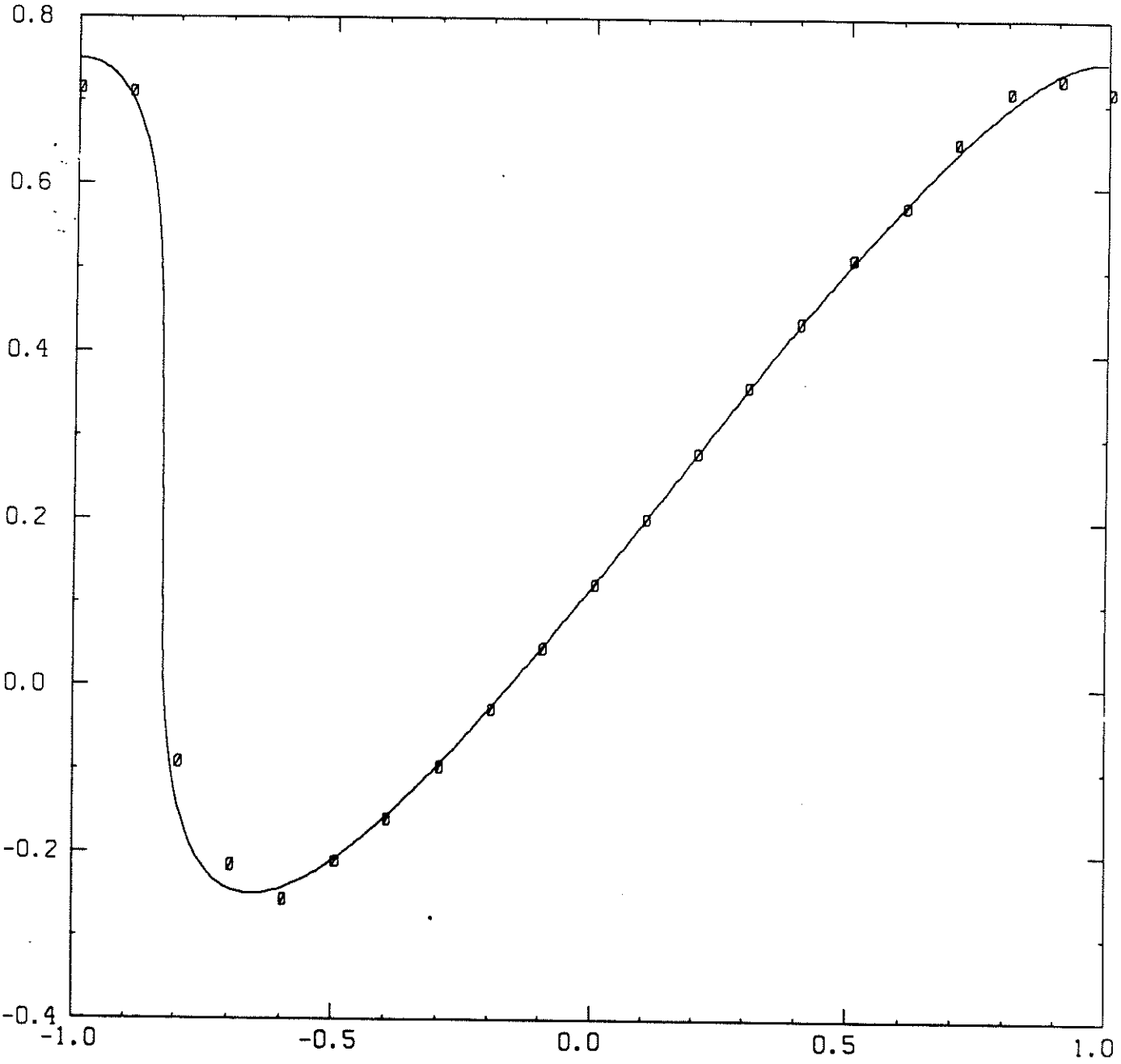

Figure 6.1-a

$T = 0.65$

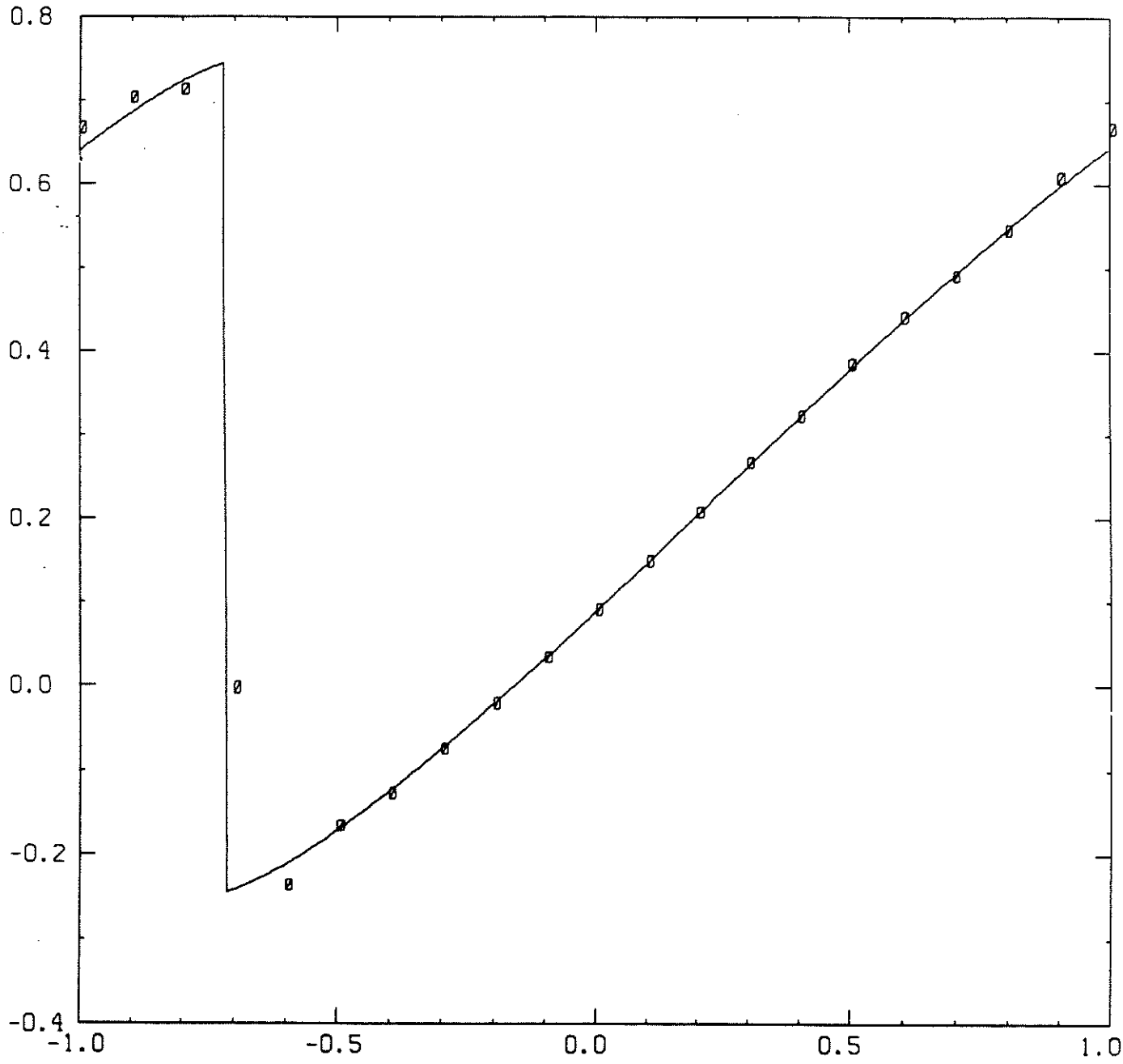

Figure 6.1-a

$T = 1.1$

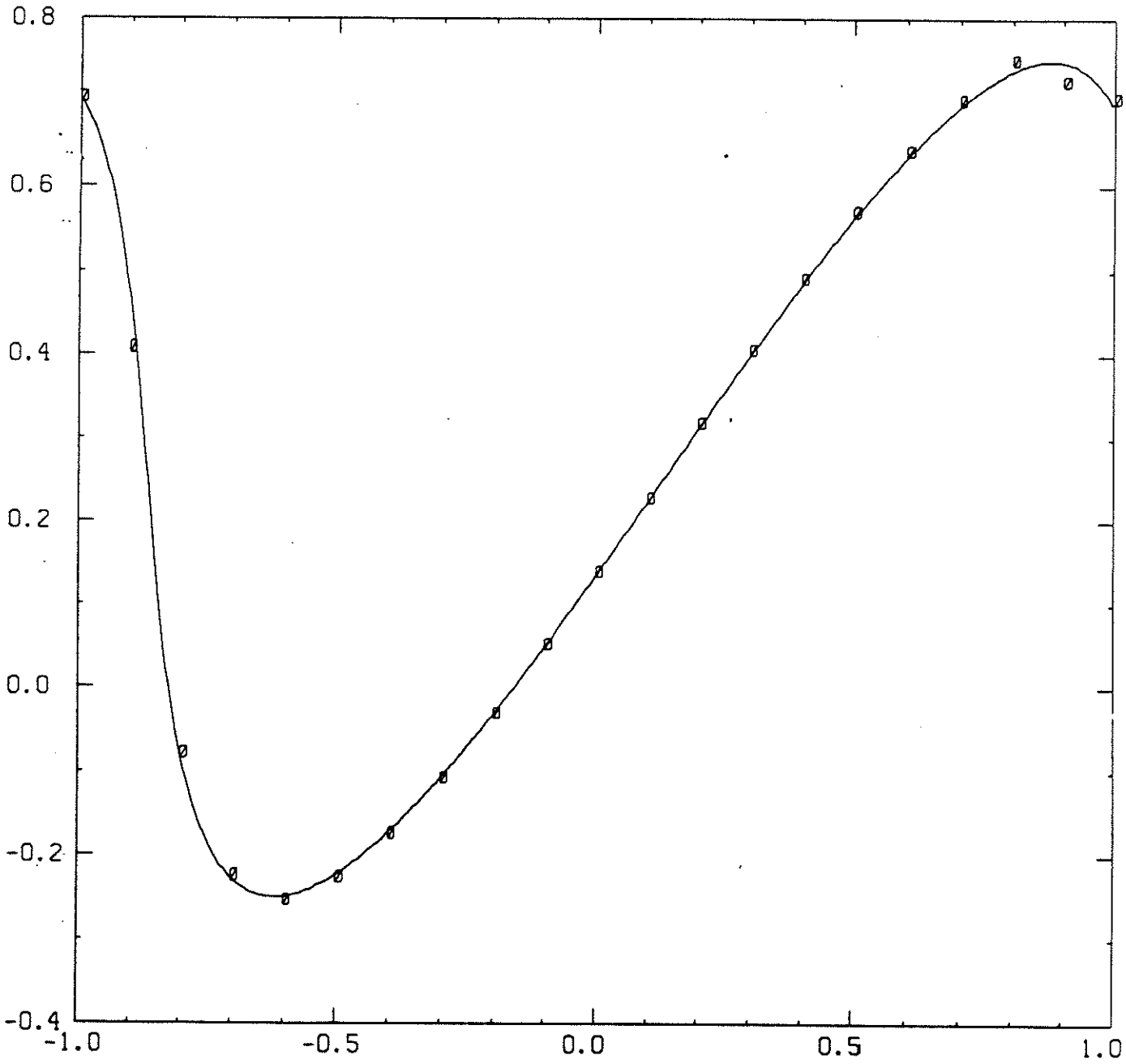

Figure 6.1 - b

$T = 0.5$

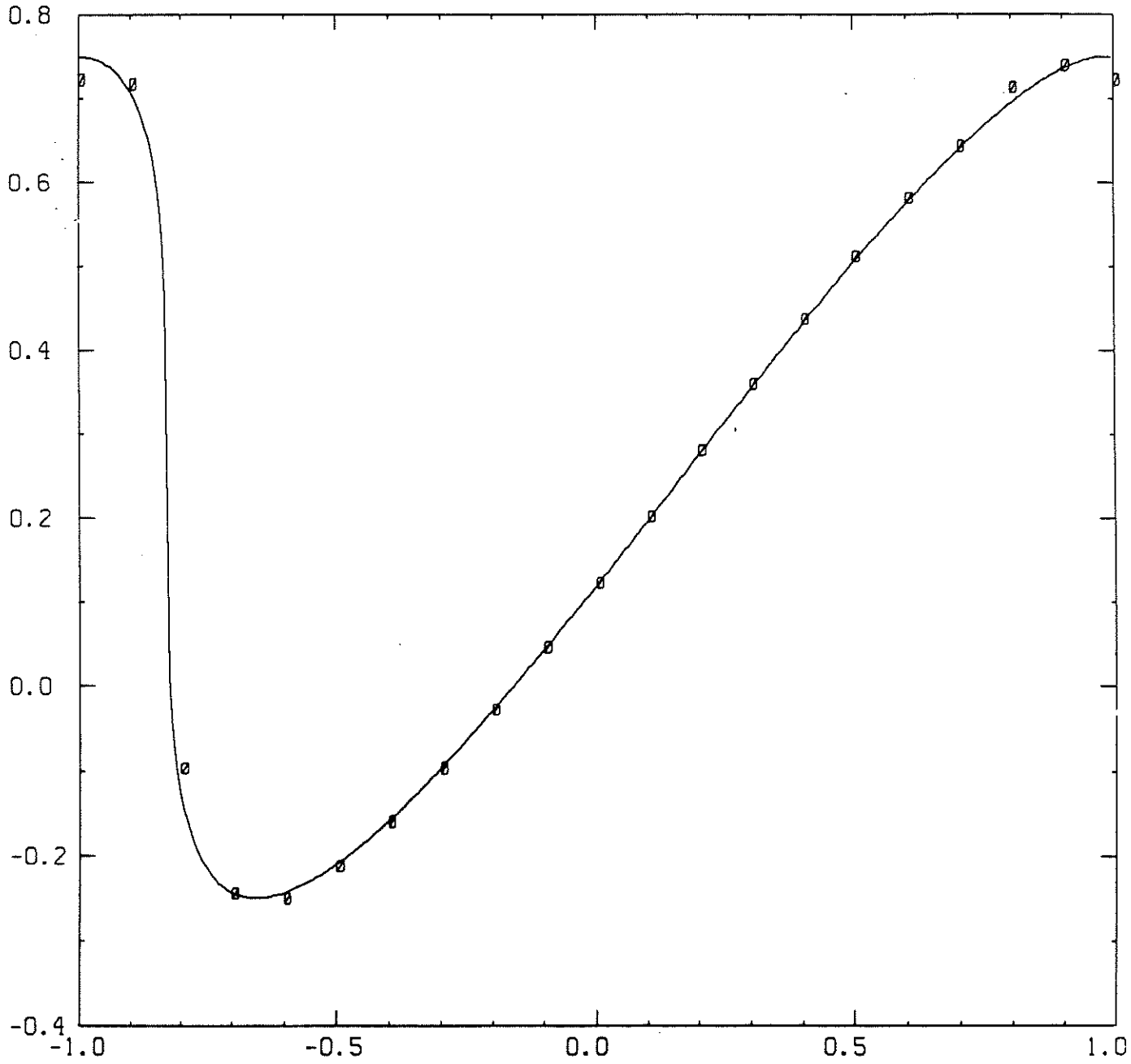

Figure 6.1-b

$T = 0.65$

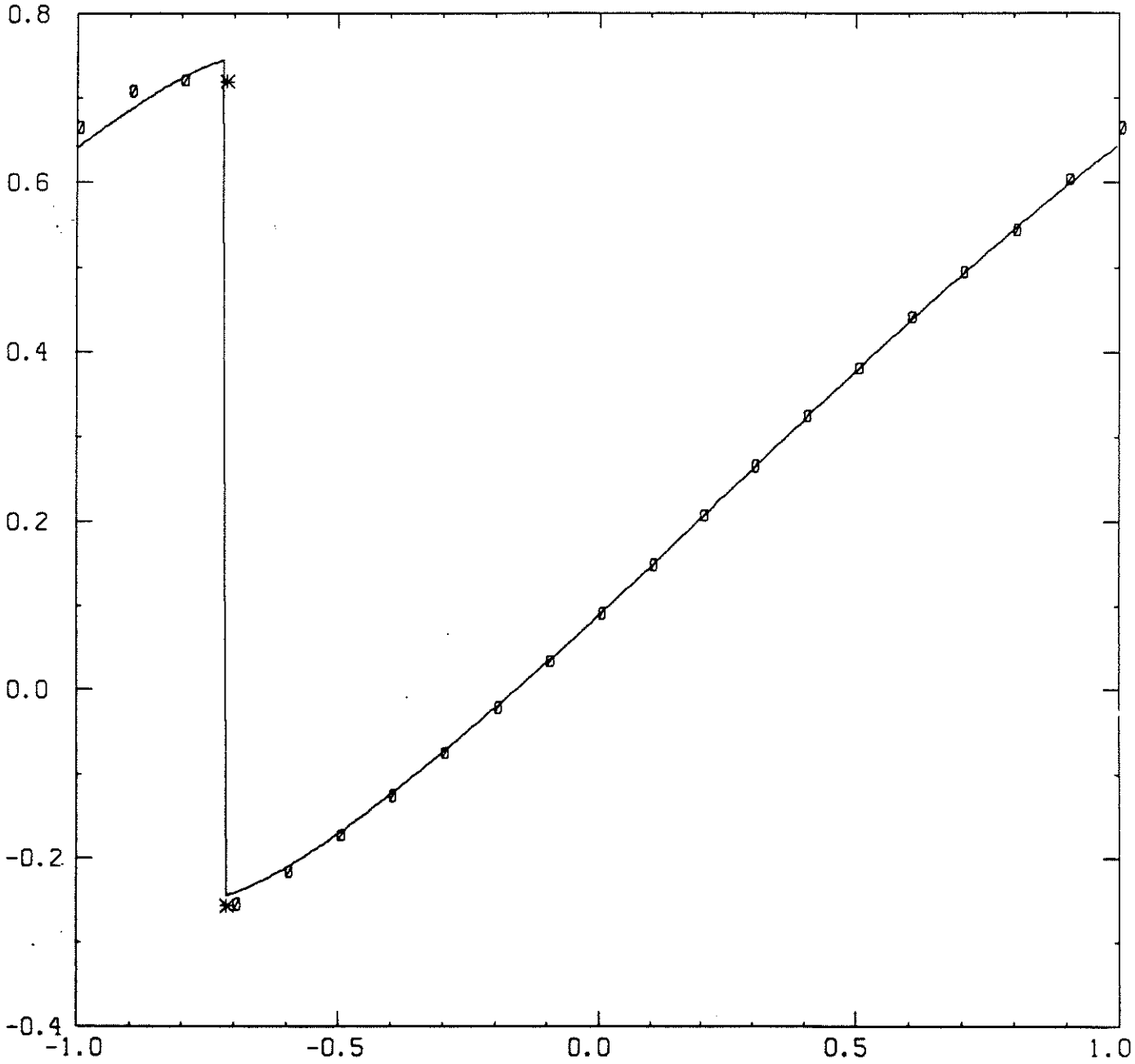

Figure 6.1 – b

$T = 1.1$

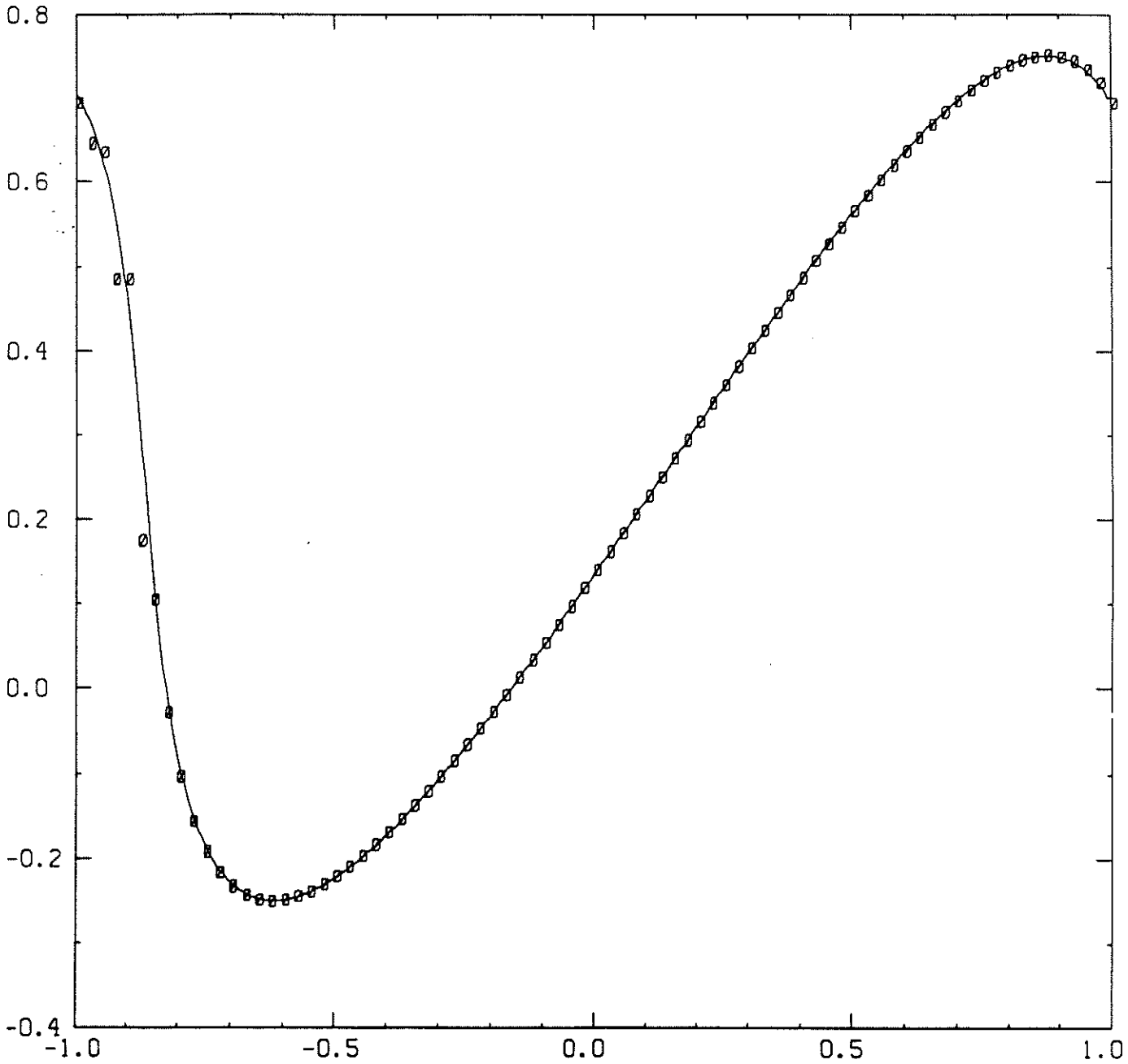

Figure 6.2 – a

$T = 0.5$

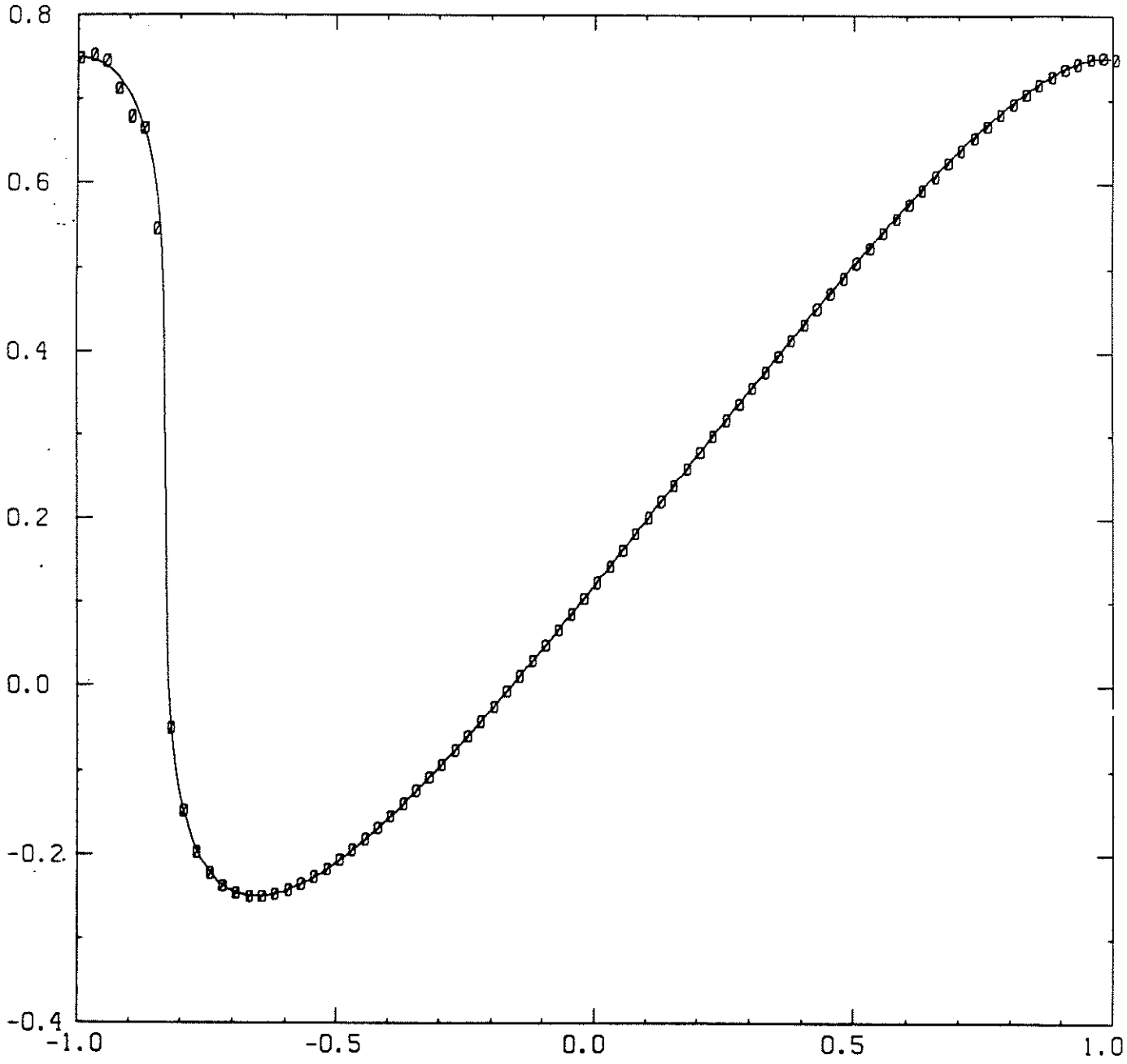

Figure 6.2-a

$T = 0.65$

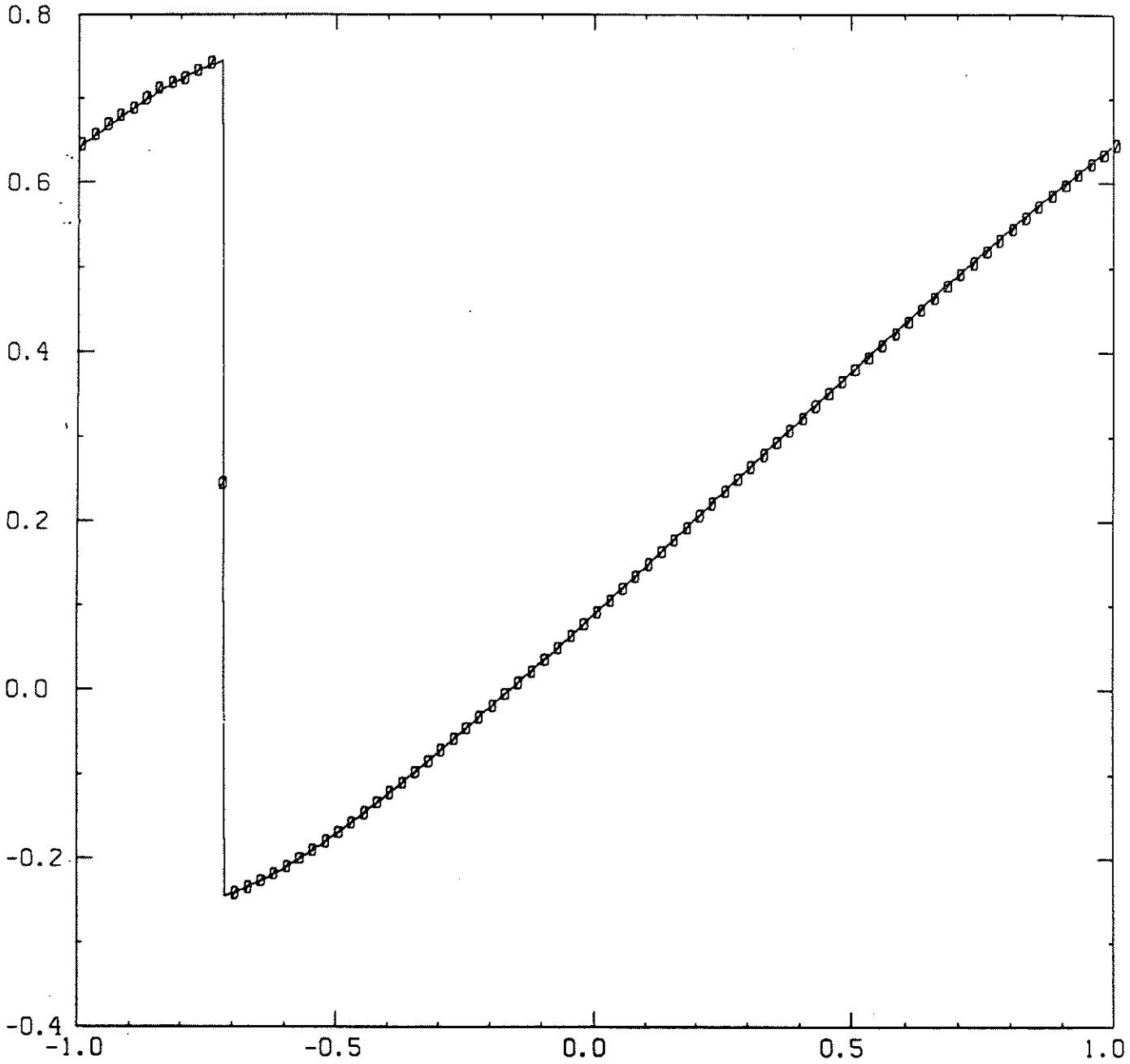

Figure 6.2-a

$T = 1.1$

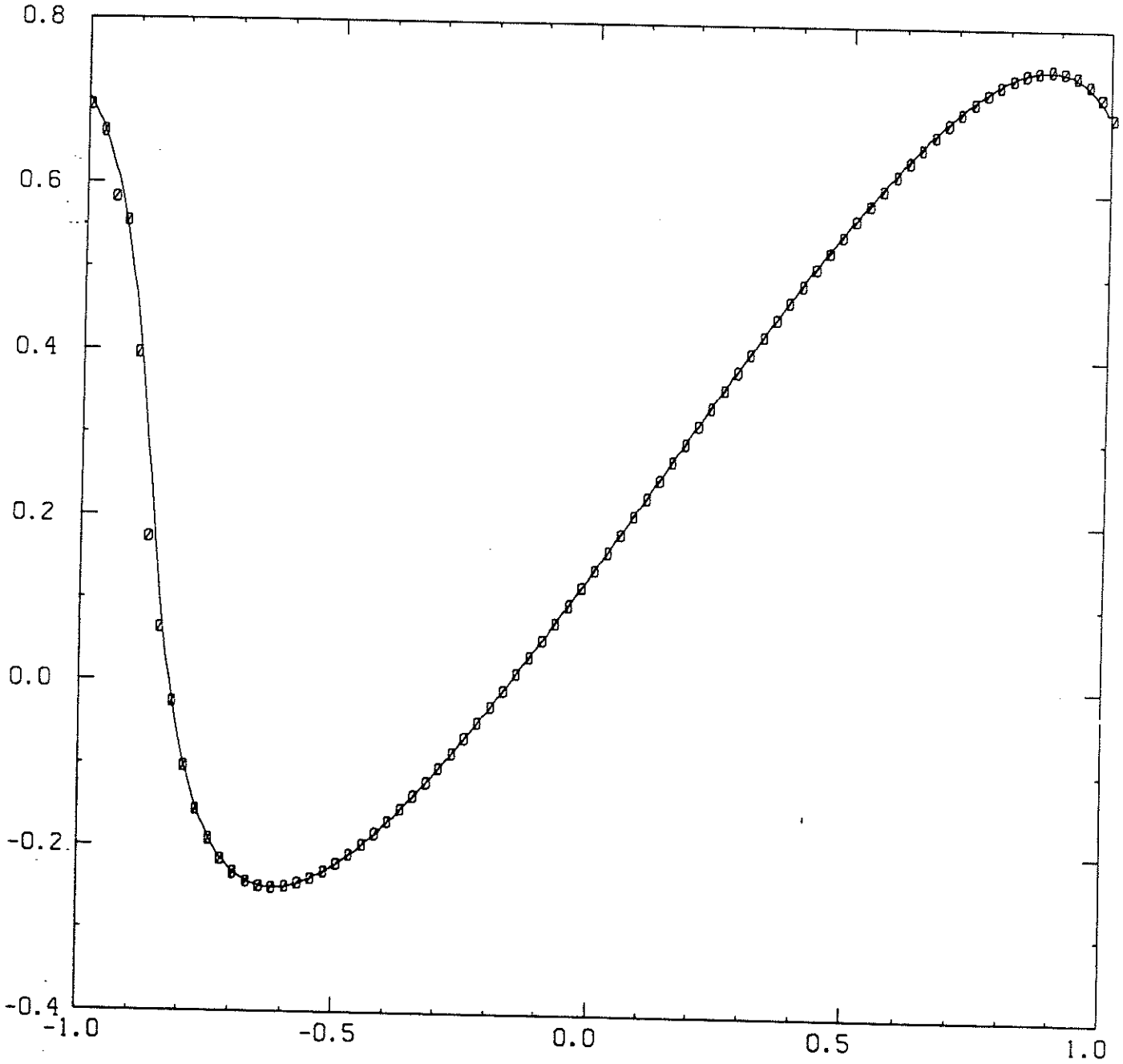

Figure 6.2-6

$T = 0.5$

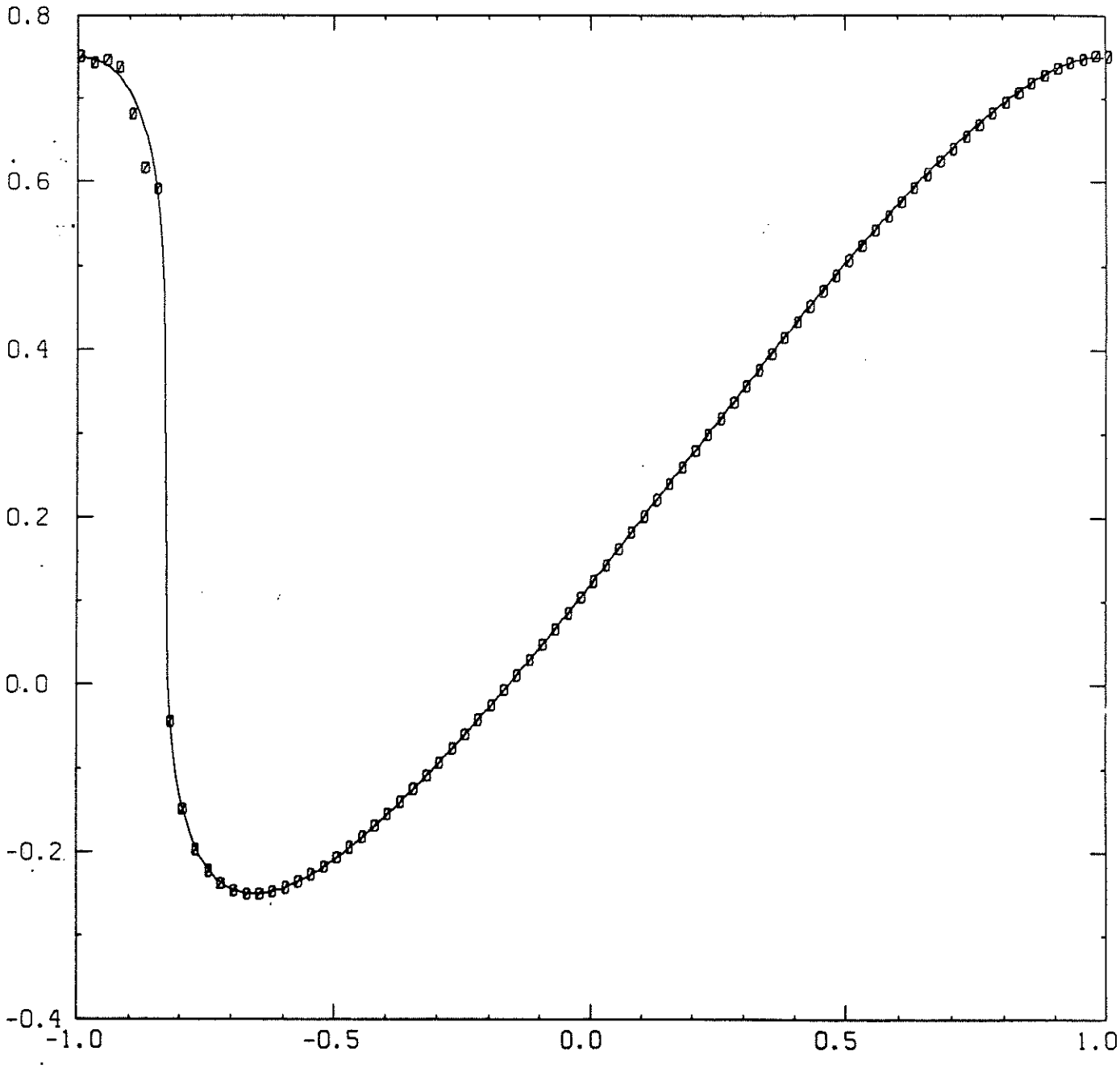

Figure 6.2— 6

$T = 0.65$

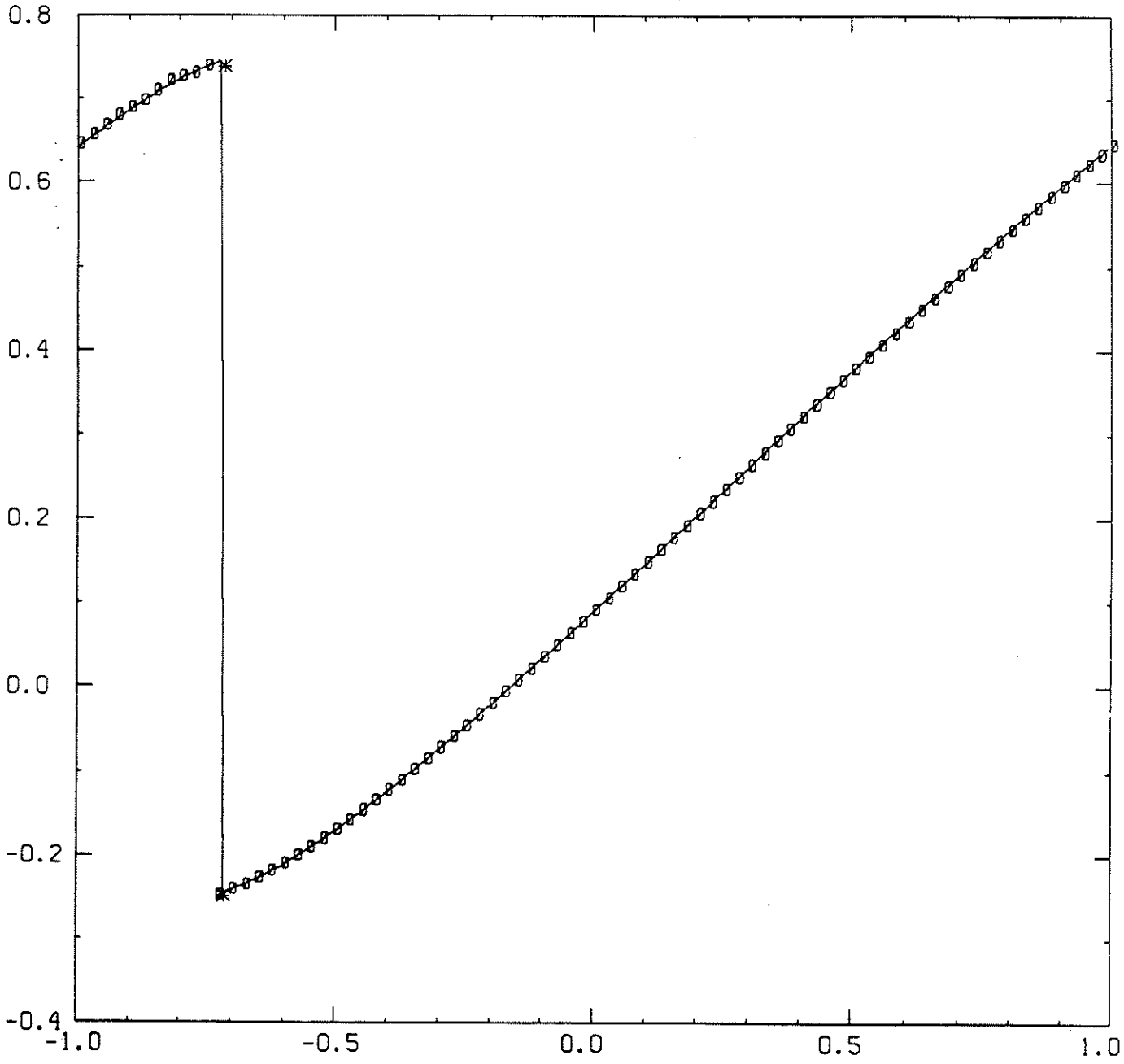

Figure 6.2-6

$T = 1.1$

EX	LF	LW	MO
-0.8250000	-0.8364334	-0.8241019	-0.8235581
-0.8125000	-0.8230240	-0.8116784	-0.8112703
-0.8000000	-0.8094509	-0.7993561	-0.7990226
-0.7875000	-0.7957033	-0.7870850	-0.7867607
-0.7750000	-0.7817740	-0.7748046	-0.7744159
-0.7625000	-0.7676604	-0.7624528	-0.7619203
-0.7500000	-0.7533634	-0.7499743	-0.7505927
-0.7375000	-0.7420182	-0.7369952	-0.7385750
-0.7250000	-0.7293629	-0.7254016	-0.7263834

Table 6.1 – a

EX	LF	LW	MO
-0.8375000	-0.8488083	-0.8384687	-0.8403274
-0.8343750	-0.8448576	-0.8350775	-0.8369125
-0.8312500	-0.8411281	-0.8317347	-0.8335727
-0.8281250	-0.8375554	-0.8284522	-0.8303084
-0.8250000	-0.8341025	-0.8231344	-0.8271104
-0.8218750	-0.8307408	-0.8203193	-0.8224791
-0.8187500	-0.8274463	-0.8174989	-0.8192699
-0.8156250	-0.8233213	-0.8146763	-0.8161011
-0.8125000	-0.8196540	-0.8118547	-0.8129746
-0.8093750	-0.8161189	-0.8090336	-0.8098869
-0.8062500	-0.8126772	-0.8062074	-0.8068277
-0.8031250	-0.8093064	-0.8033639	-0.8037825
-0.8000000	-0.8059886	-0.8004860	-0.8007355
-0.7968750	-0.8027091	-0.7967674	-0.7967654
-0.7937500	-0.7989069	-0.7938213	-0.7937031
-0.7906250	-0.7954147	-0.7908556	-0.7906504
-0.7875000	-0.7920048	-0.7878712	-0.7876069
-0.7843750	-0.7886513	-0.7848648	-0.7845677
-0.7812500	-0.7853393	-0.7818301	-0.7815251
-0.7781250	-0.7820576	-0.7787599	-0.7784705
-0.7750000	-0.7787967	-0.7756485	-0.7753965
-0.7718750	-0.7755489	-0.7723584	-0.7718992
-0.7687500	-0.7720225	-0.7691954	-0.7688425
-0.7656250	-0.7686651	-0.7660306	-0.7657788
-0.7625000	-0.7653494	-0.7628636	-0.7627079
-0.7593750	-0.7620615	-0.7596936	-0.7596282
-0.7562500	-0.7587928	-0.7565193	-0.7565369
-0.7531250	-0.7555370	-0.7533406	-0.7534313
-0.7500000	-0.7522890	-0.7501586	-0.7503106
-0.7468750	-0.7488993	-0.7470106	-0.7471527
-0.7437500	-0.7456065	-0.7438717	-0.7440282
-0.7406250	-0.7423366	-0.7407333	-0.7409001
-0.7375000	-0.7390810	-0.7375951	-0.7377681
-0.7343750	-0.7358351	-0.7344573	-0.7346318
-0.7312500	-0.7325952	-0.7313206	-0.7314907
-0.7281250	-0.7293584	-0.7281857	-0.7283449
-0.7250000	-0.7261226	-0.7250538	-0.7251932

Table 6.1-b

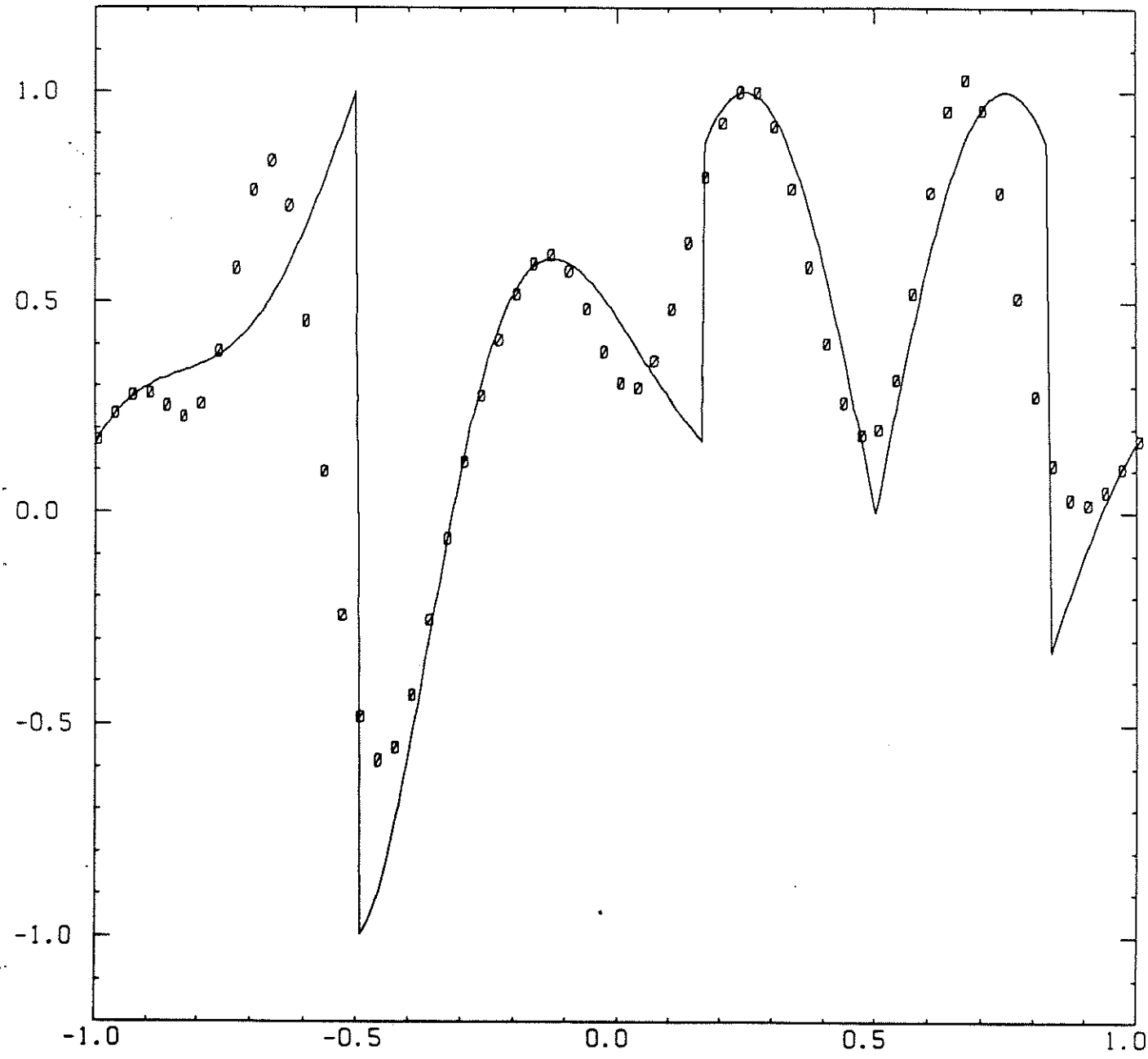

Figure 6.3-a

T = 2.

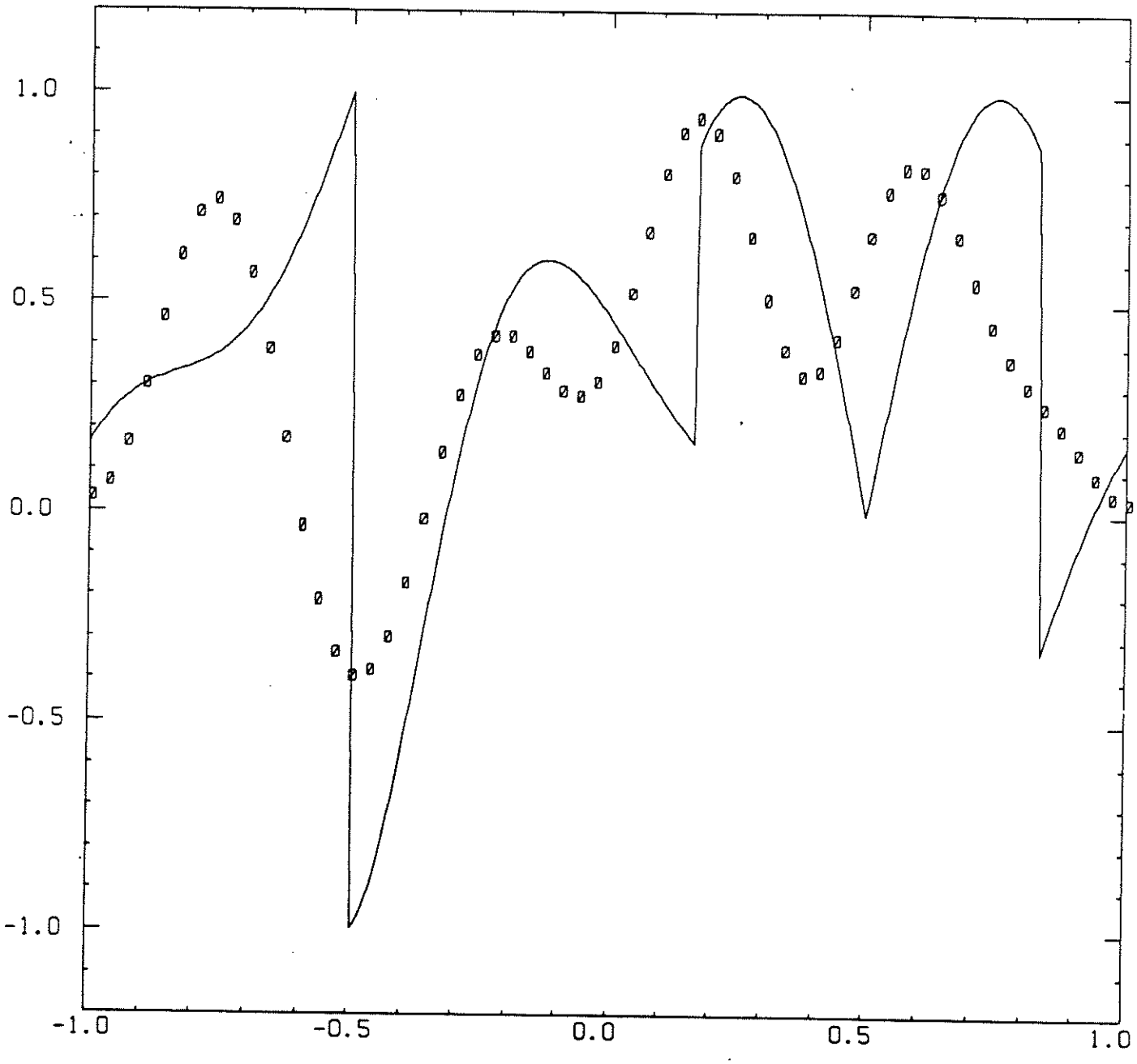

Figure 6.3-a

T = 8.

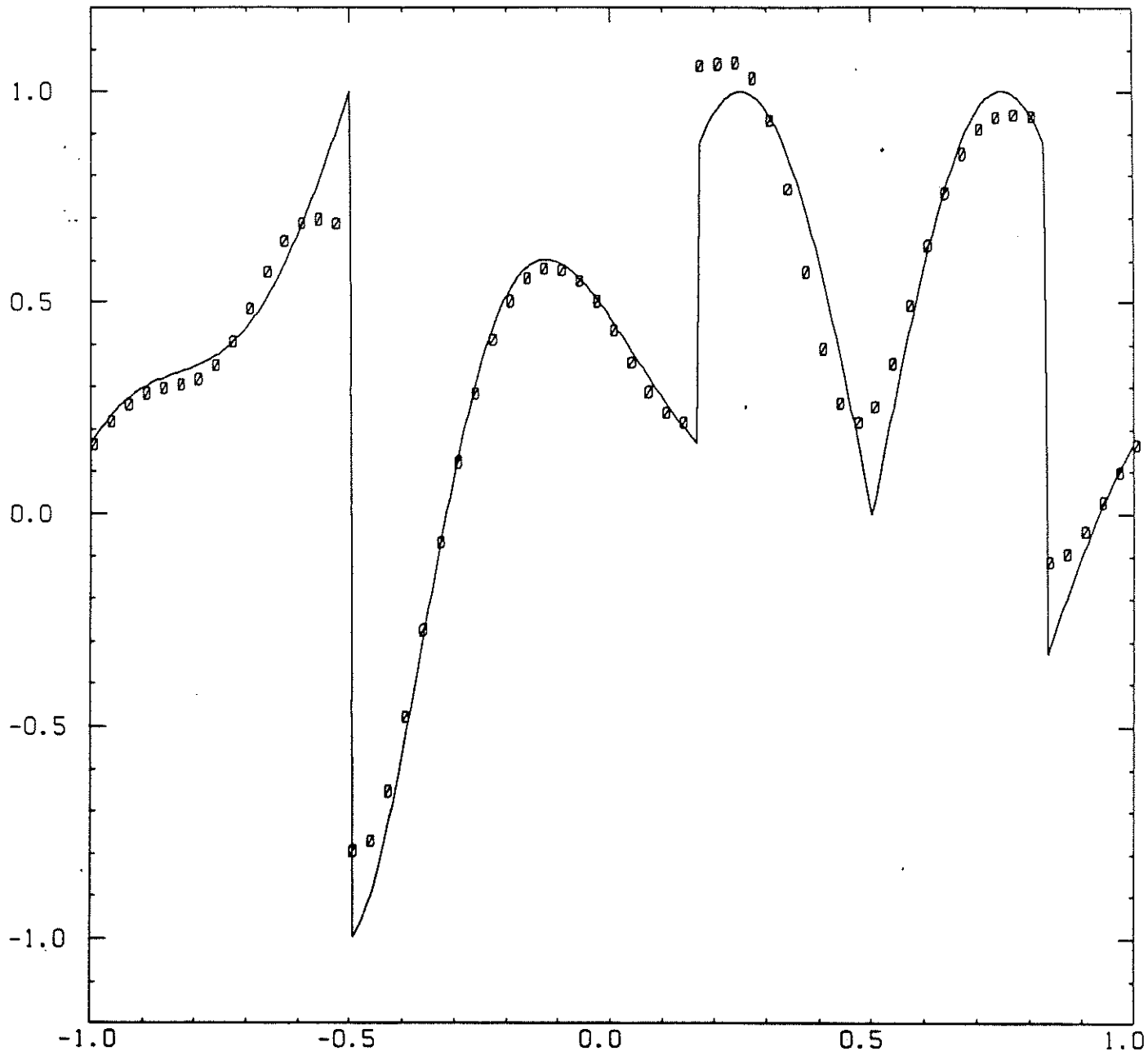

Figure 6.3-6

T = 2.

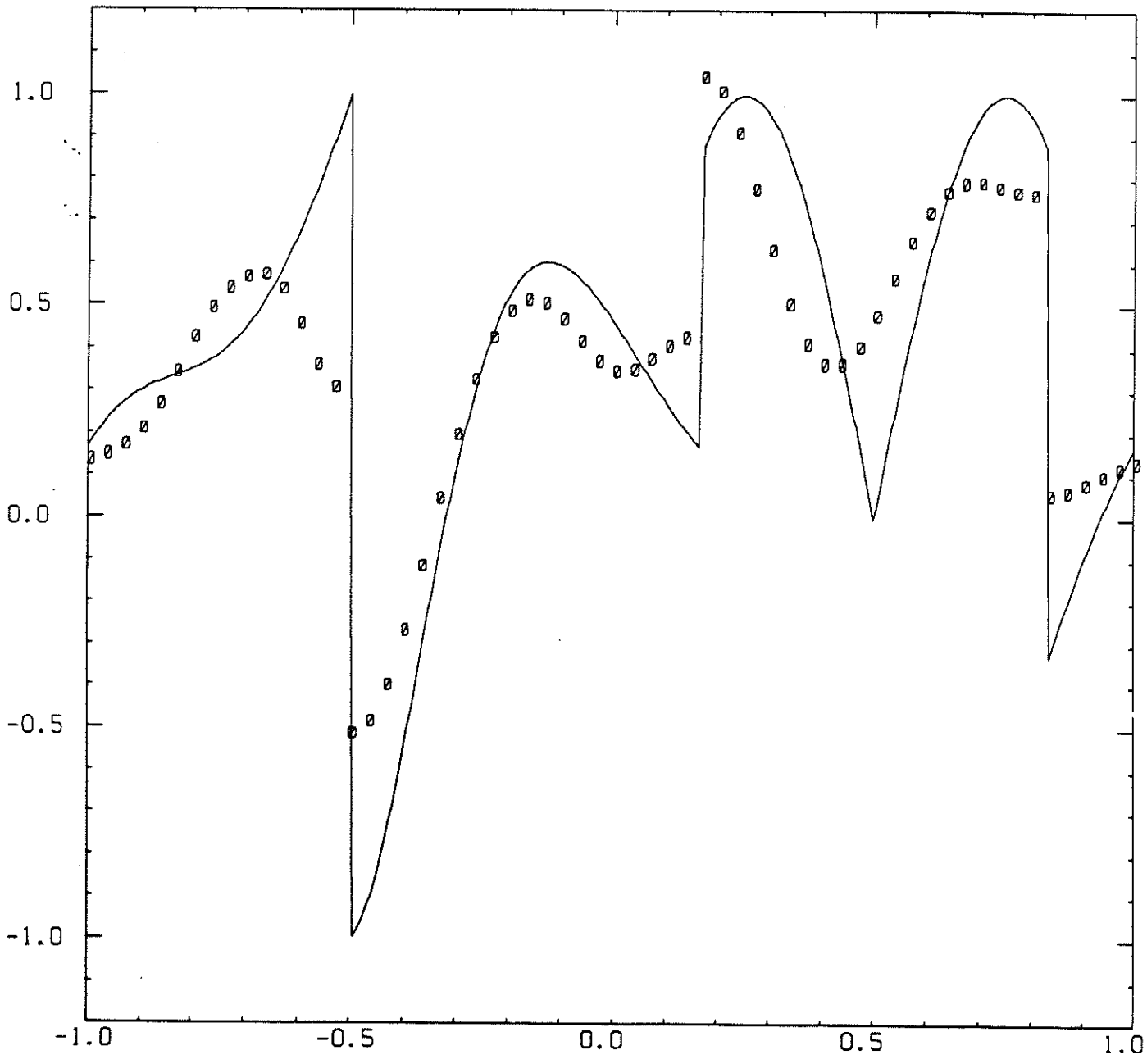

Figure 6.3-b

T = 8.

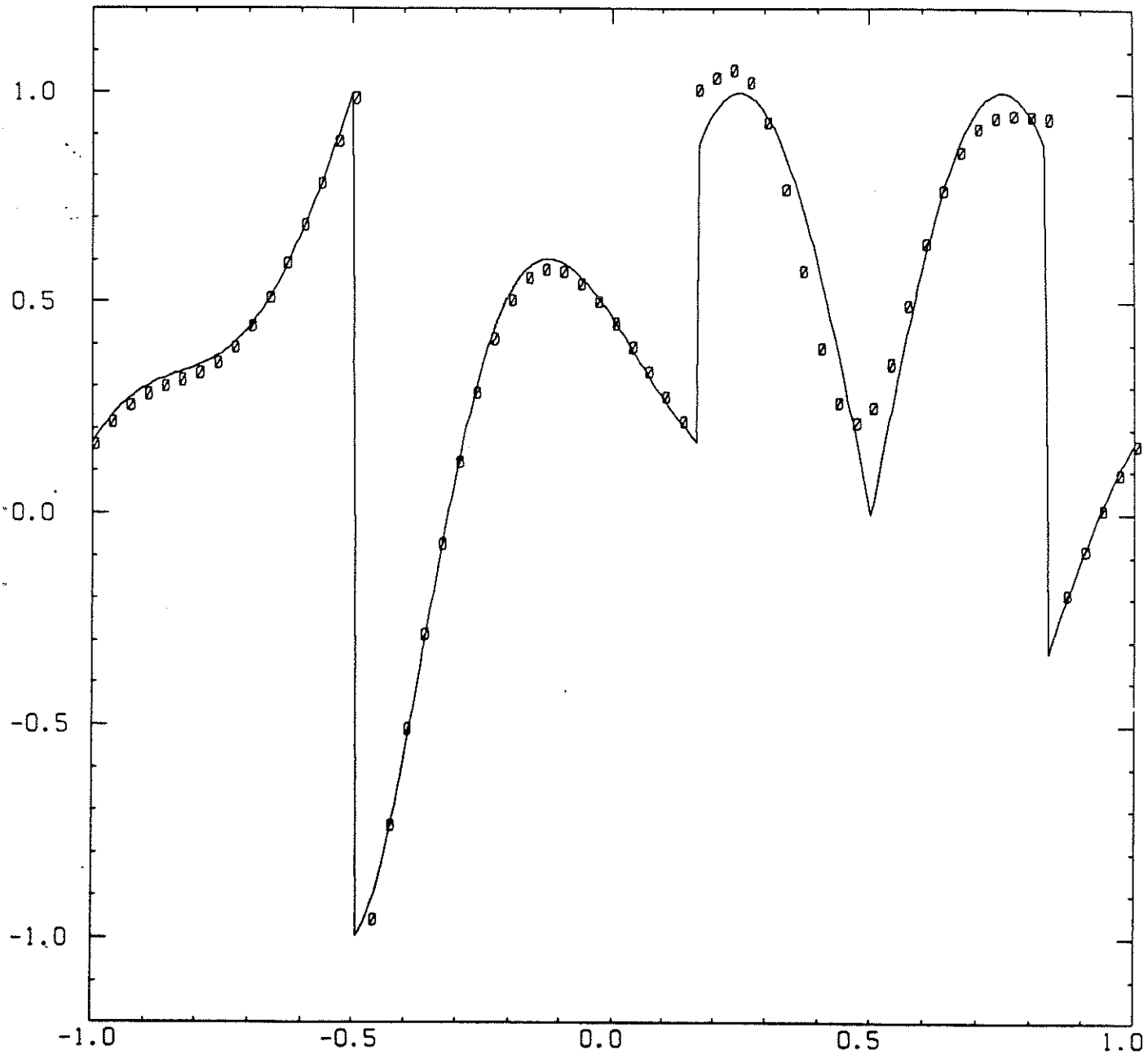

Figure 6.3-C

T = 2.

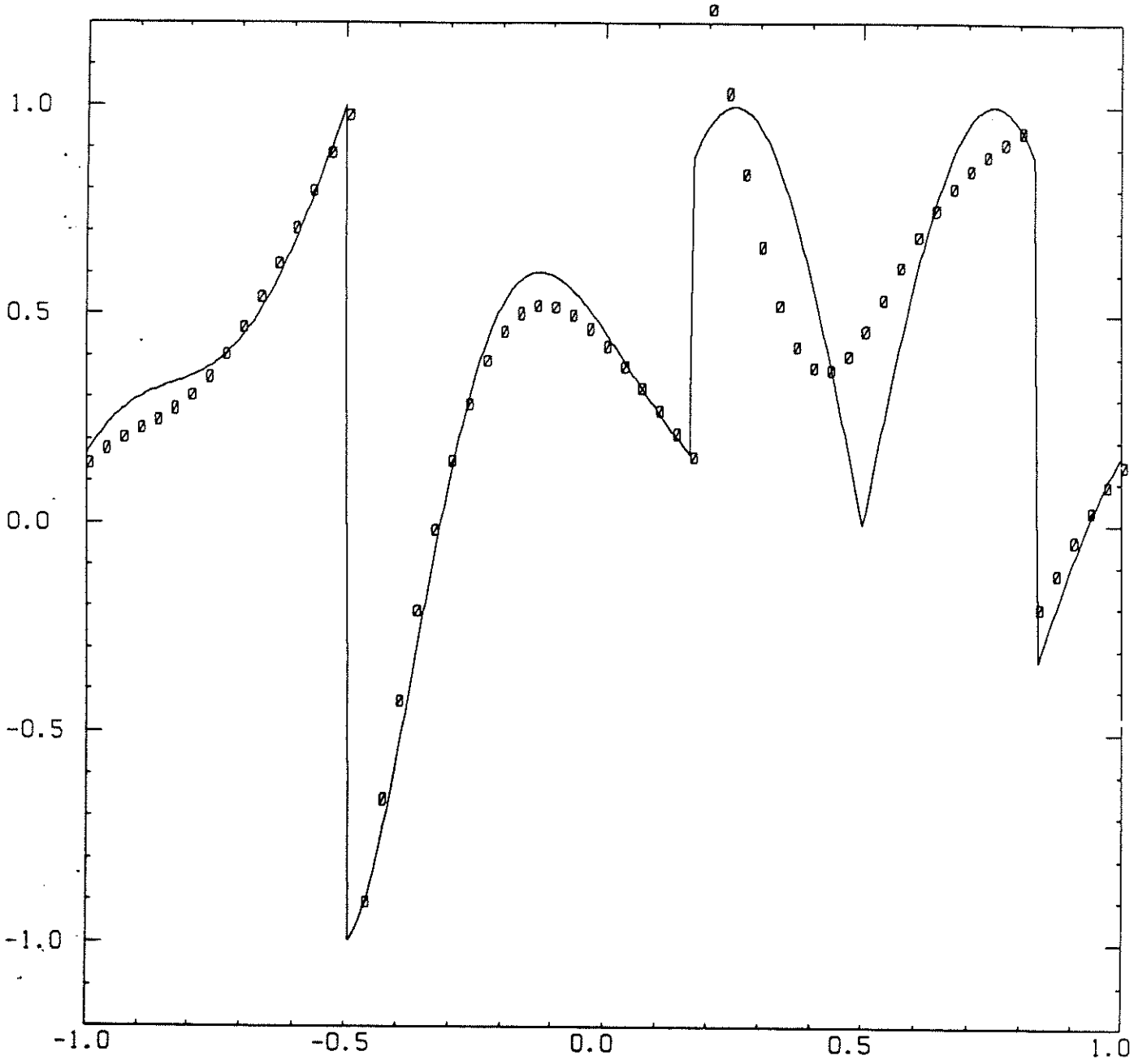

Figure 6.3 – C

T = 8.

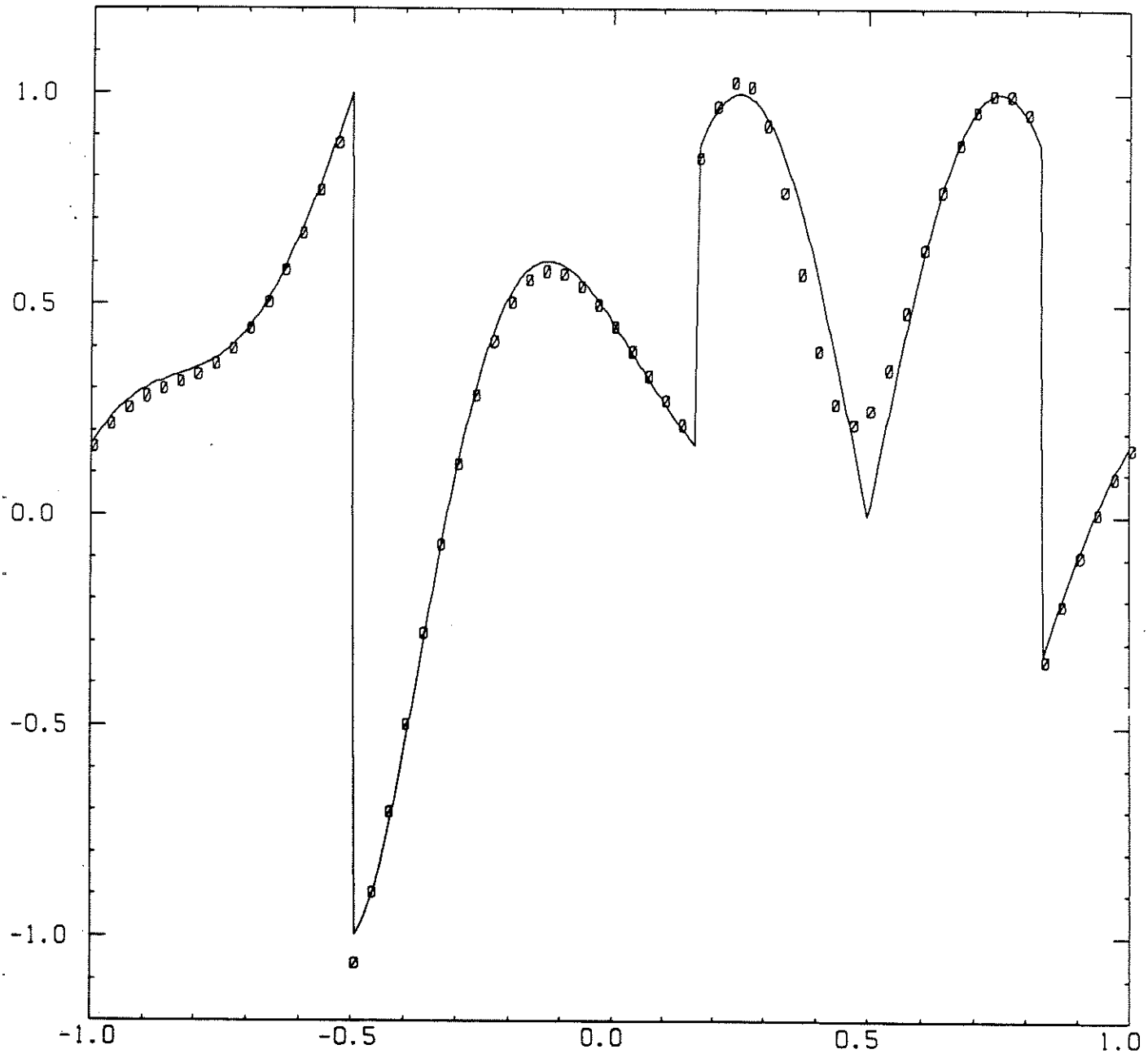

Figure 6.3-d

T = 2.

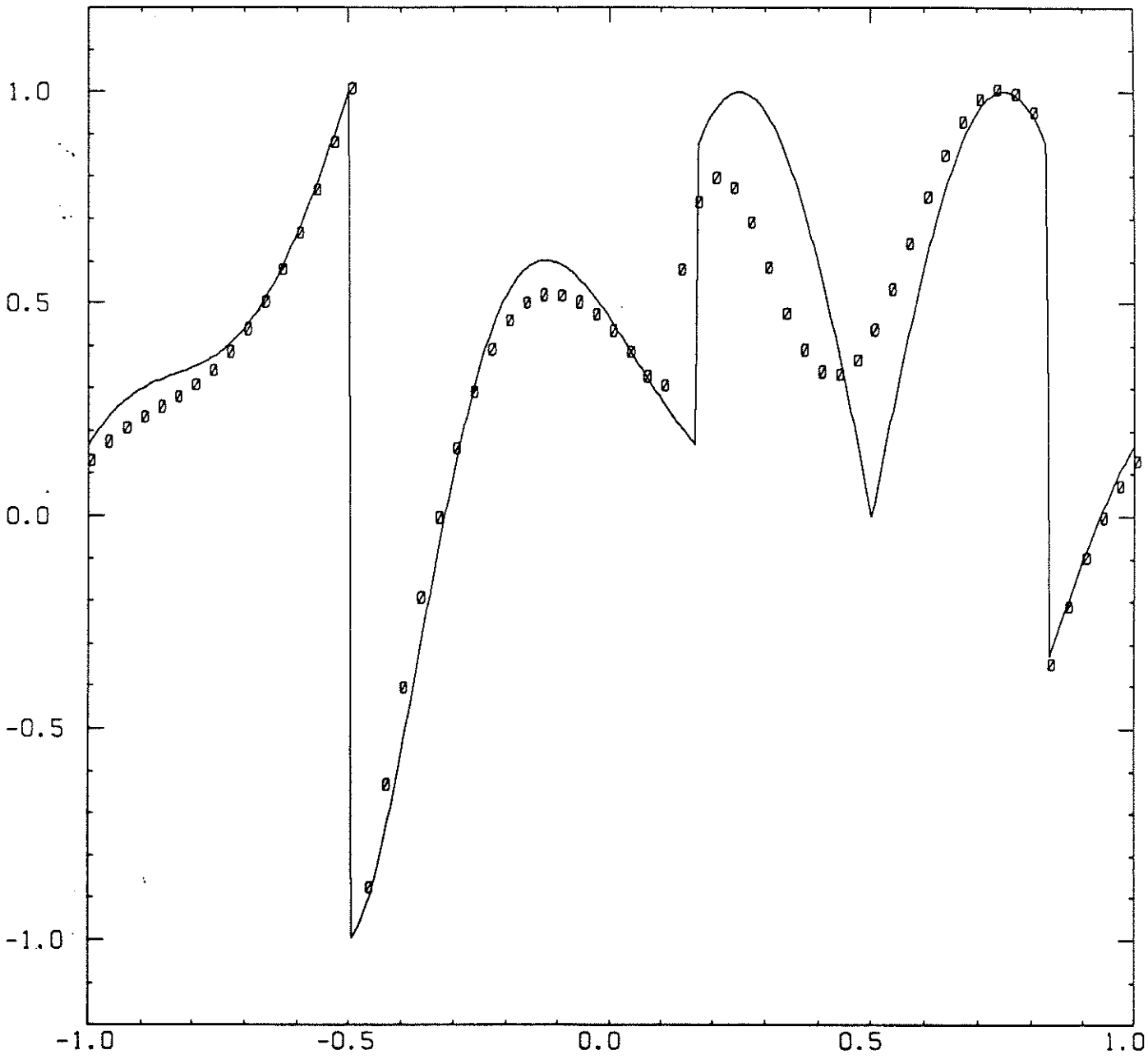

Figure 63-d

T = 8.

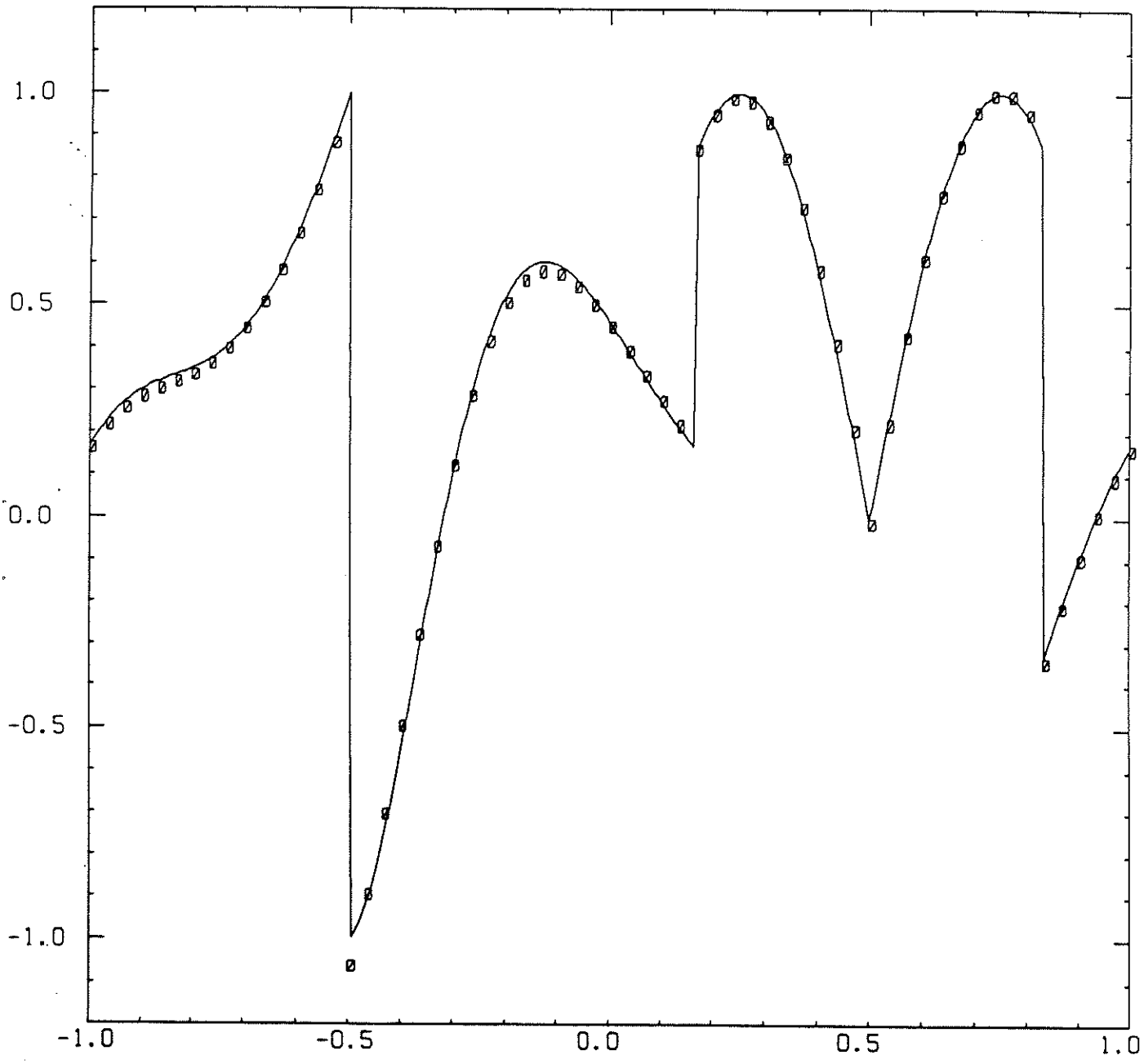

Figure 6.3-e

T = 2.

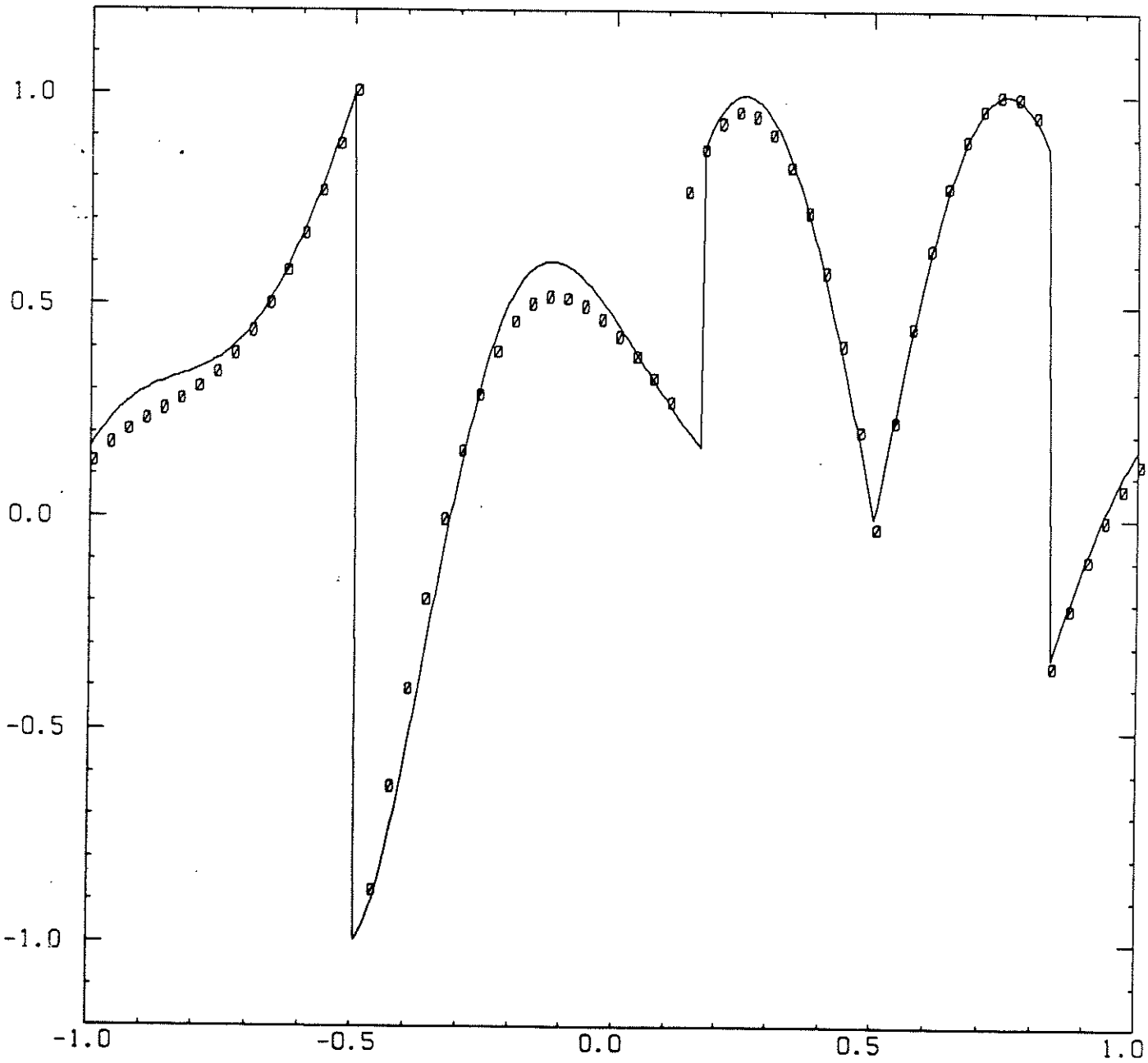

Figure 6.3-e

$T = 8.$

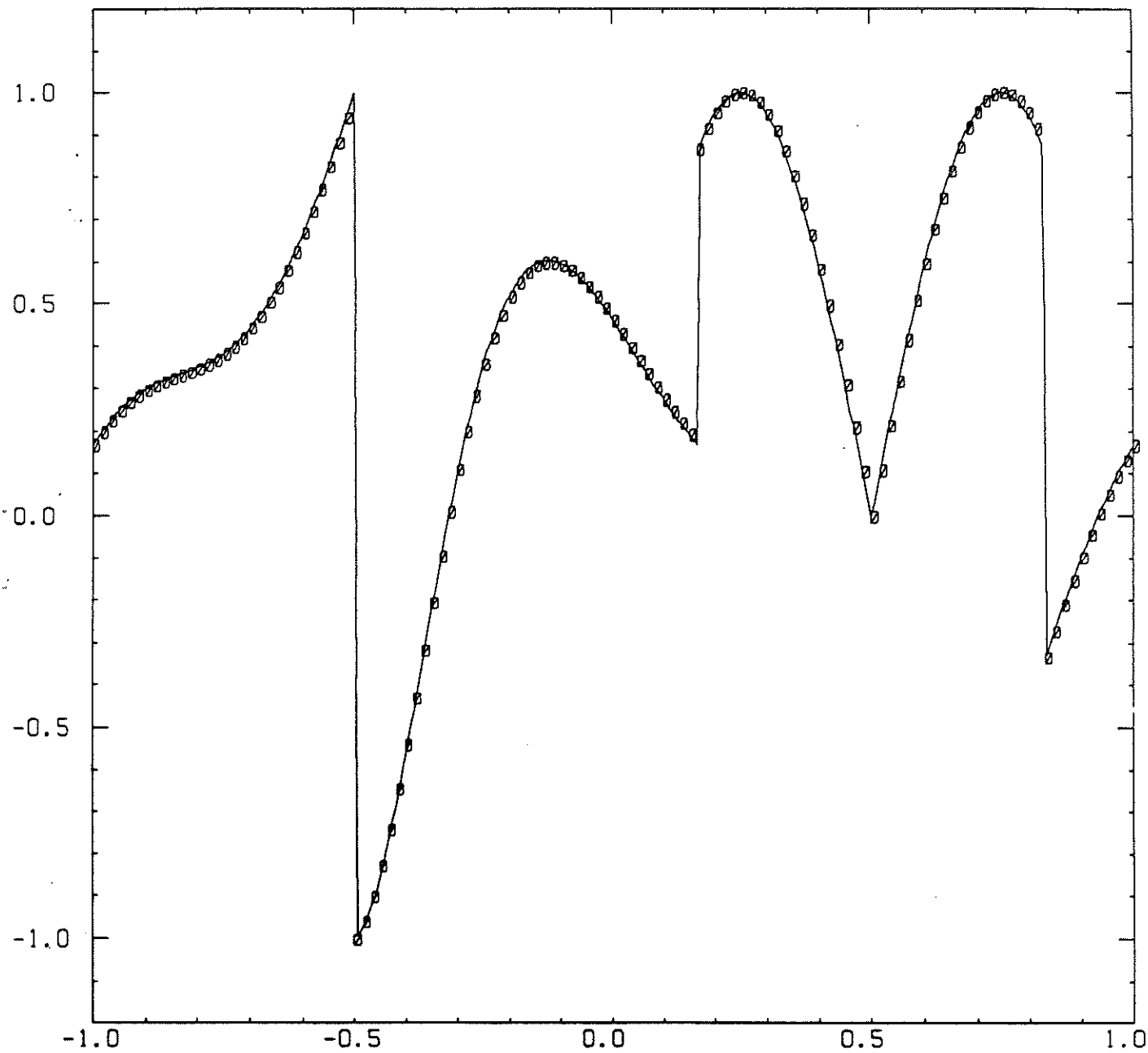

Figure 6.4

T=2.

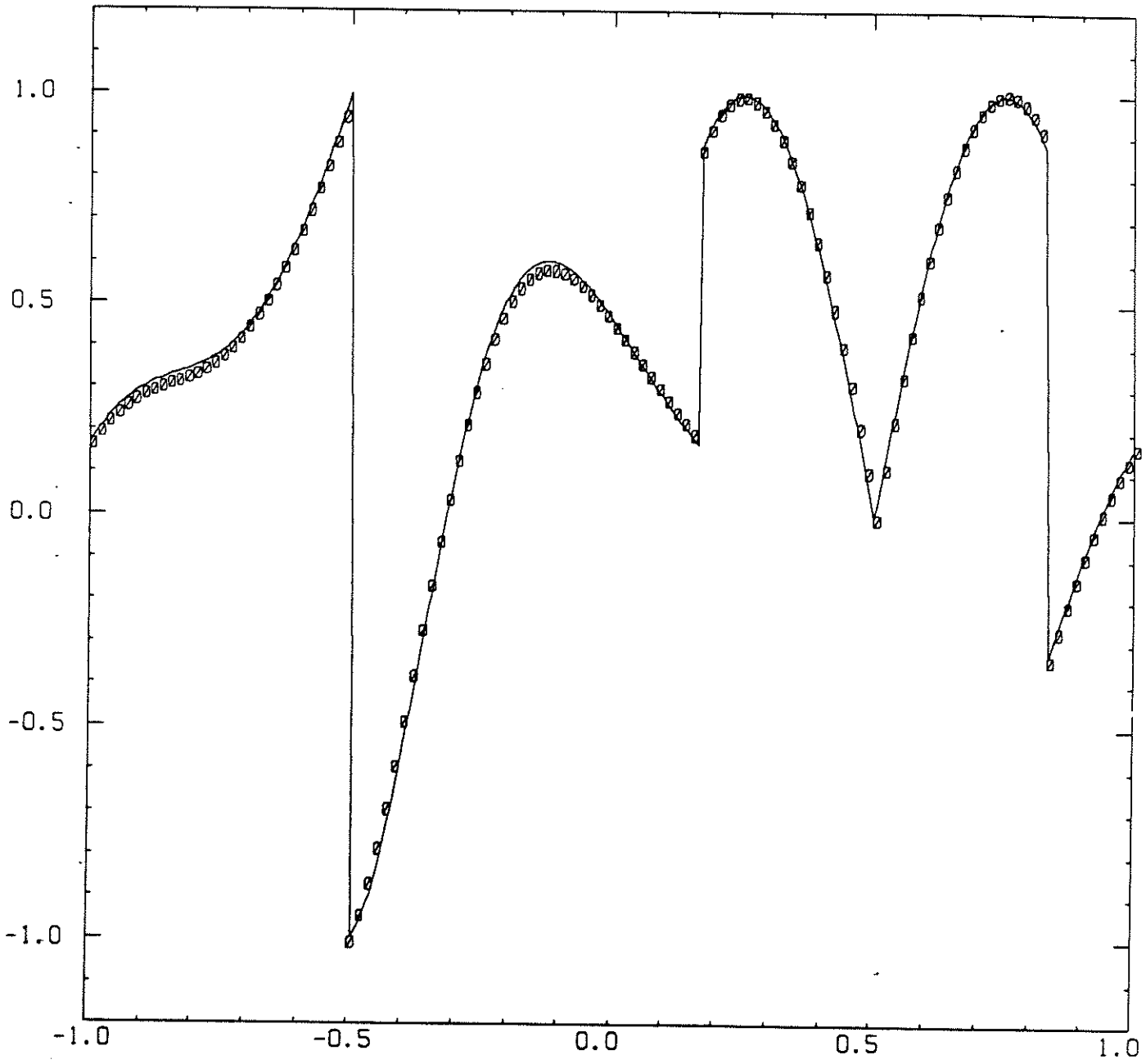

Figure 6.4

$T = 8.$

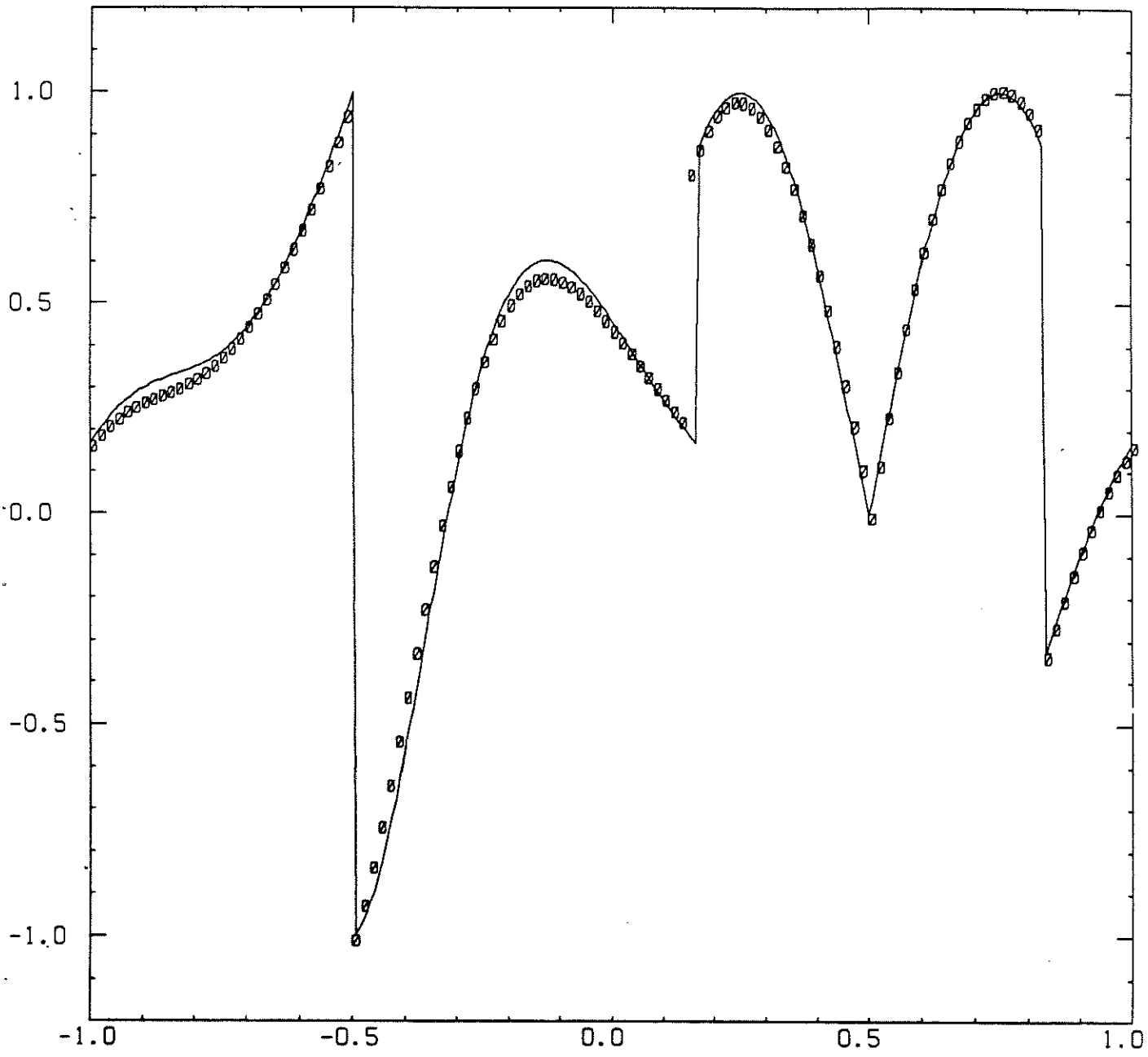

Figure 6.4

$T = 16.$

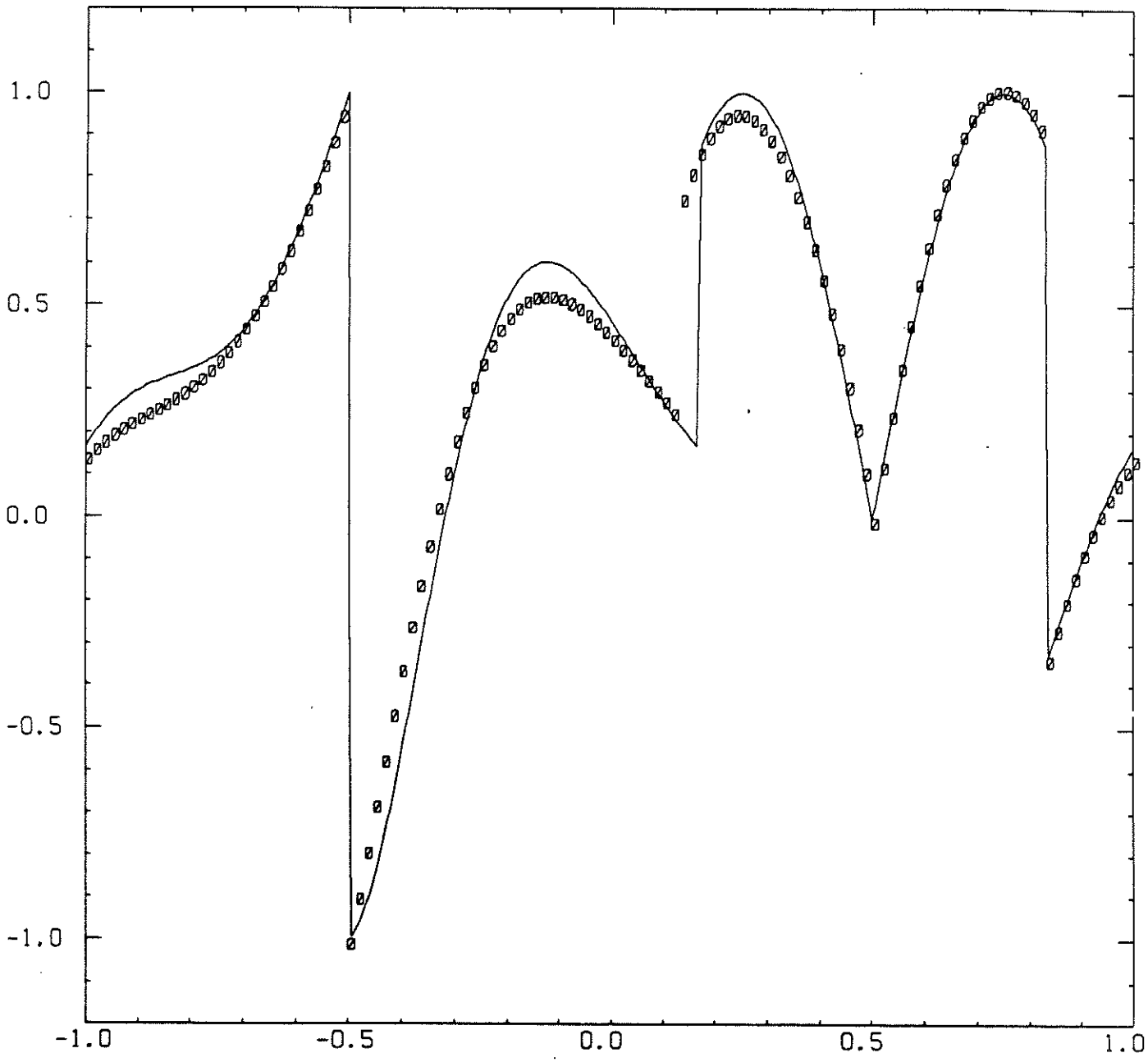

Figure 6.4

$T = 32.$

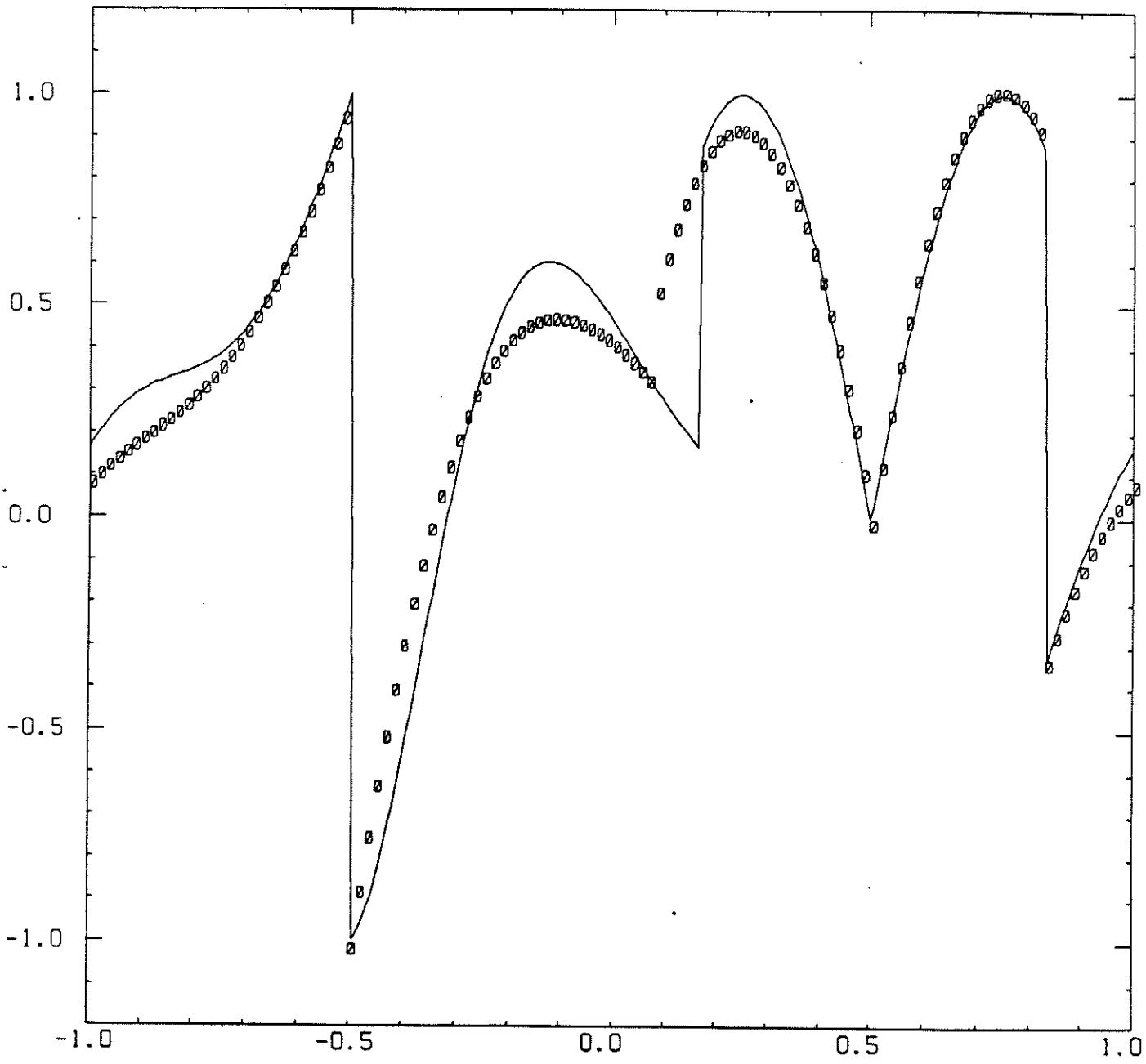

Figure 6.4

T = 64

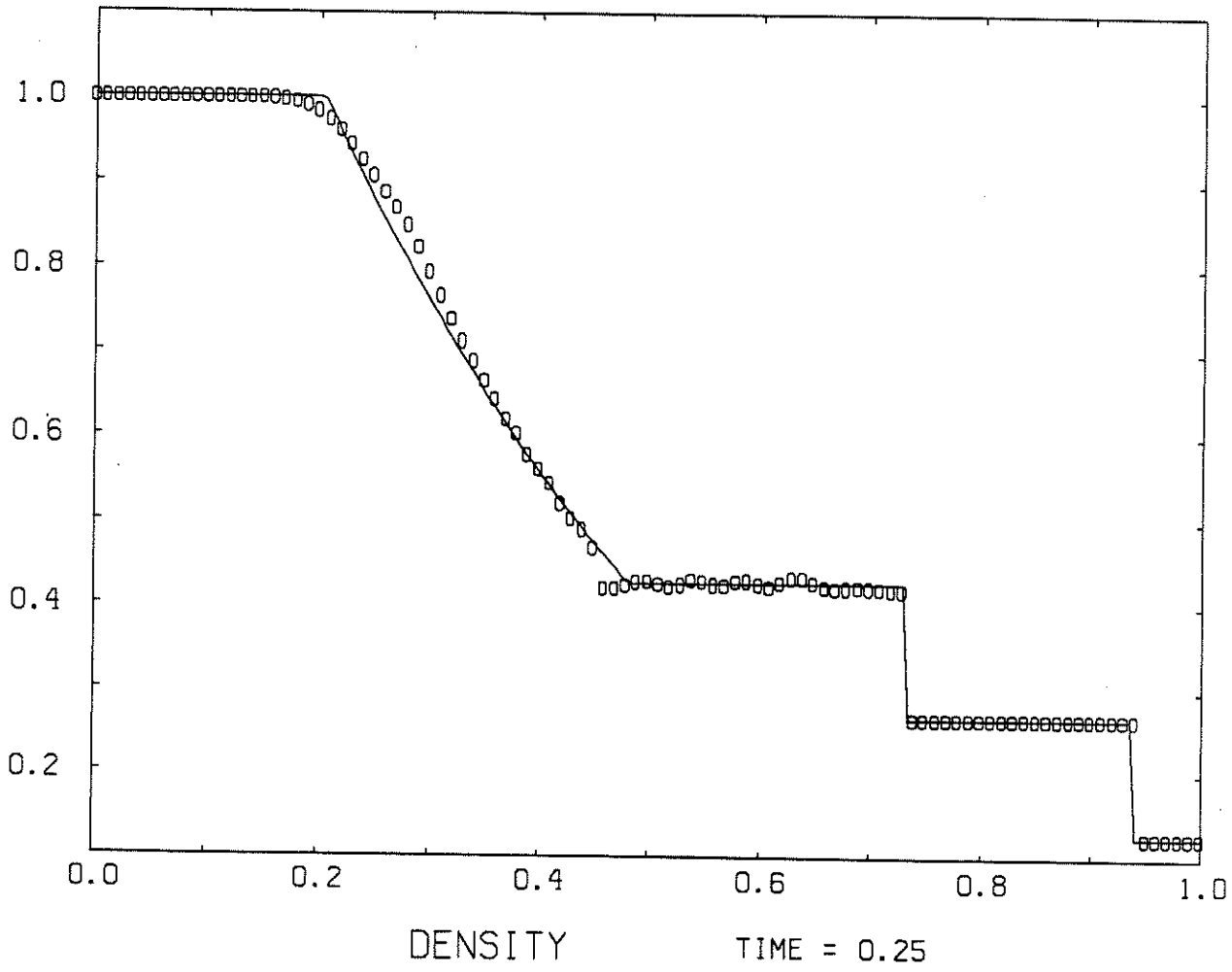

Fig. 6.5 – a

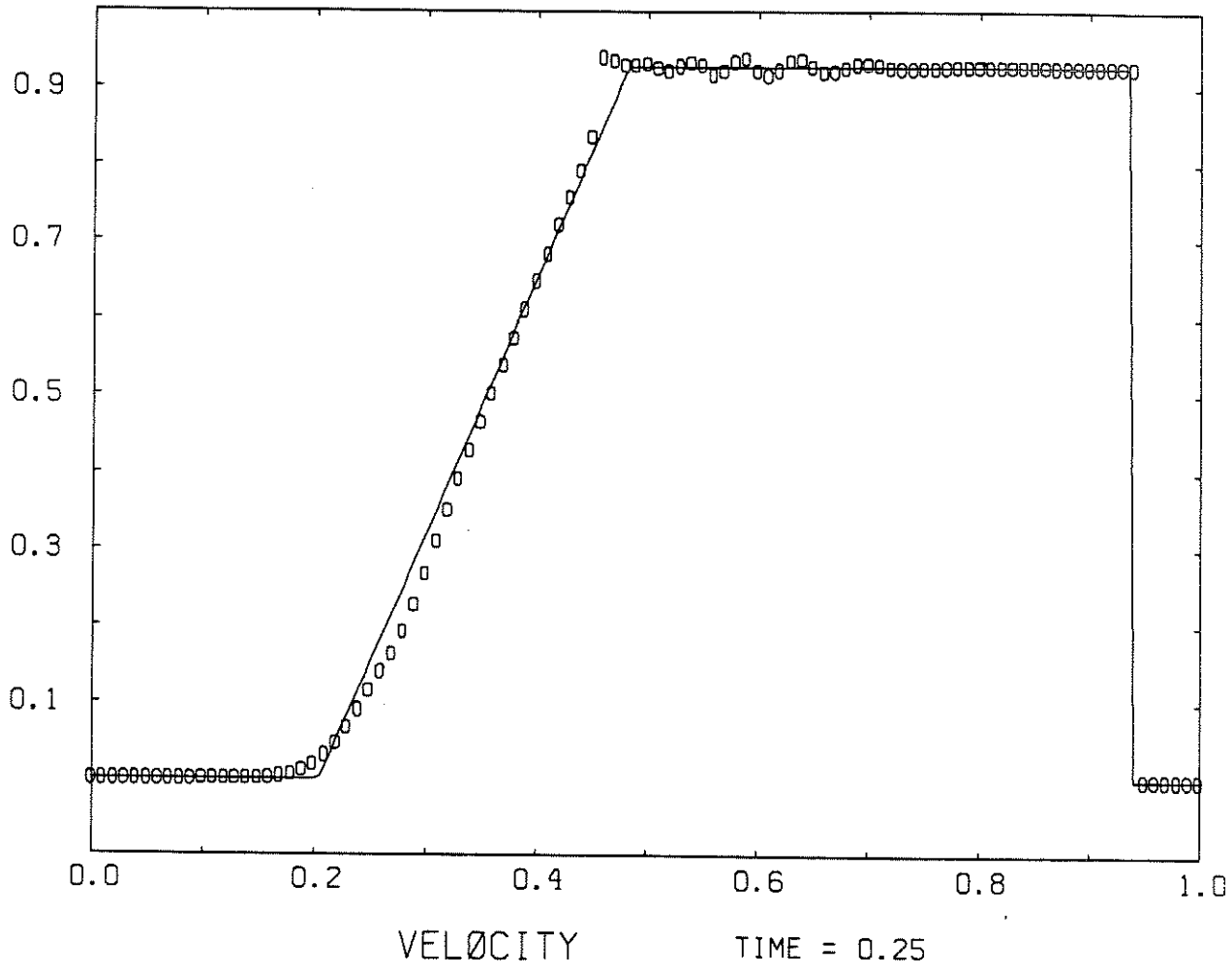

Fig. 6.5 - a

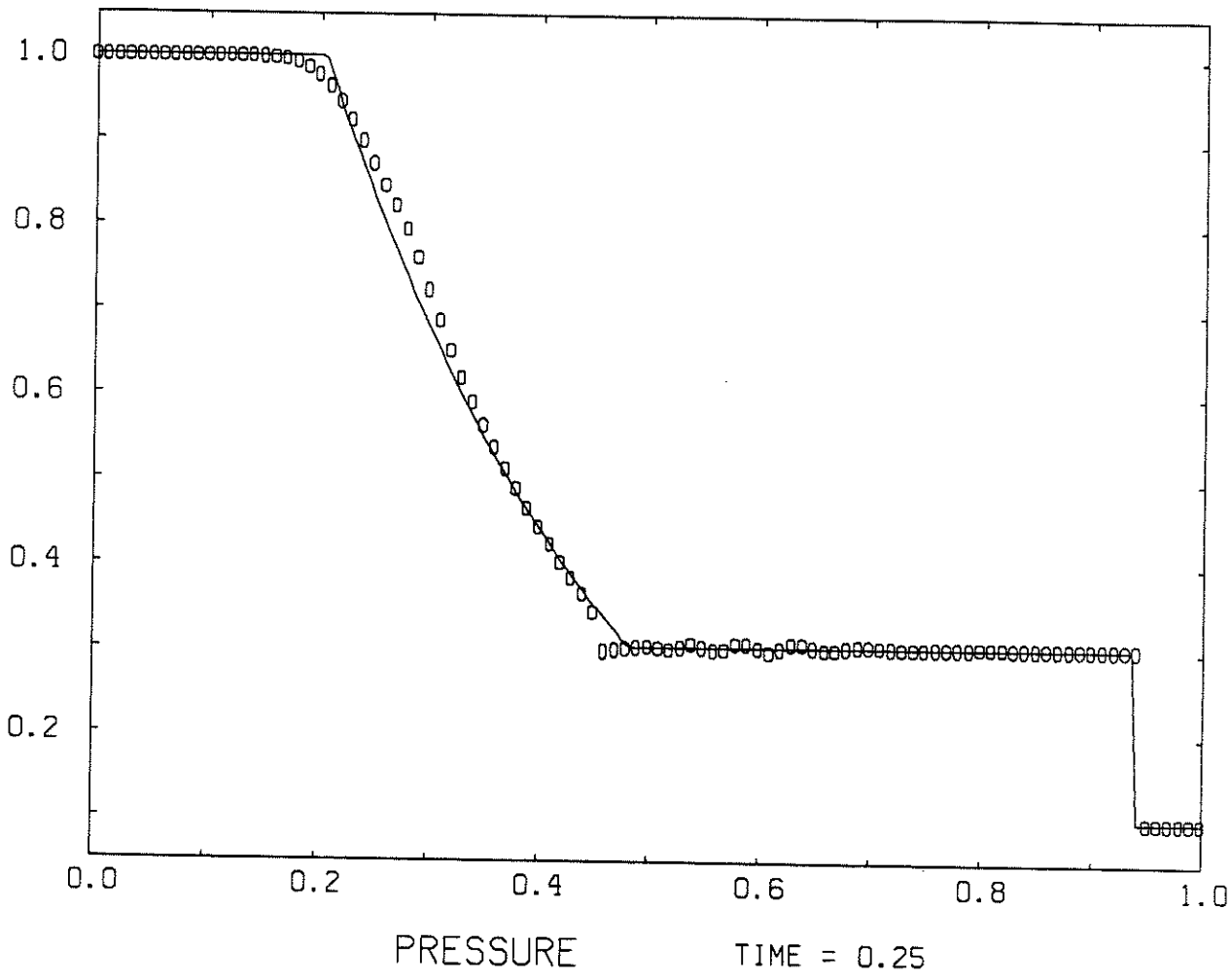

Fig. 6.5 — a

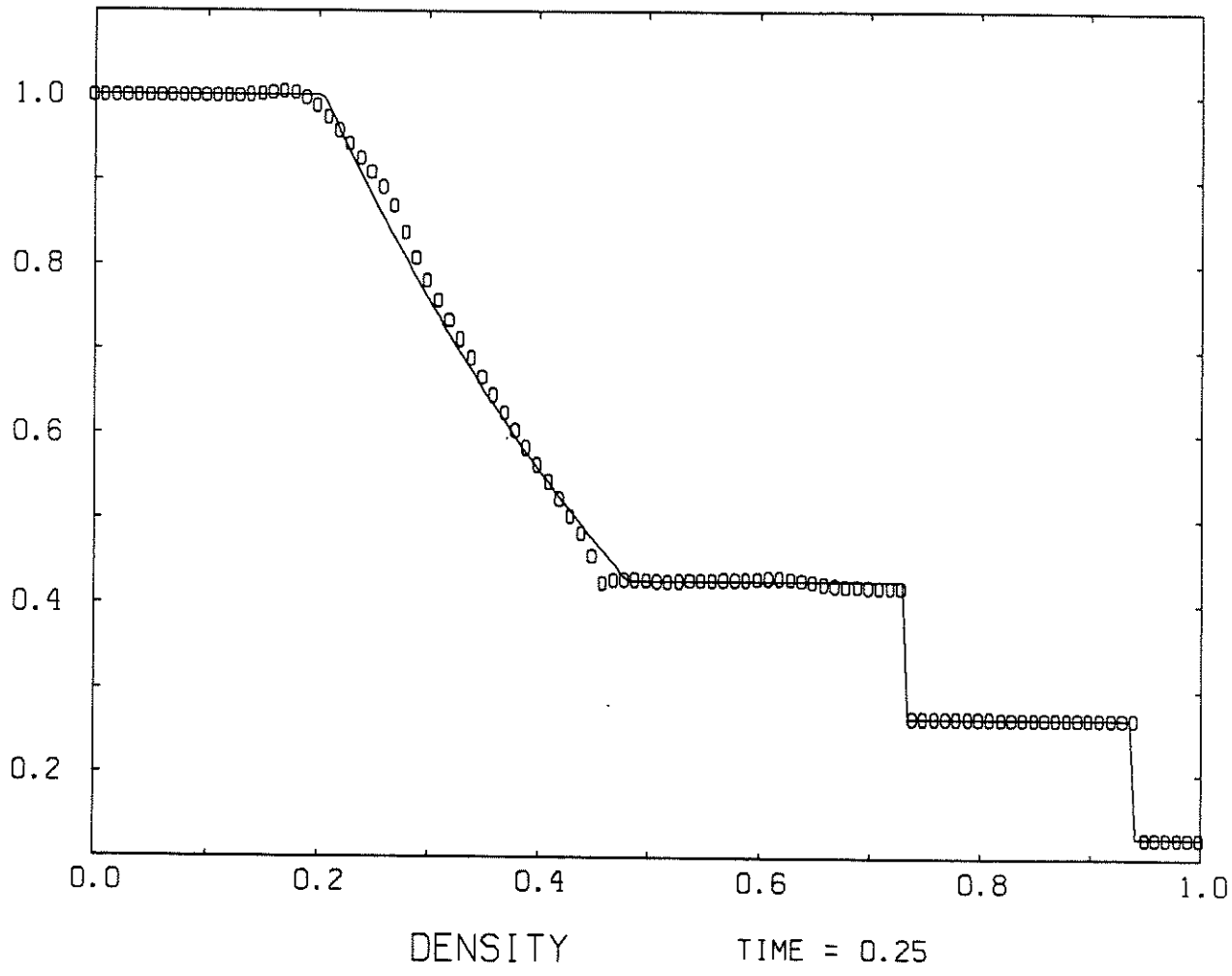

Fig. 6.5—6

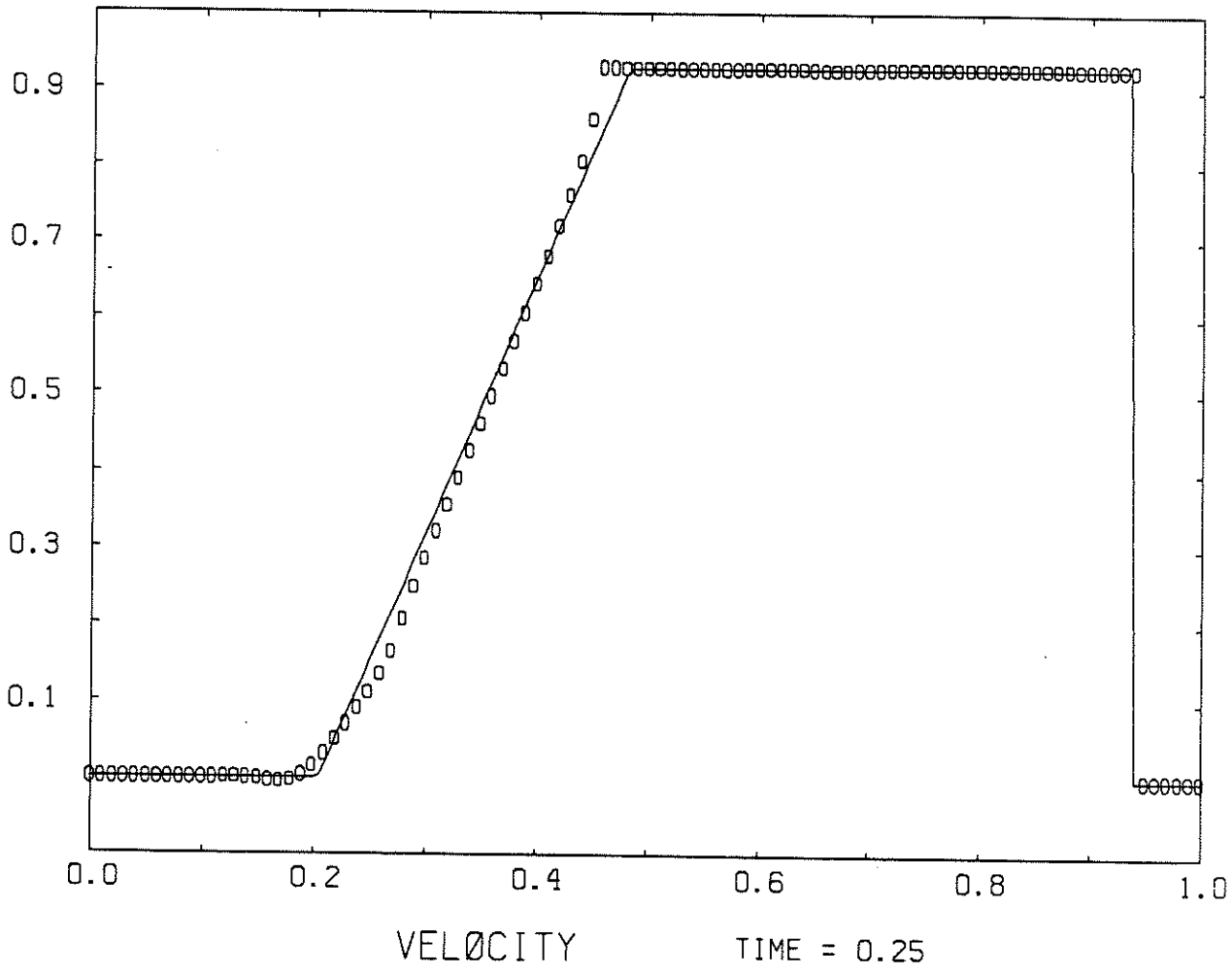

Fig. 6.5 — b

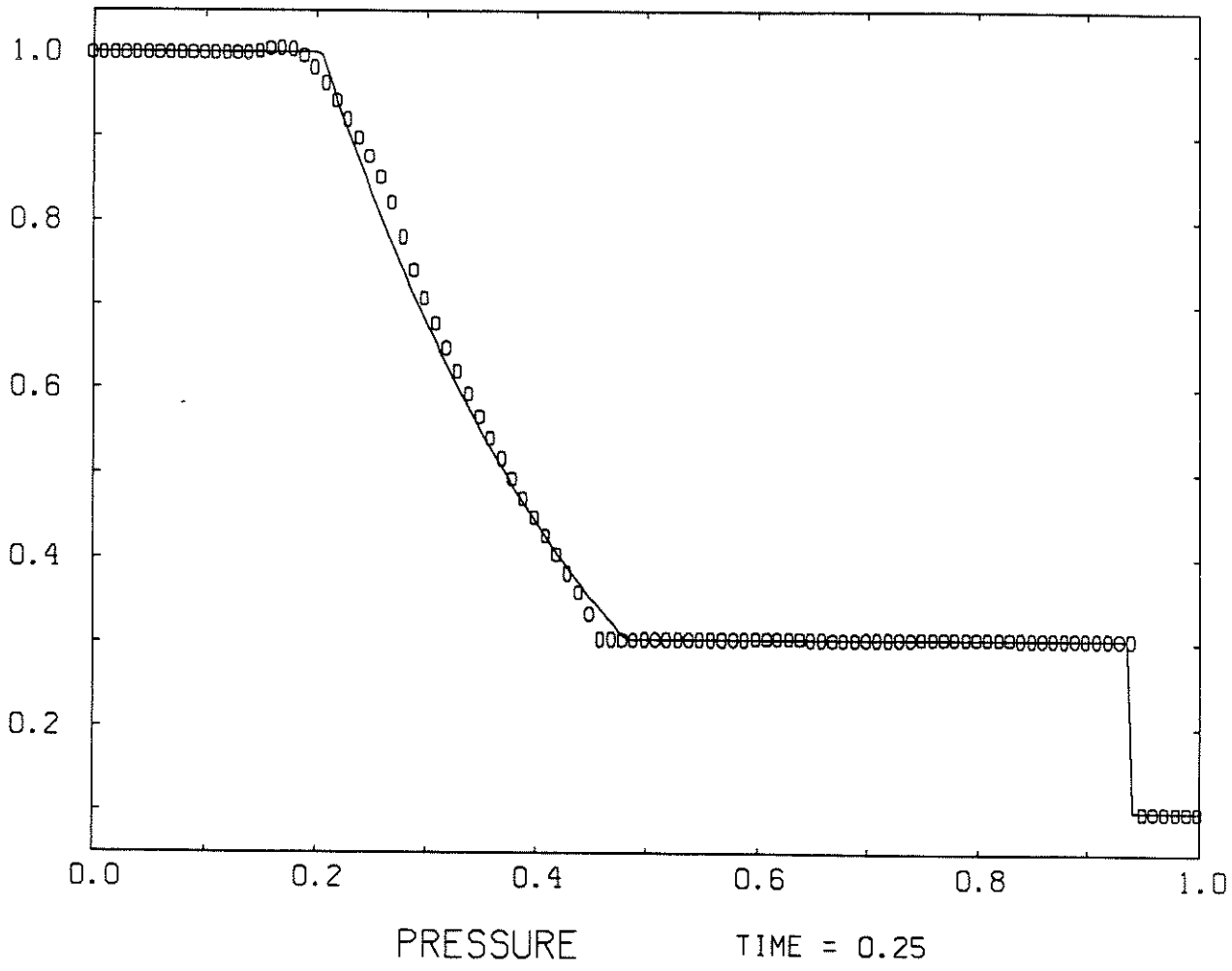

Fig. 6.5 — 6

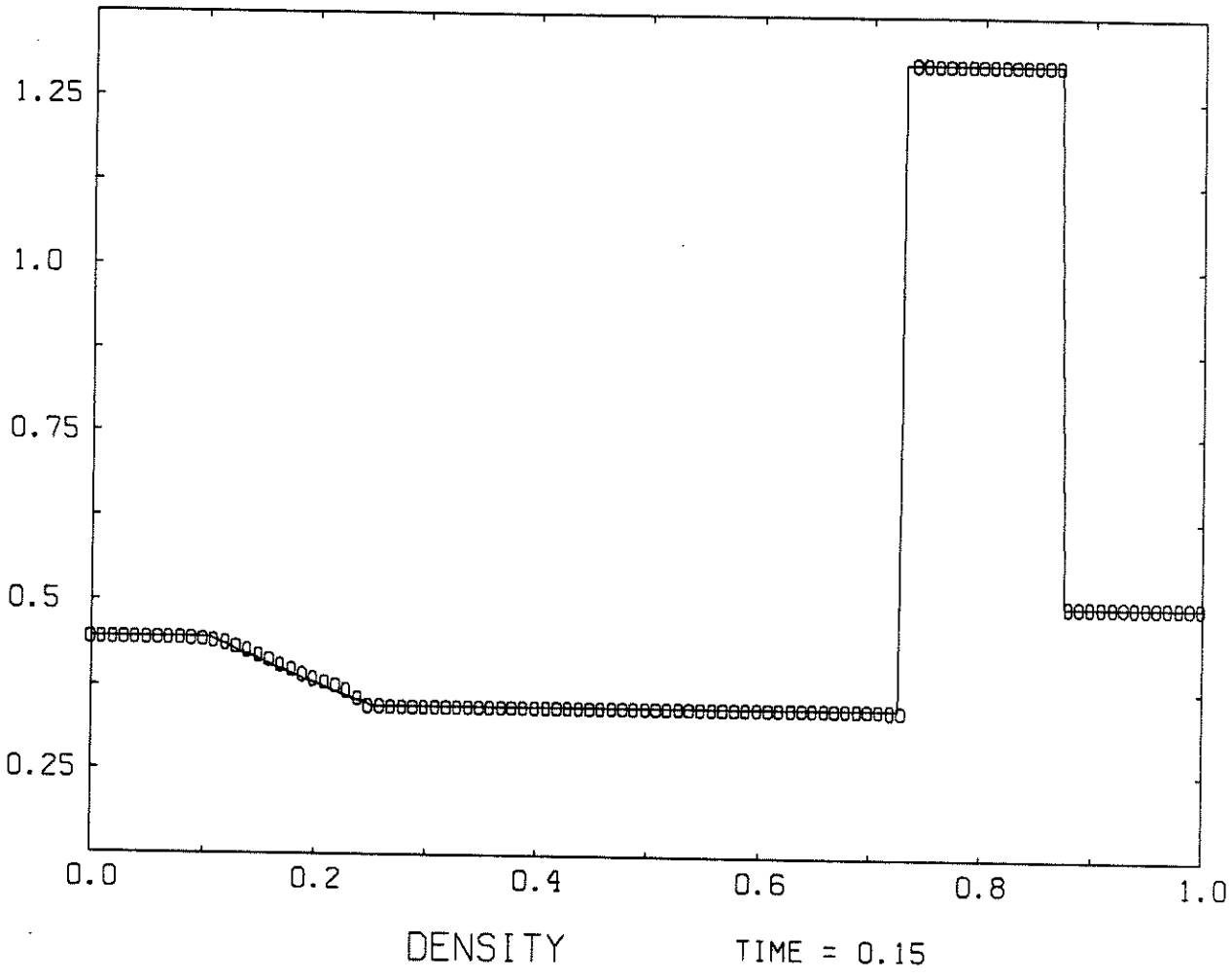

Fig. 6.6

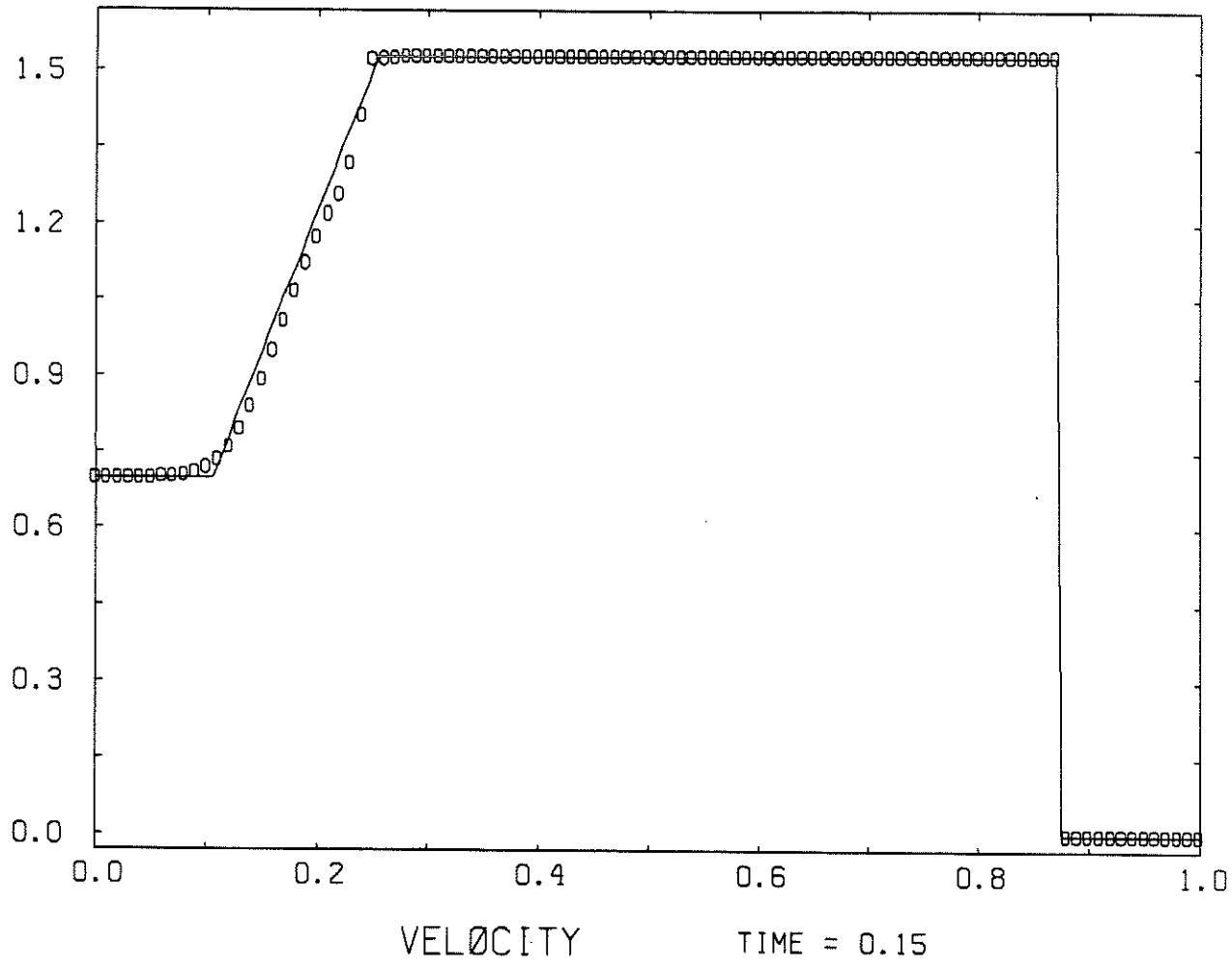

Fig. 6.6

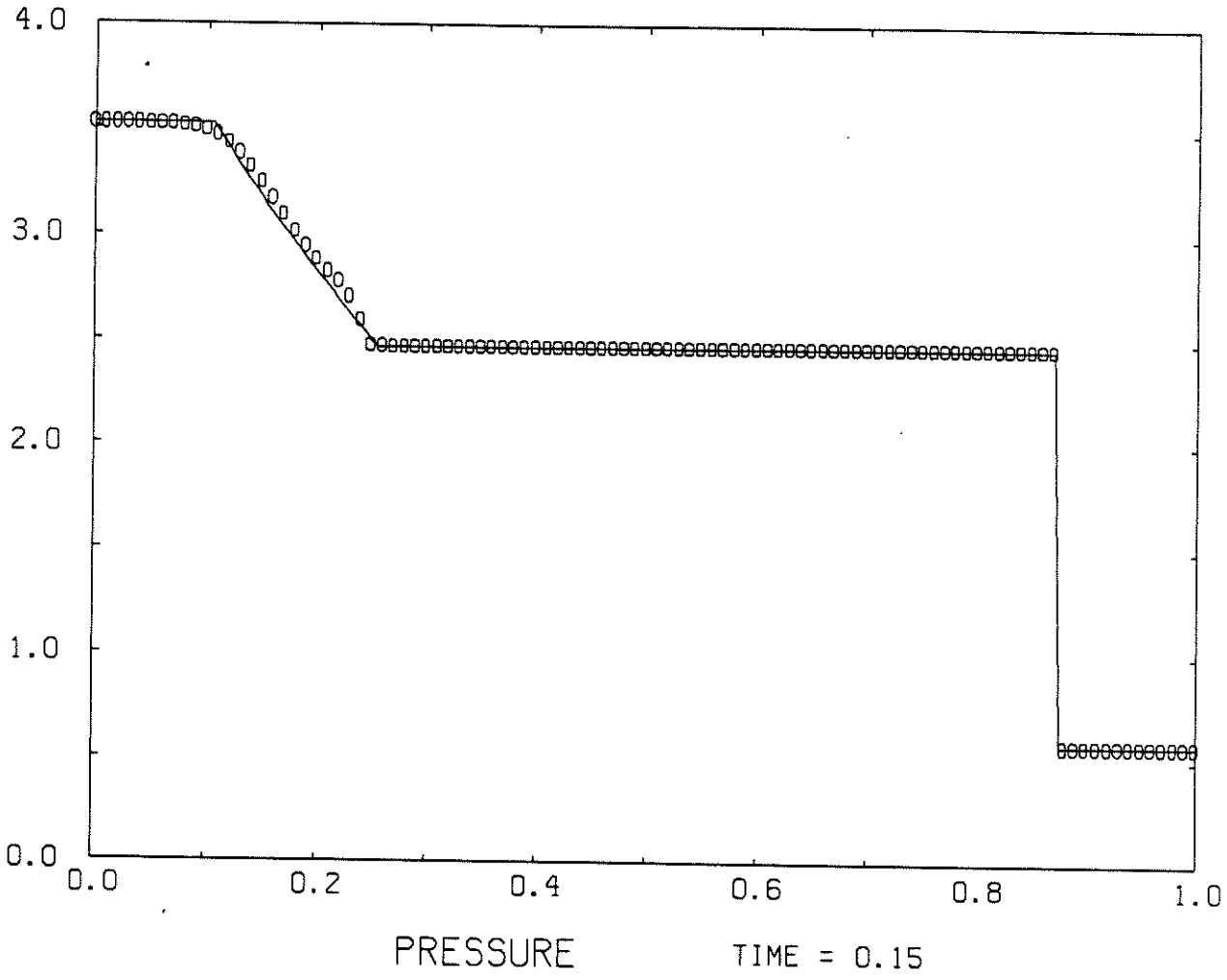

Fig. 6.6

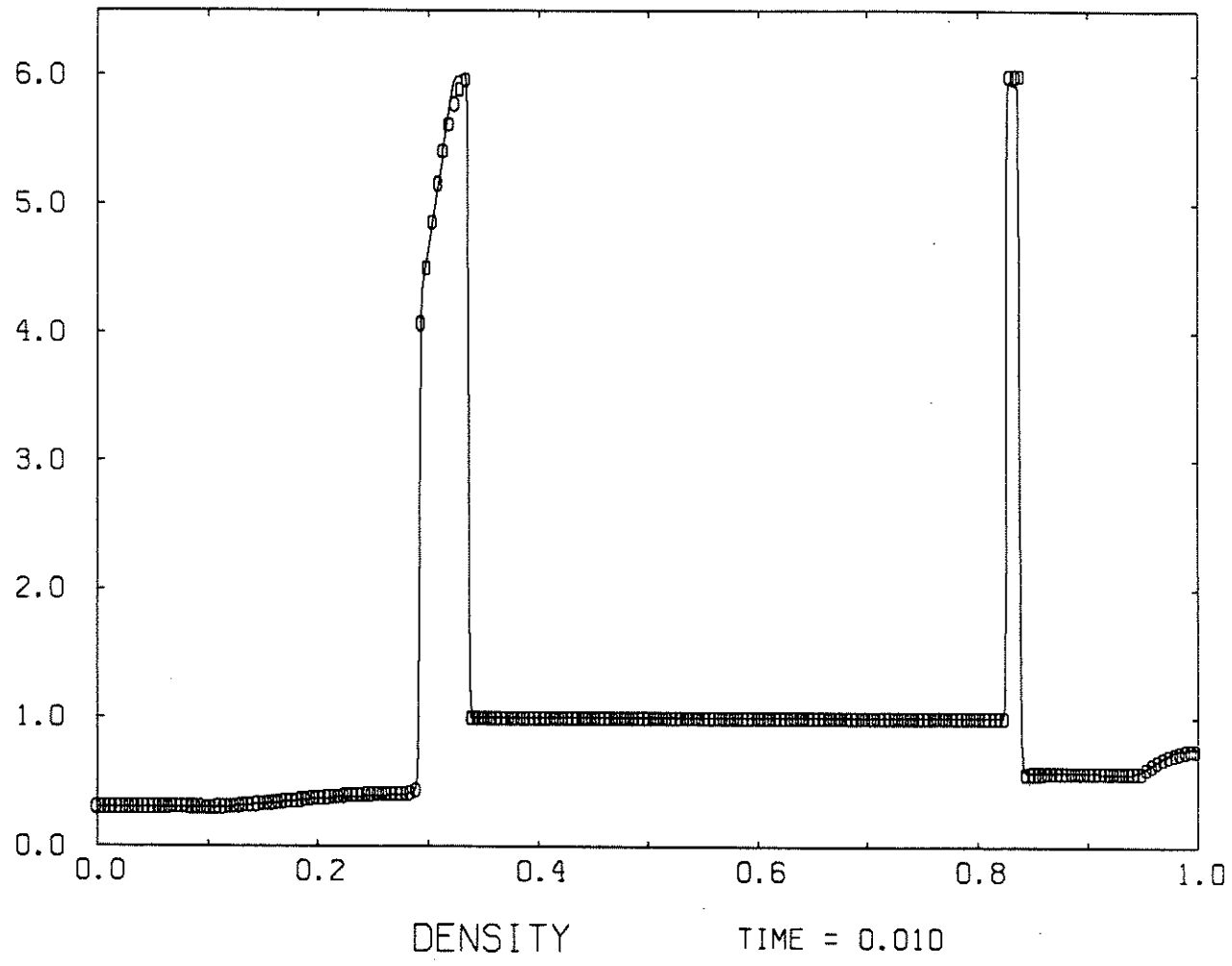

Fig. 6.7 — a

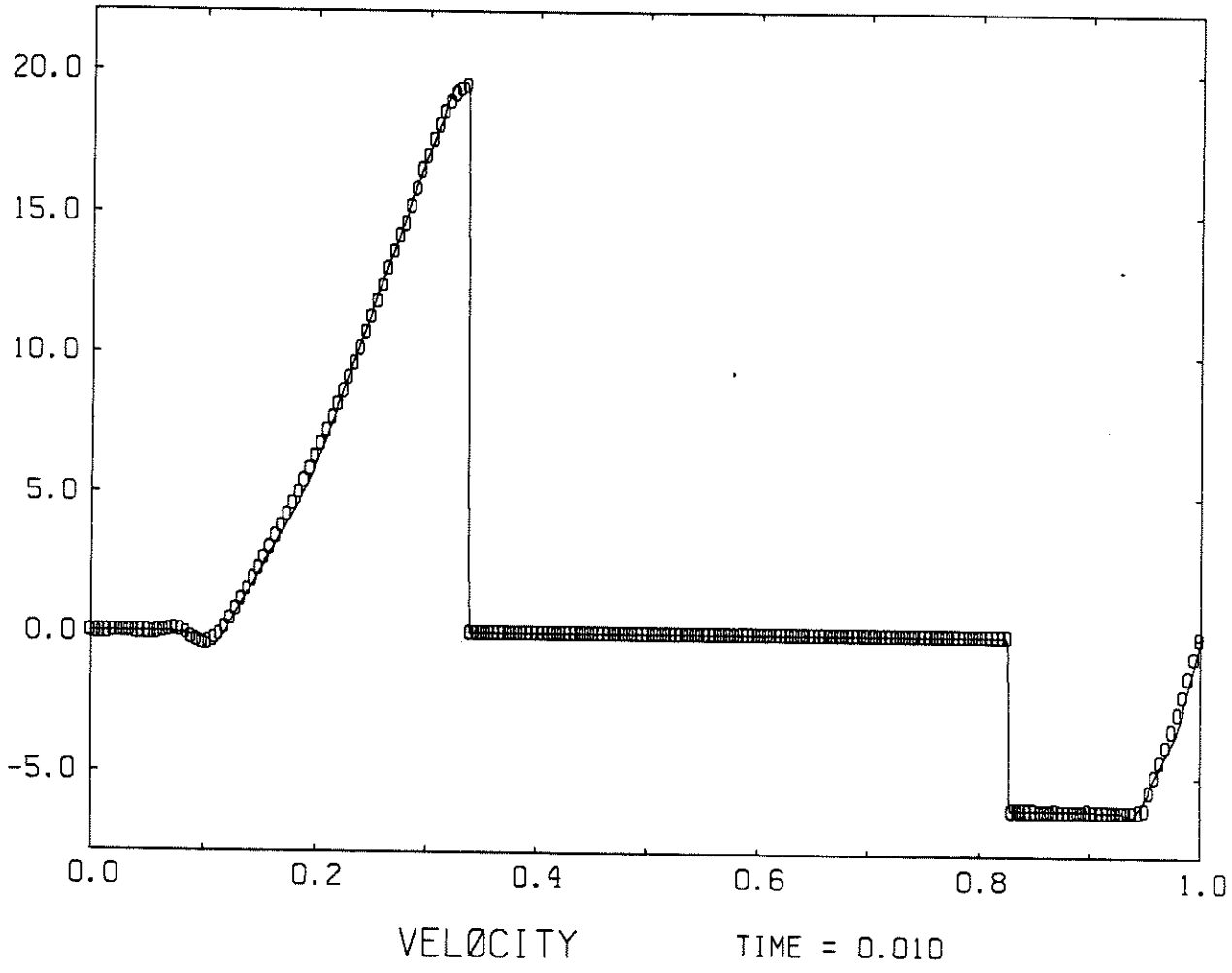

Fig. 6.7 – a

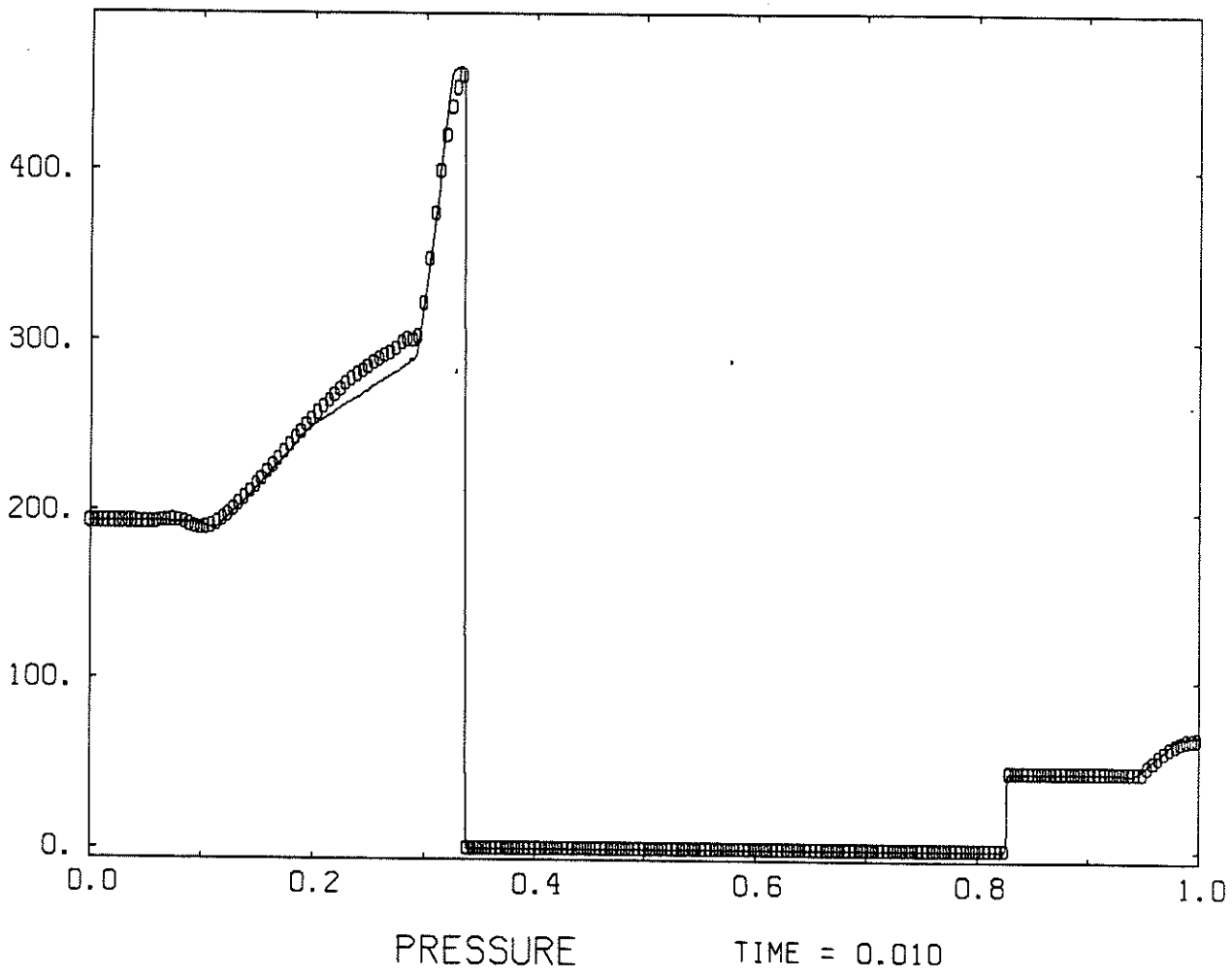

Fig. 6.7 — a

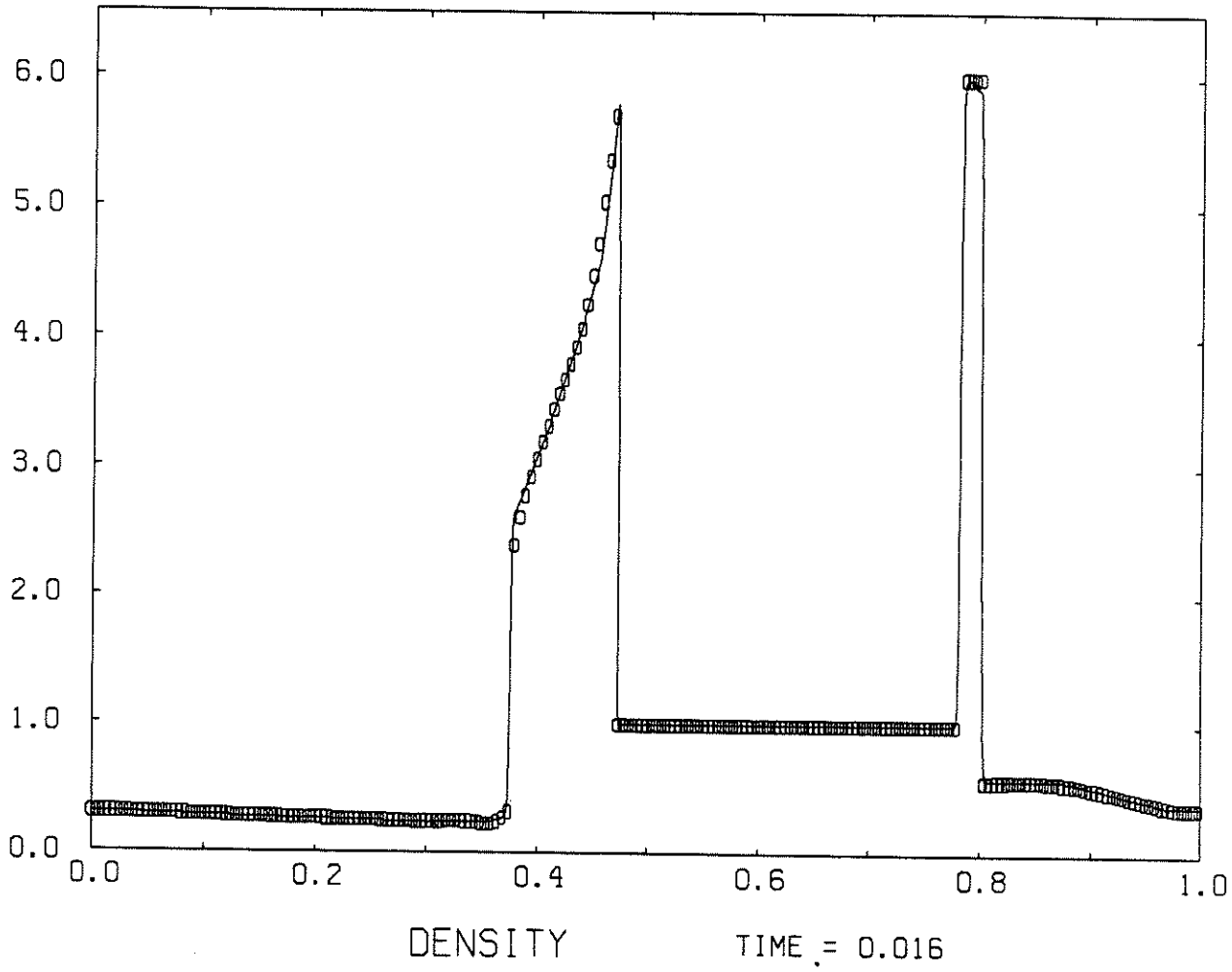

Fig. 6.7 — b

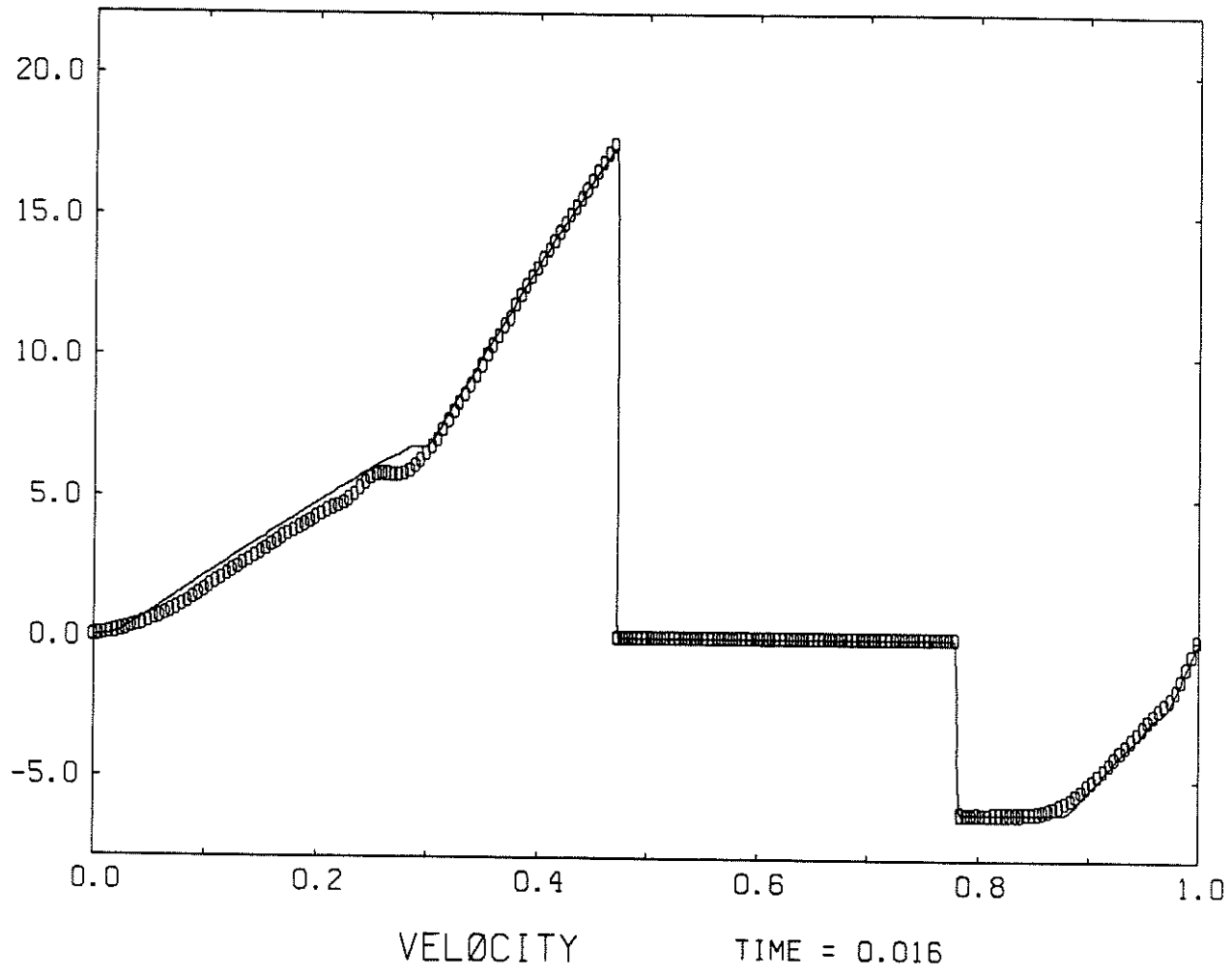

Fig. 6.7—6

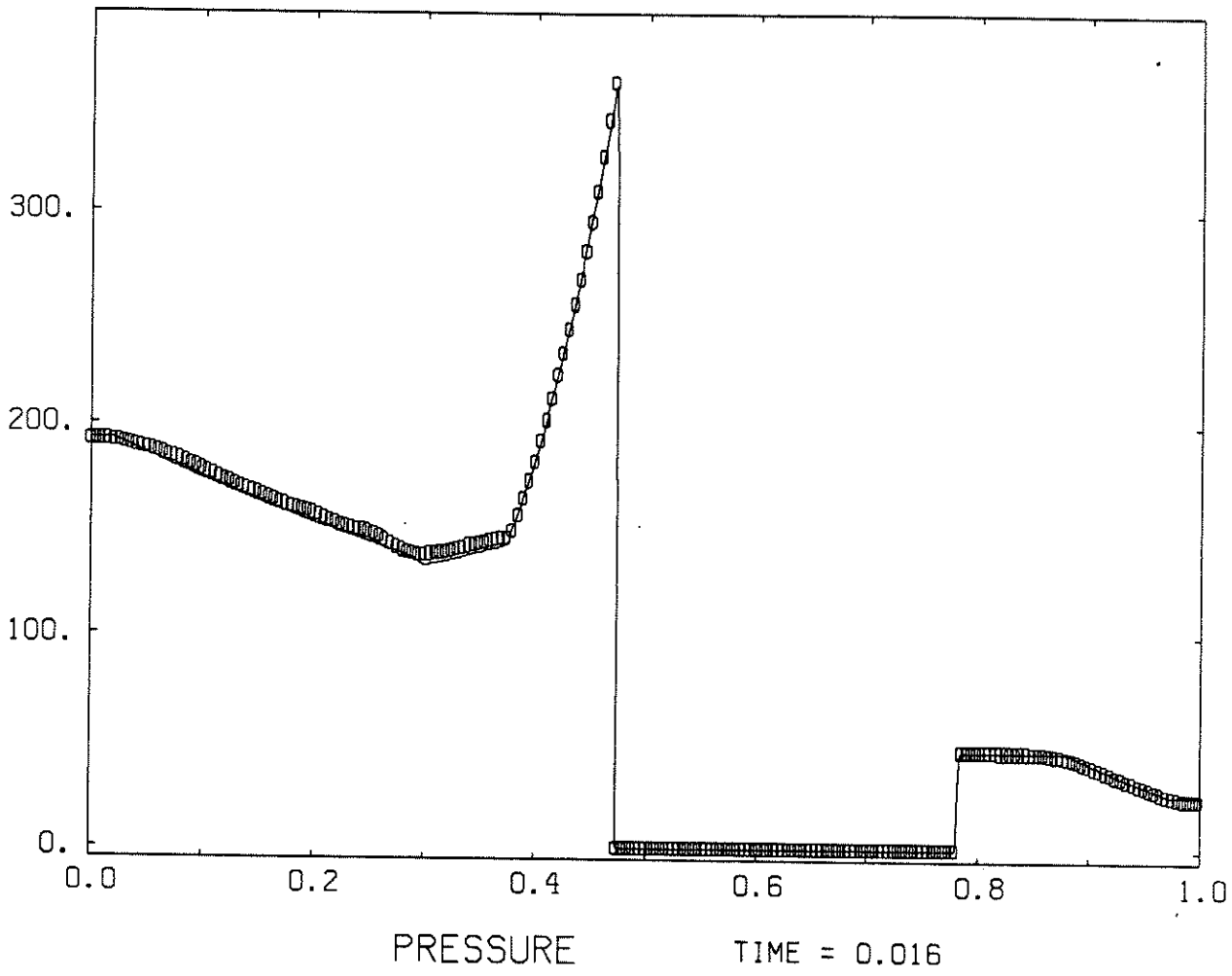

Fig. 6.7 — 6

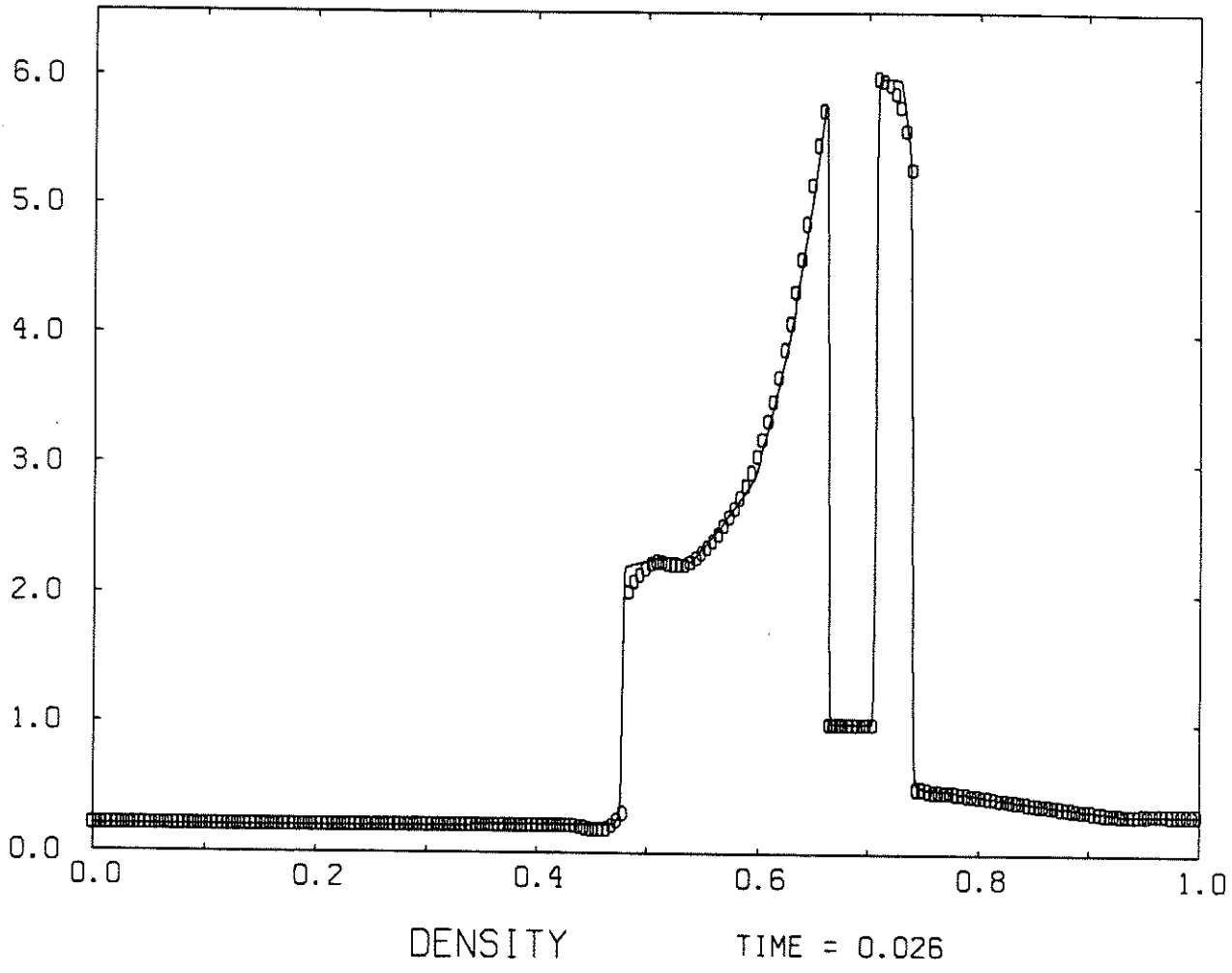

Fig. 6.7 — c

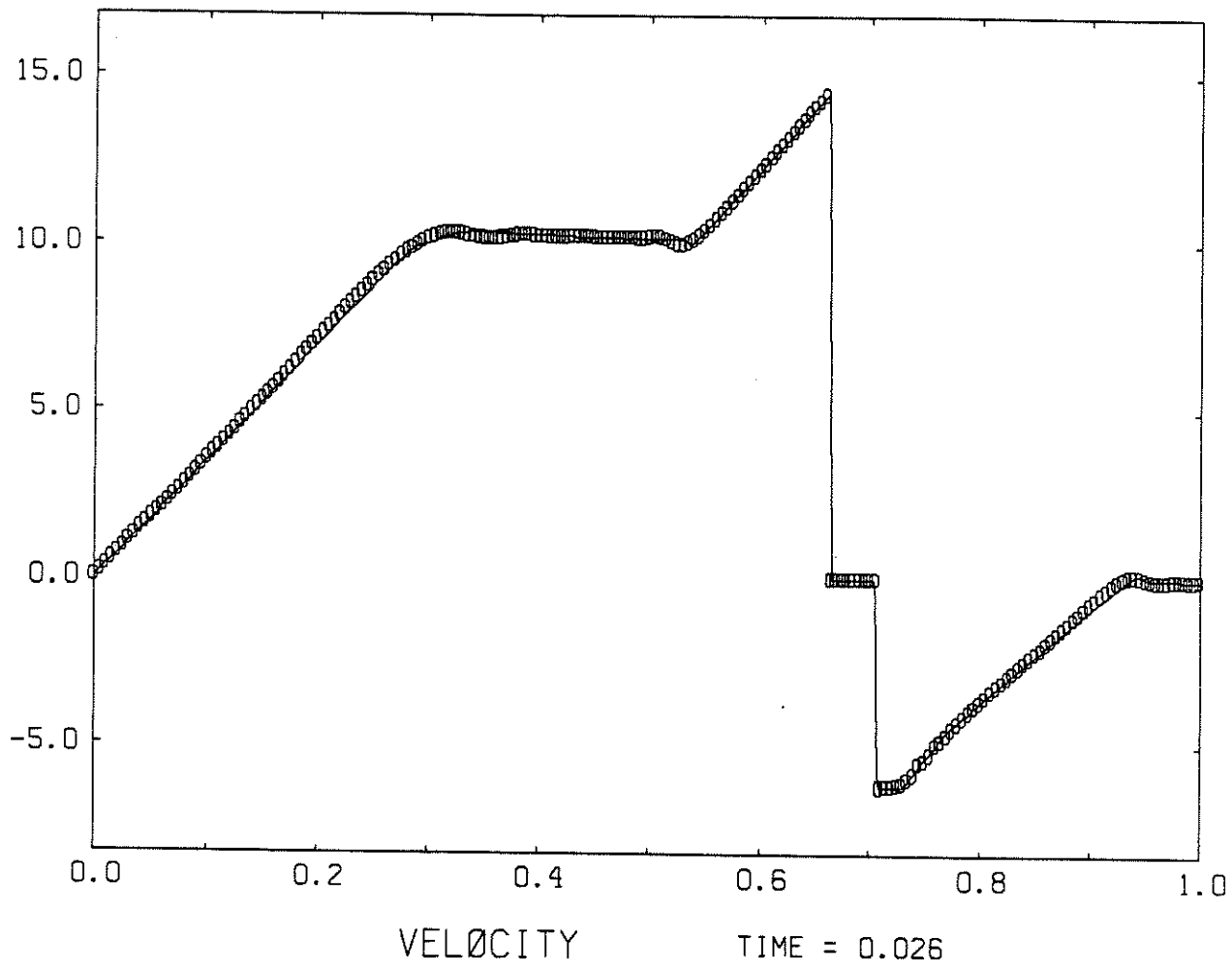

Fig. 6.7 – c

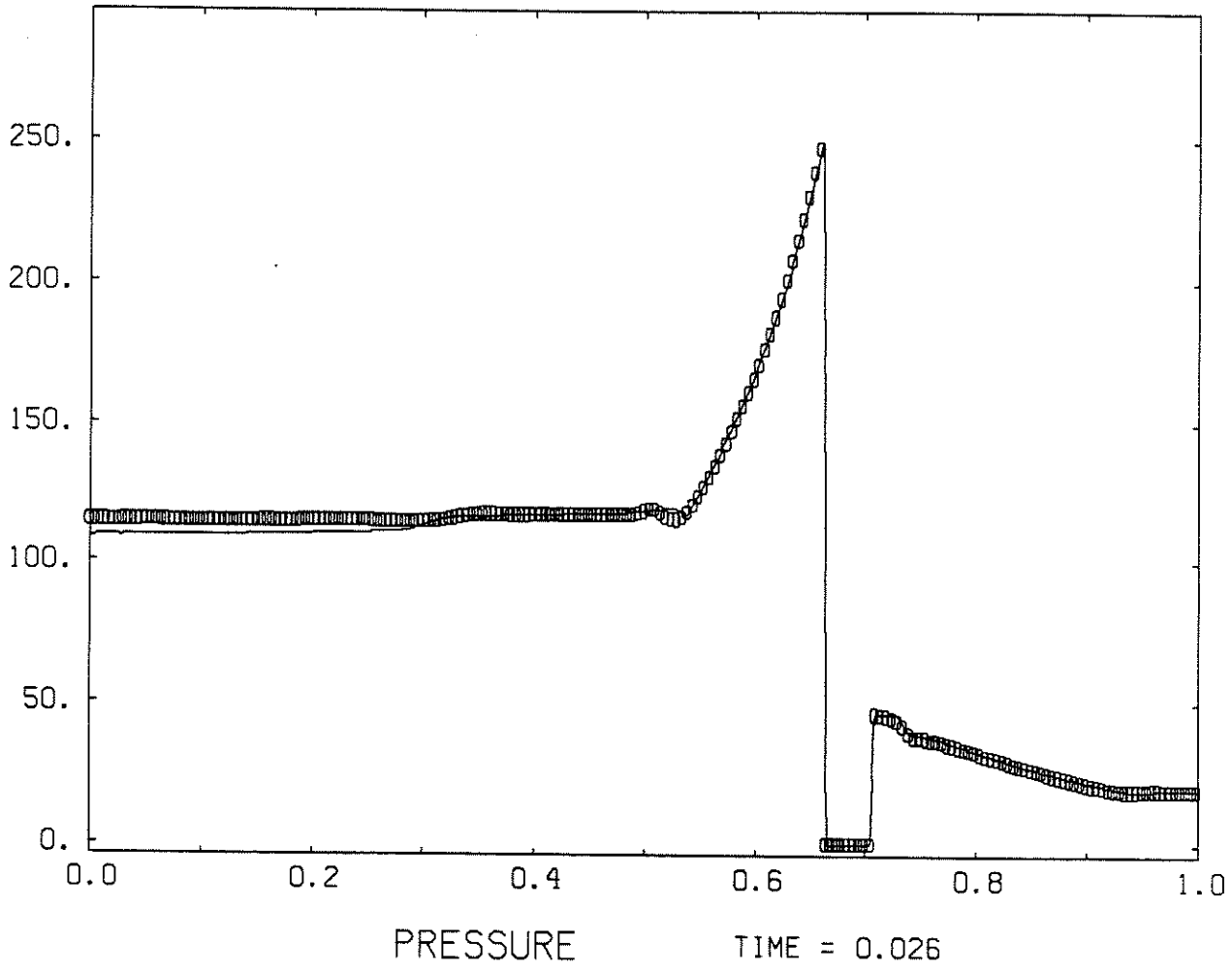

Fig. 6.7 – c

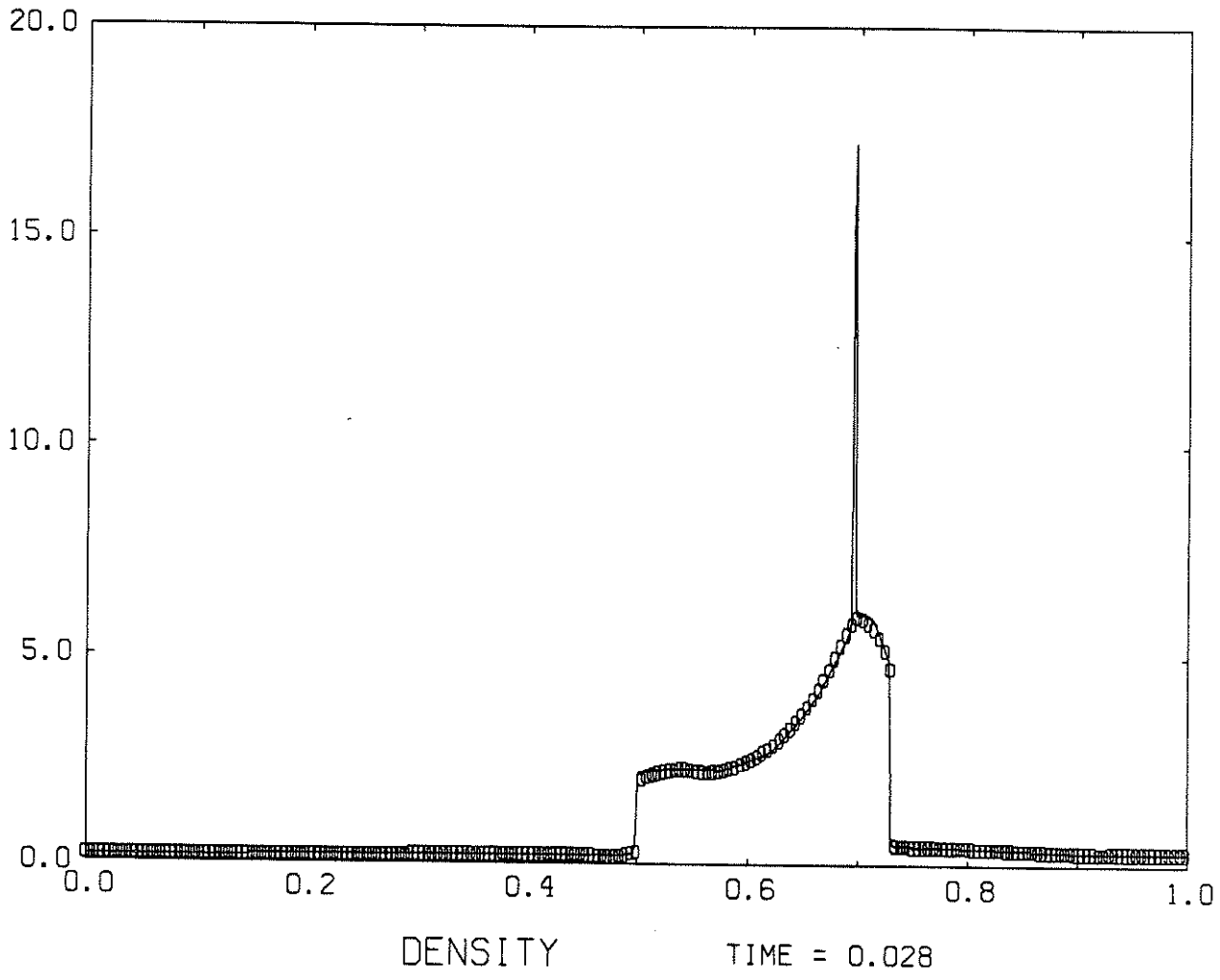

Fig. 6.7 – d

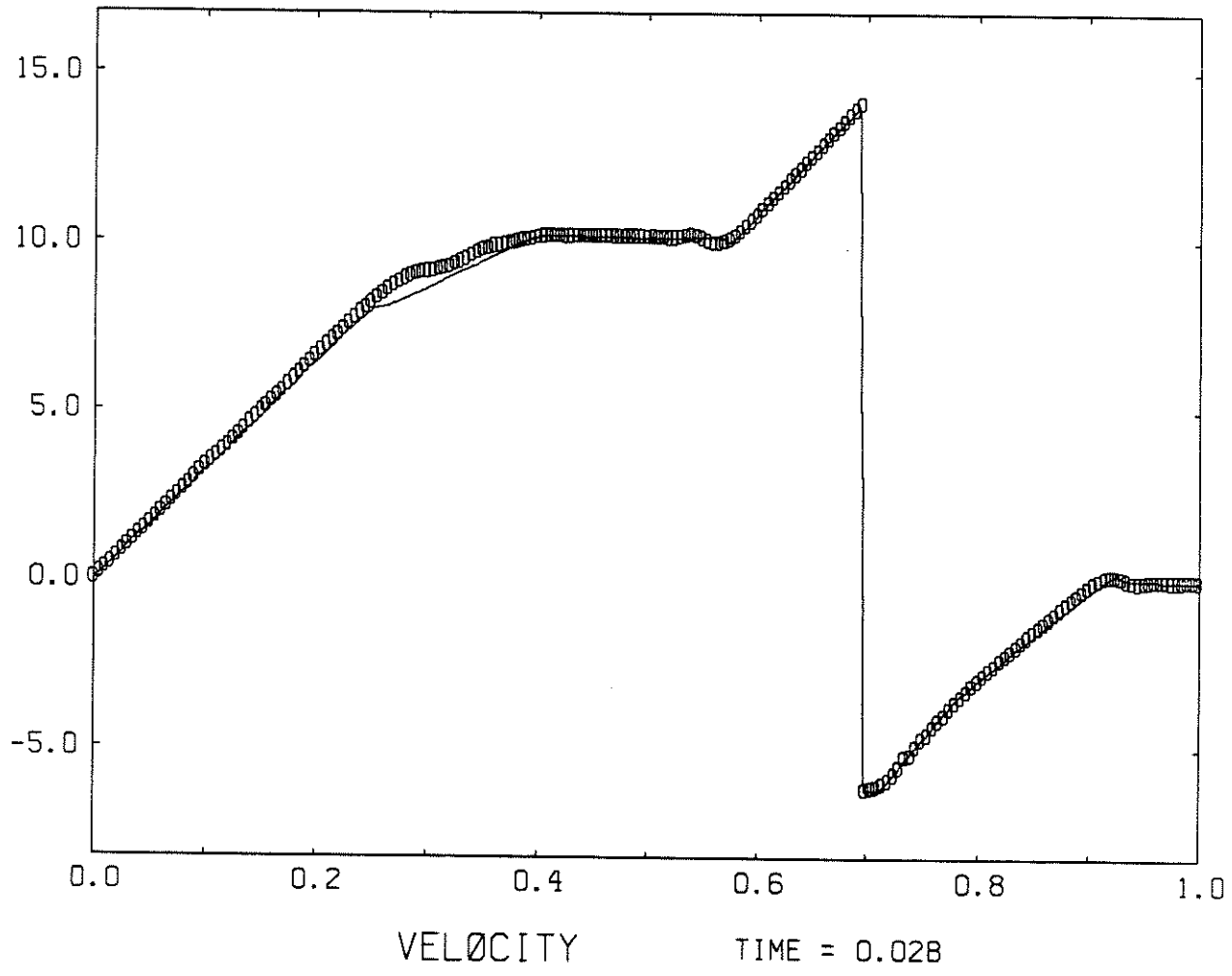

Fig. 6.7 — d

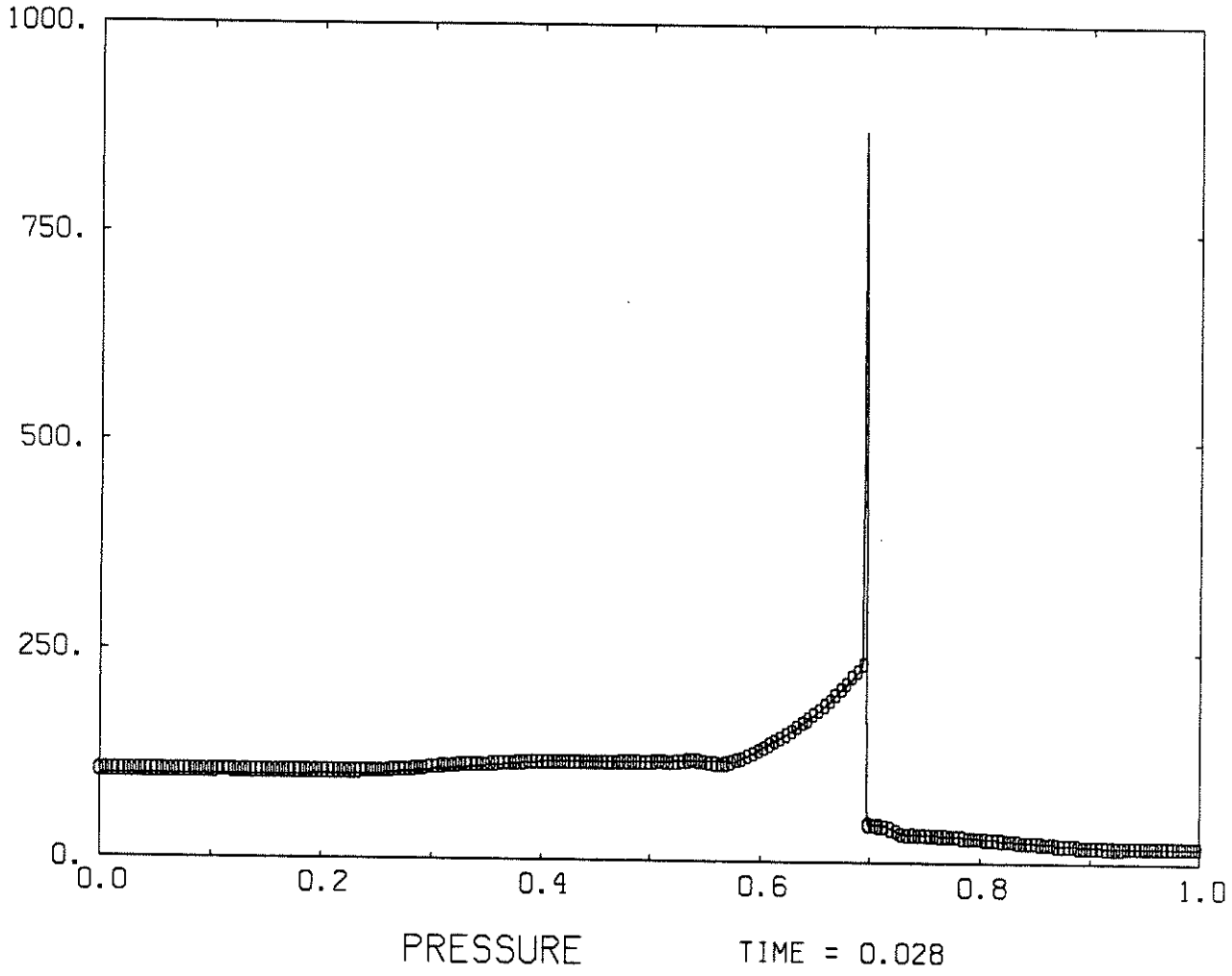

Fig. 6.7 — d

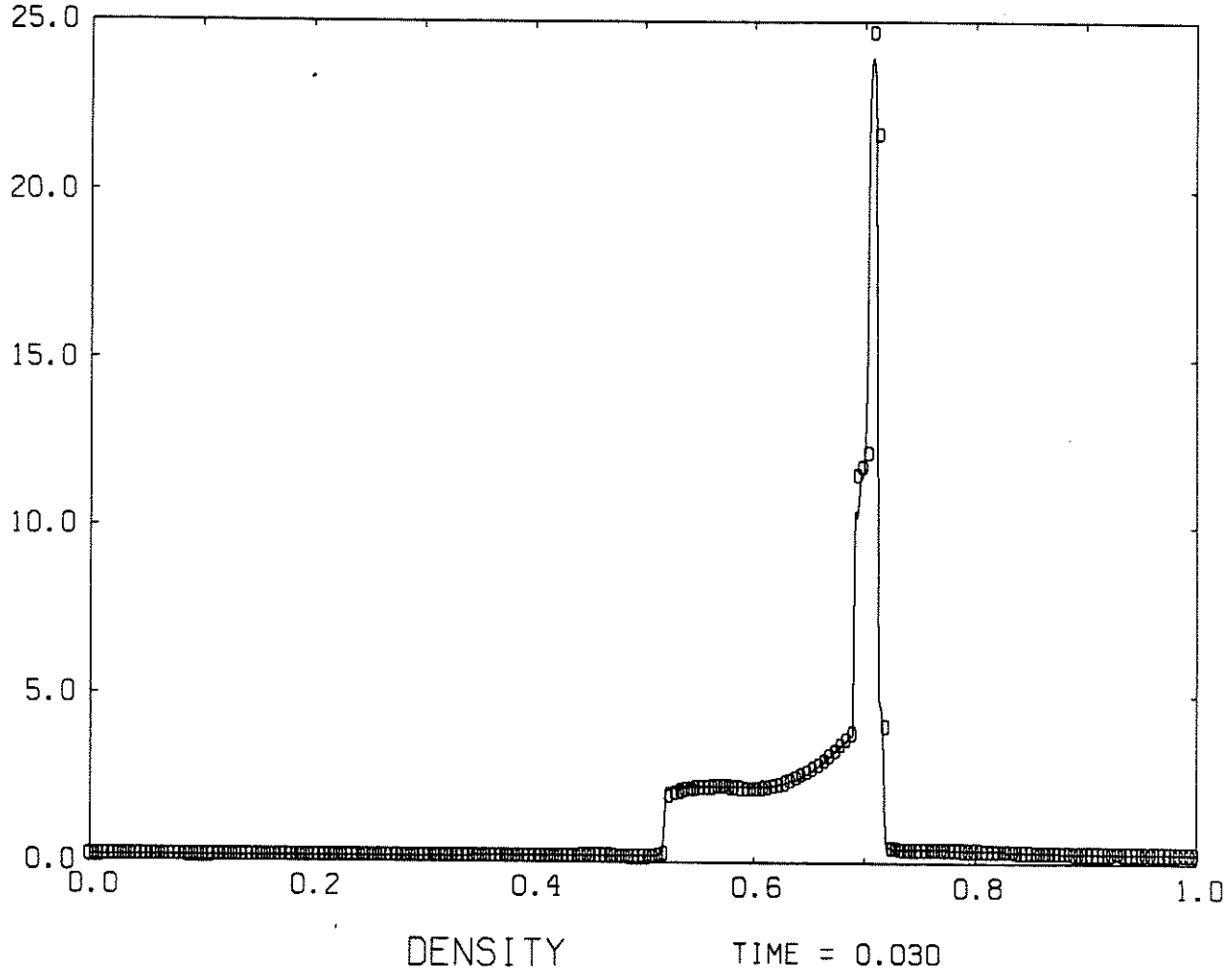

Fig. 6.7 — e

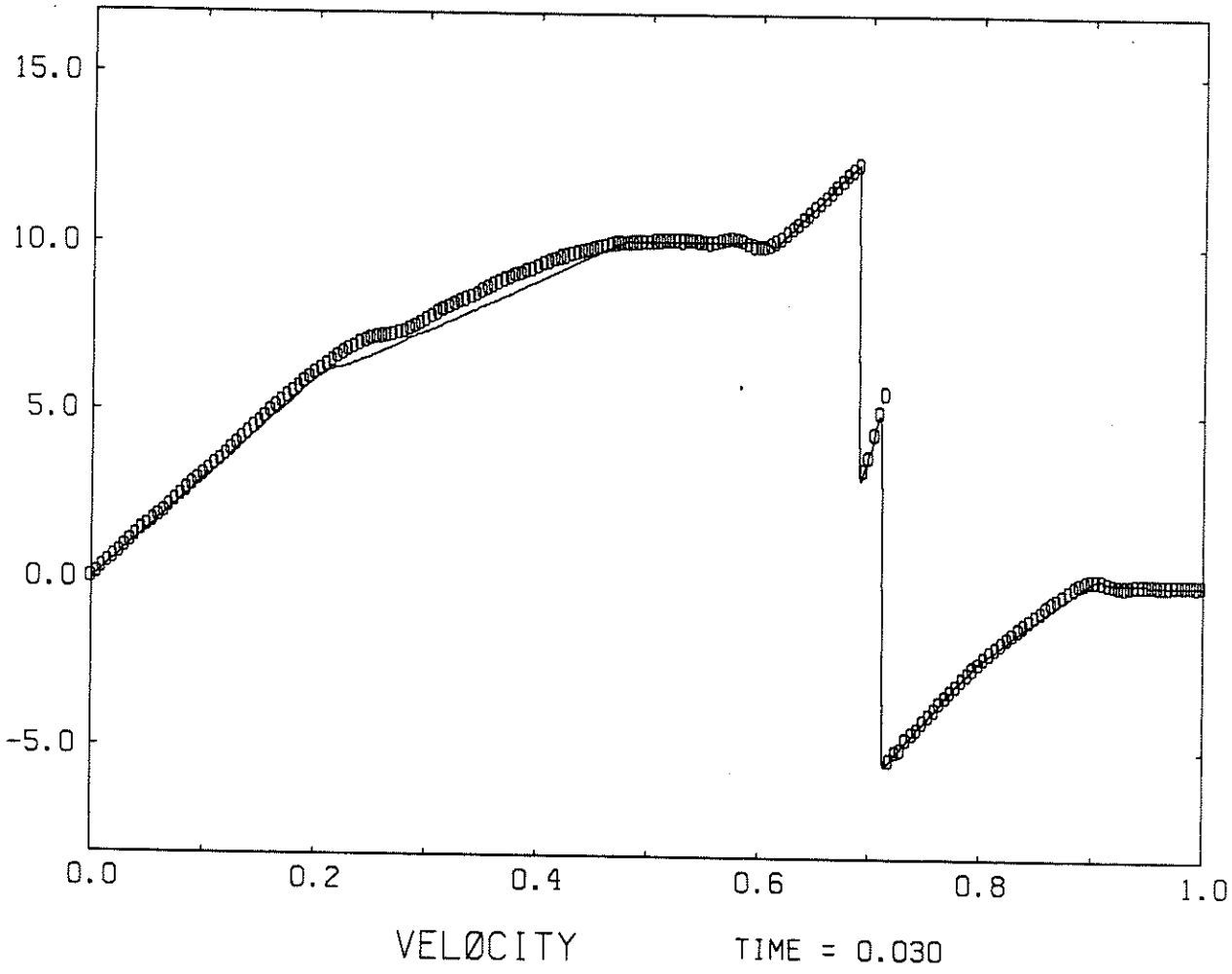

Fig. 6.7 — e

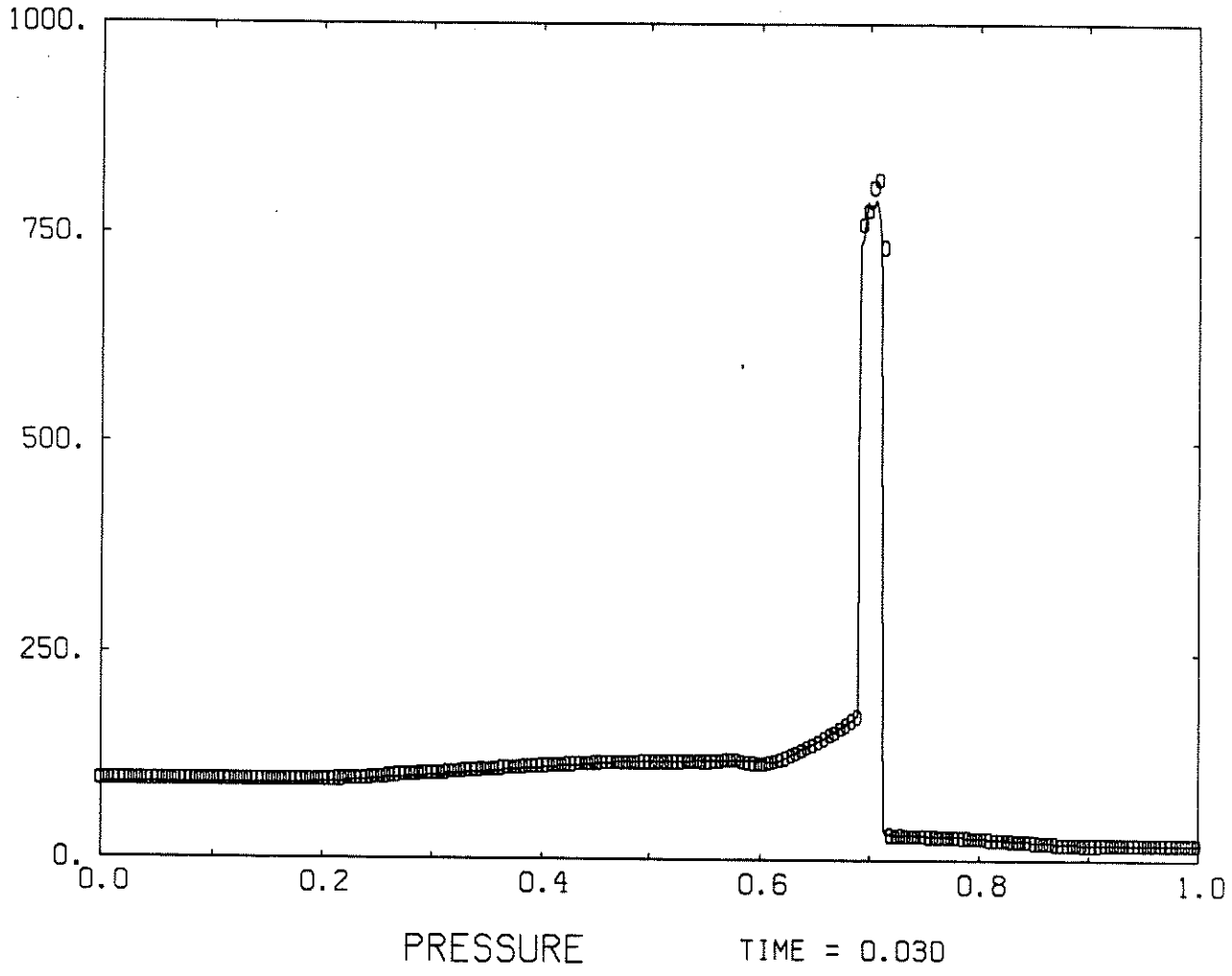

Fig. 6.7 — e

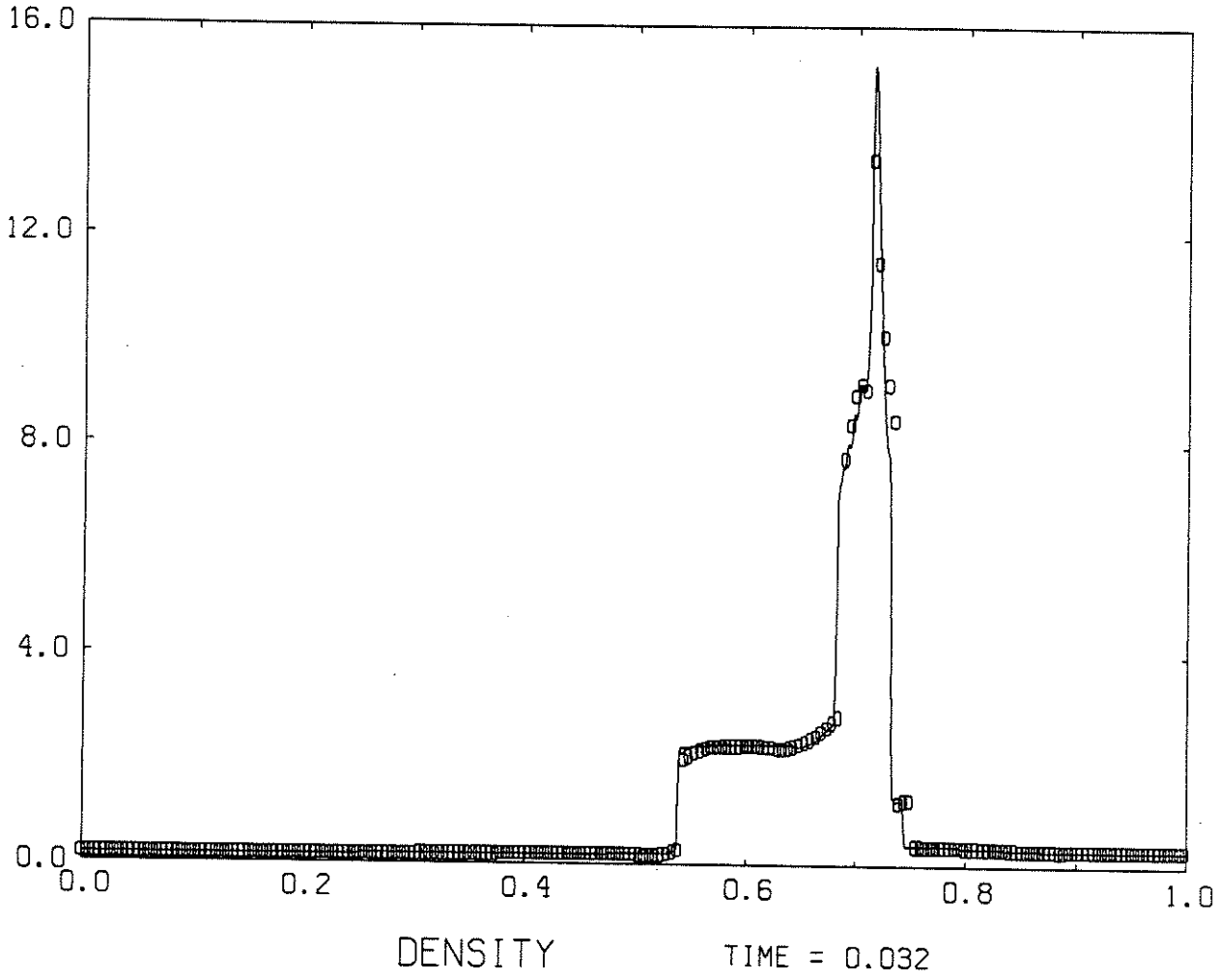

Fig. 6.7 – f

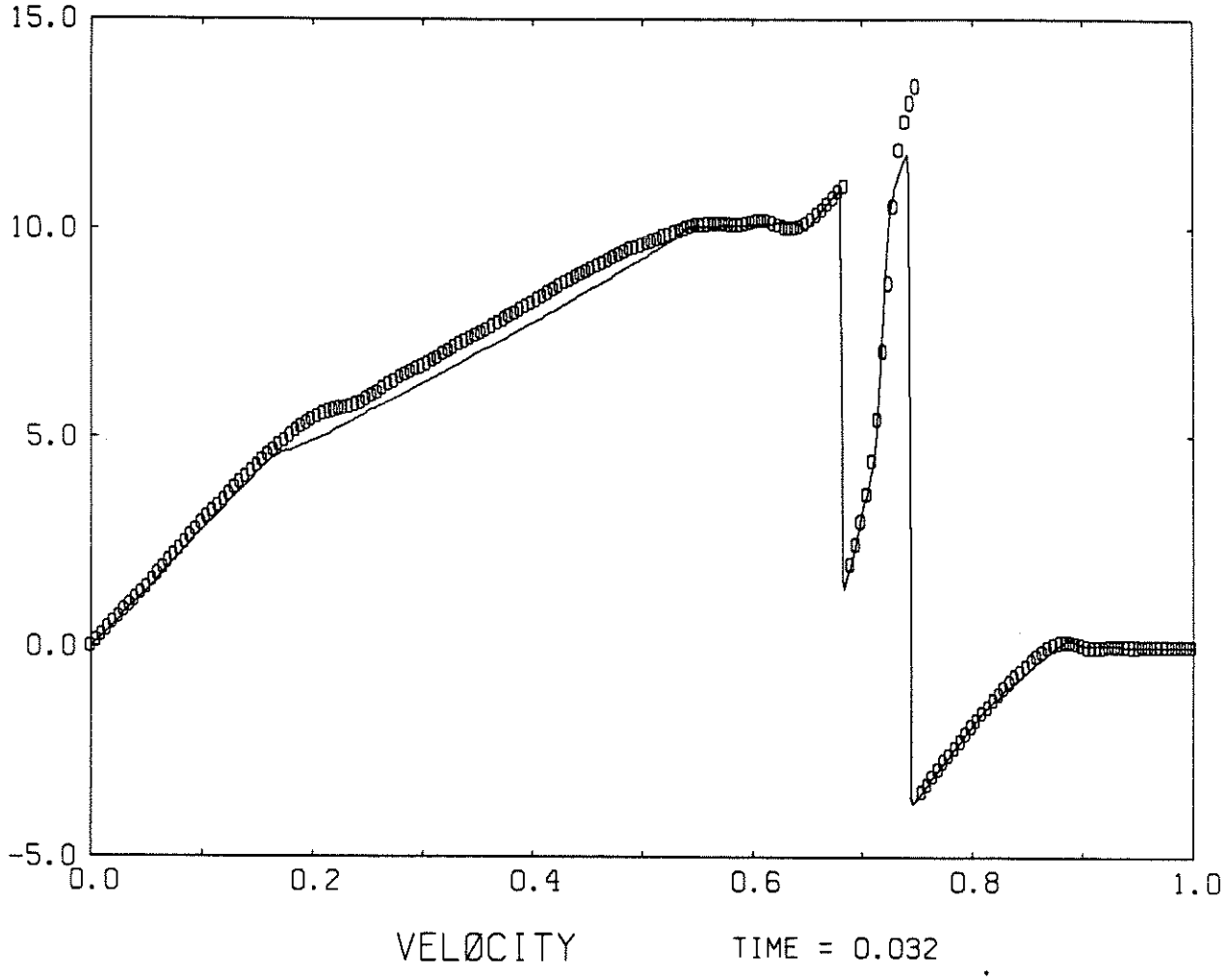

Fig. 6.7 — f

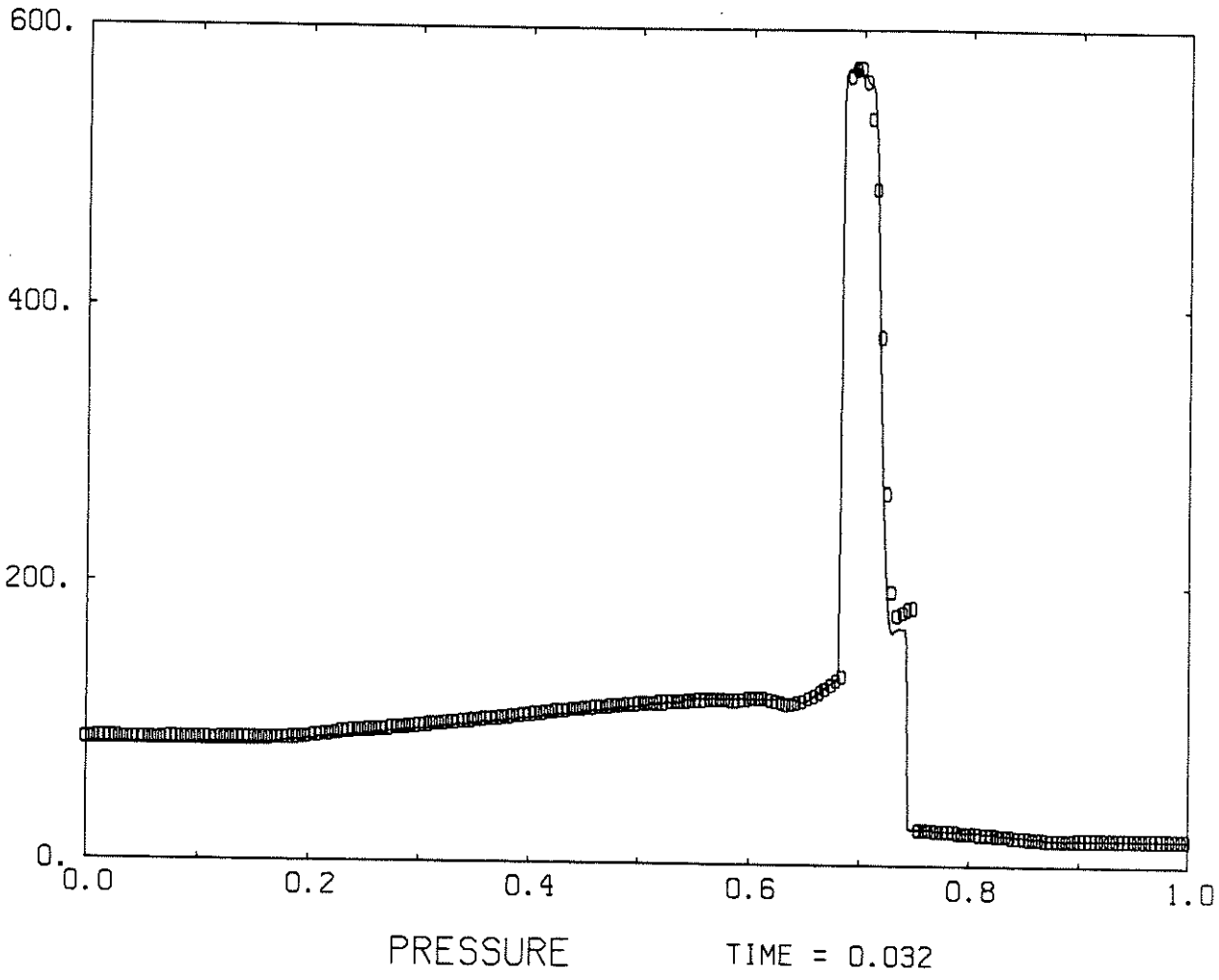

Fig. 6.7 — f

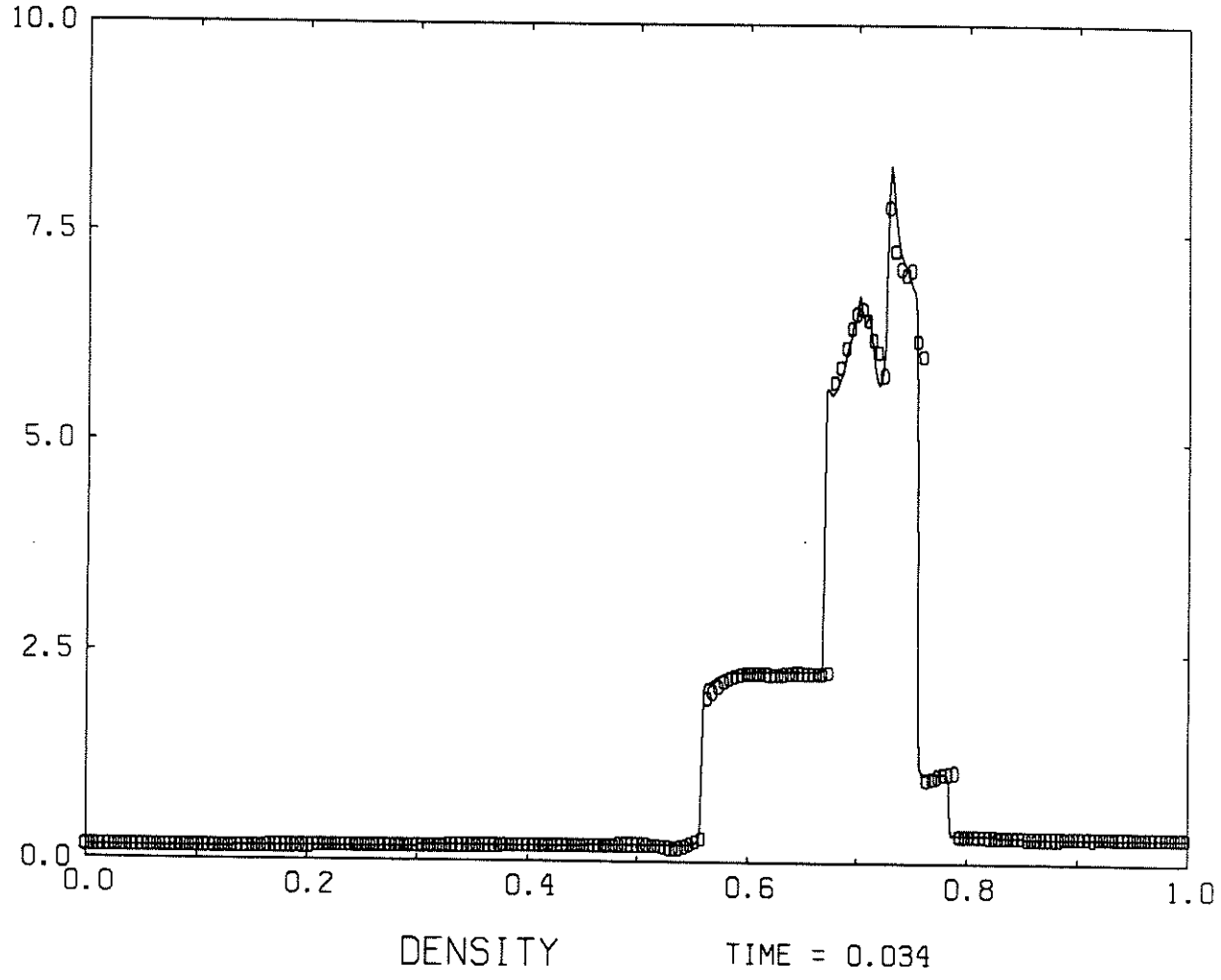

Fig. 6.7 — g

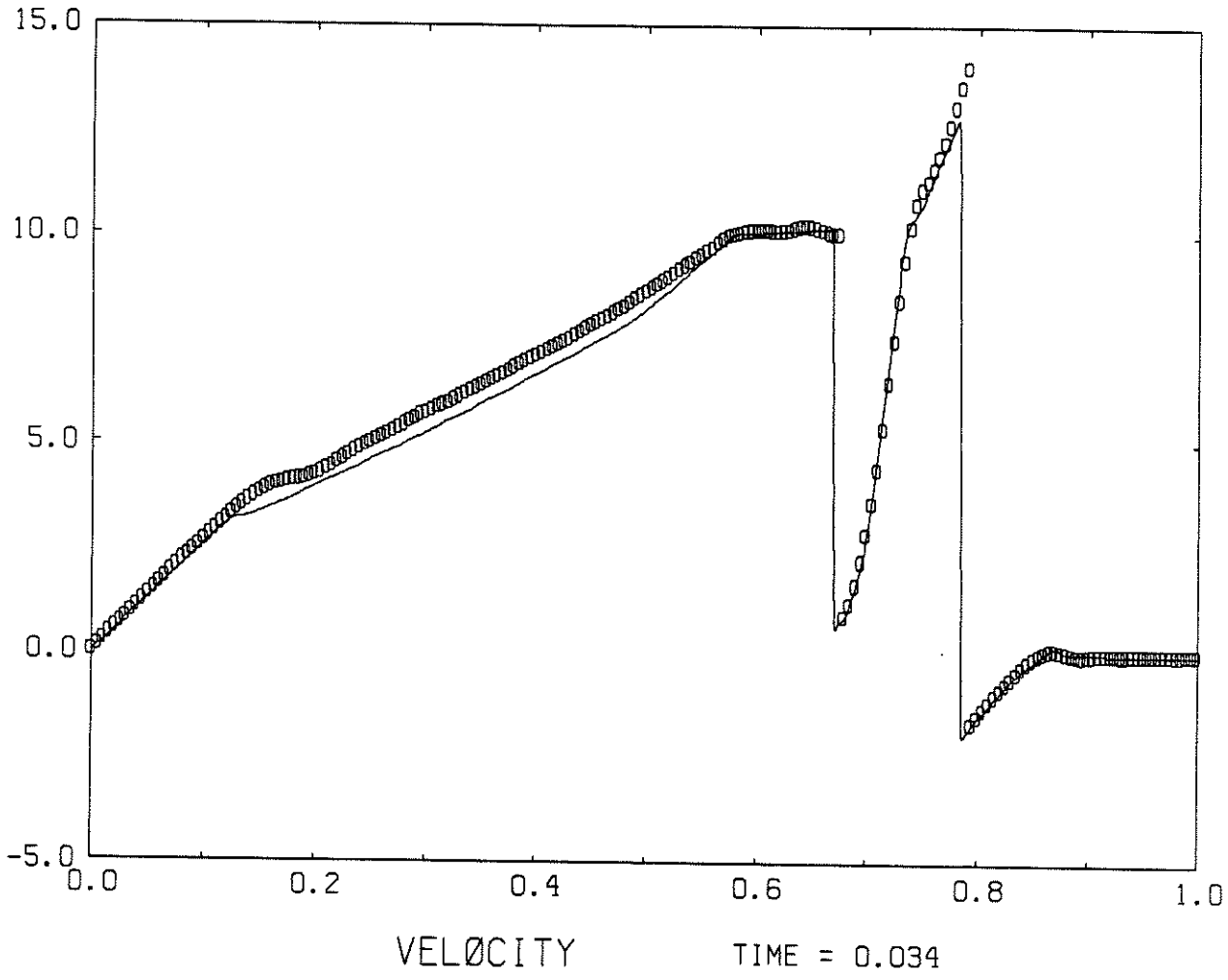

Fig. 6.7 — g

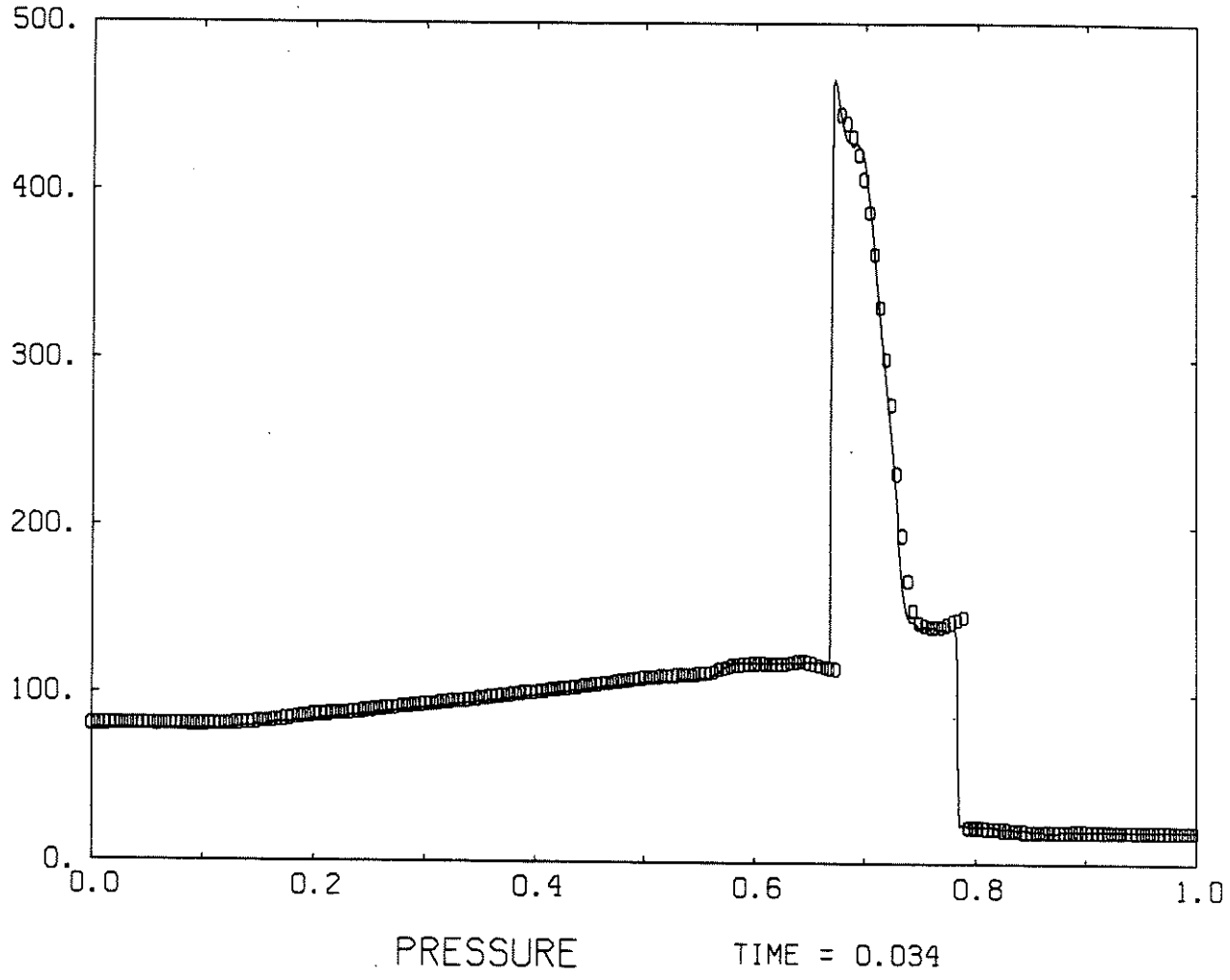

Fig. 6.7 — g

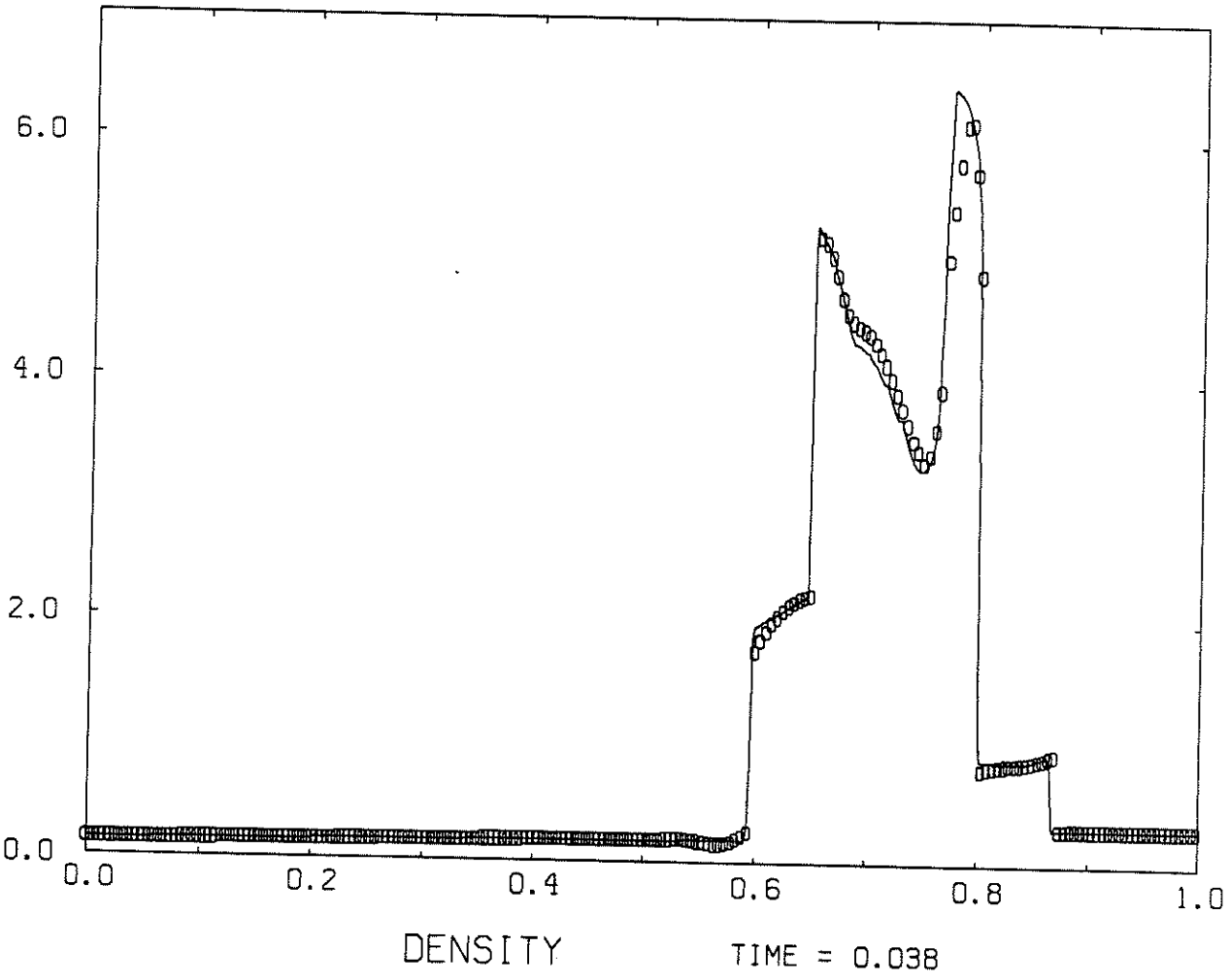

Fig. 6.7 — h

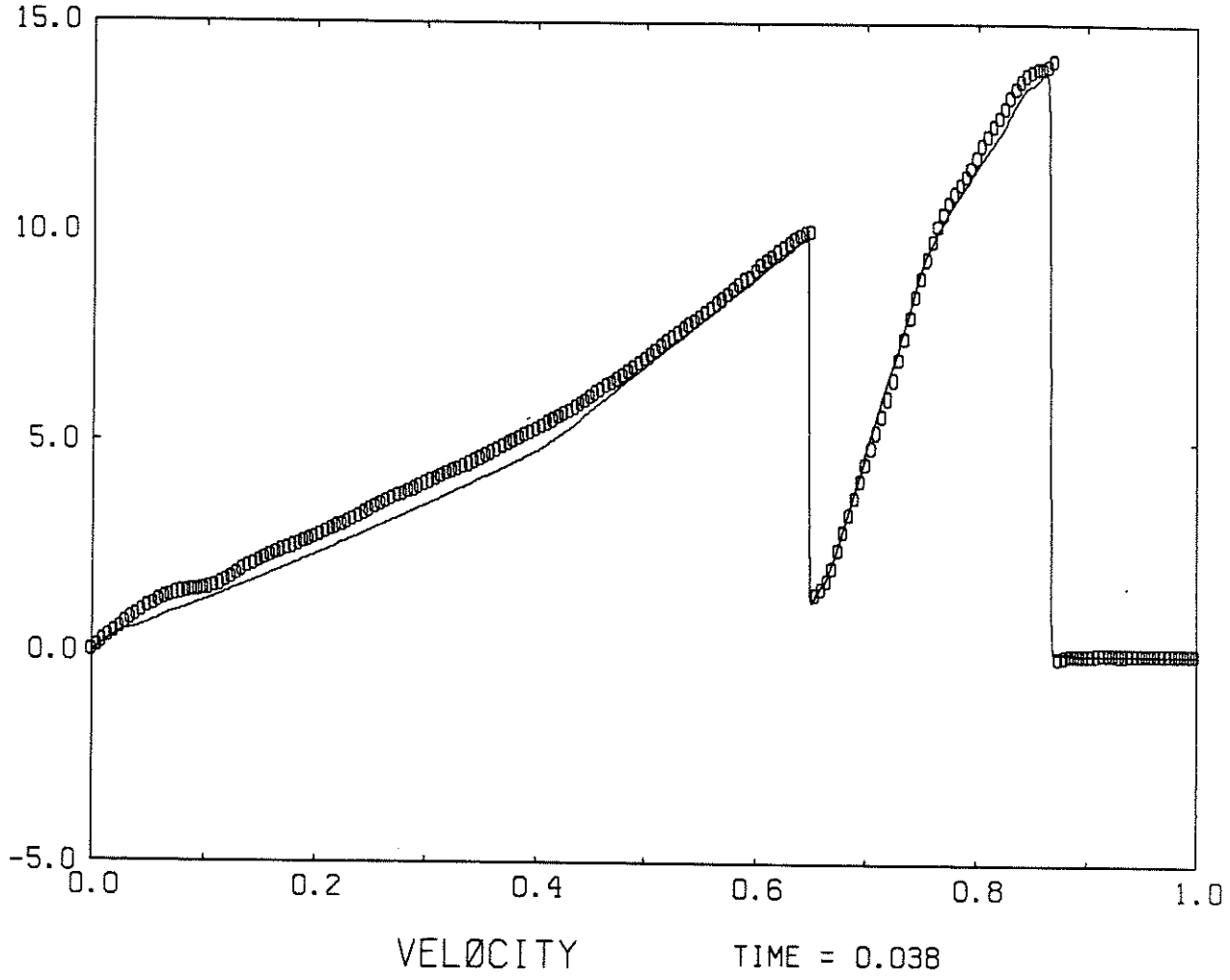

Fig. 6.7 — h

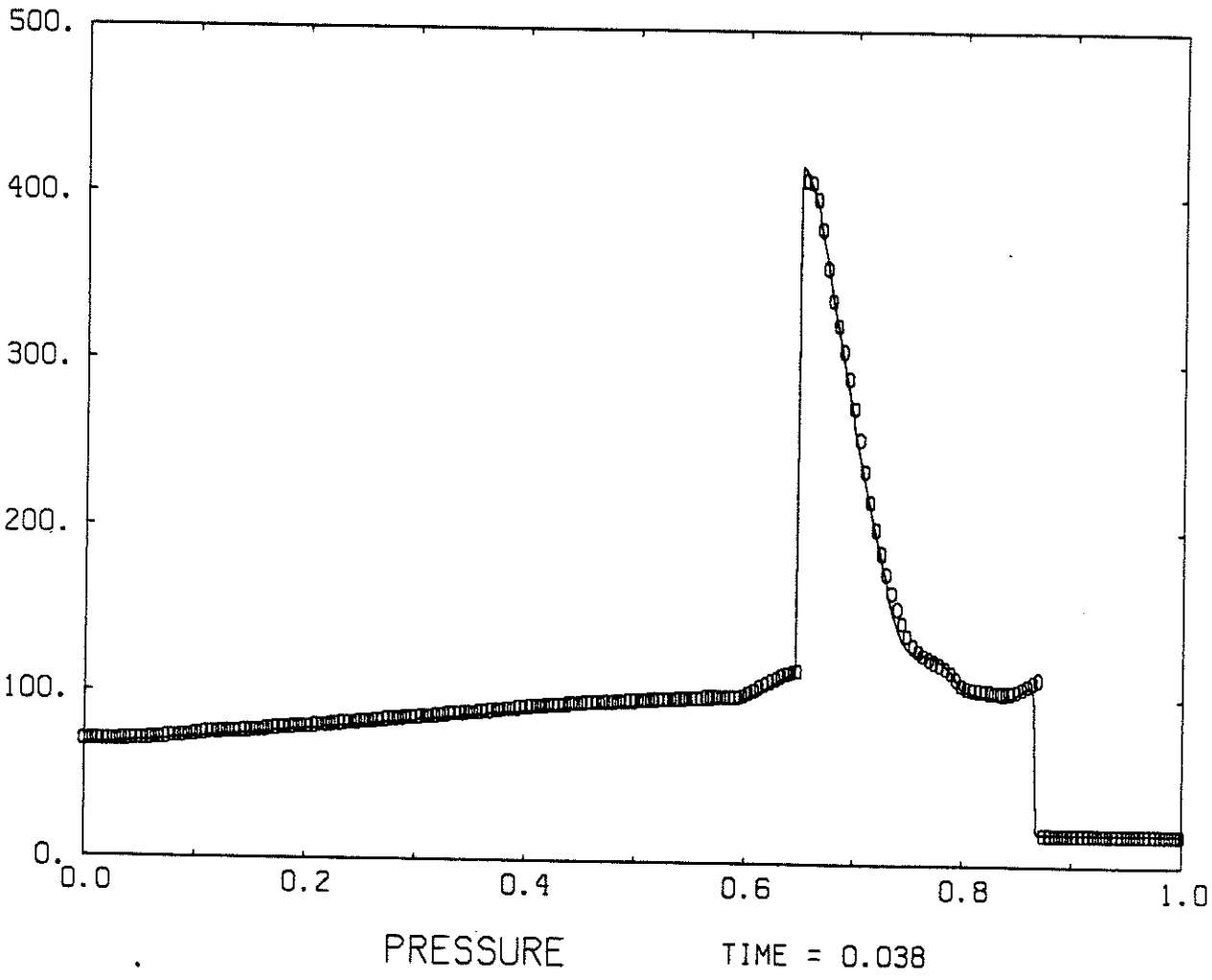

Fig. 6.7—h